Synthesis and Solution Properties of Semi-rigid Polyelectrolytes and Polyampholytes

Alice M. Savage

Dissertation submitted to the faculty of the Virginia Polytechnic Institute and State University in partial fulfillment of the requirements for the degree of

Doctor of Philosophy
In
Chemistry

S. Richard Turner, Committee Chair
Timothy E. Long
Richey M. Davis
Alan R. Esker

August 29, 2014
Blacksburg, VA

Keywords: controlled radical polymerizations, semi-rigid, alternating copolymers, polyelectrolytes

Abstract: Synthesis and Solution Properties of Semi-rigid Polyelectrolytes and Polyampholytes

Alice M. Savage

The incorporation of substituted stilbenes in copolymers affects the resulting solution properties and their controlled radical polymerizations. Substituted stilbene monomers readily polymerize in an alternating fashion with acceptor comonomers such as maleic anhydride and maleimide. These sterically crowded polymer backbones are classified as semi-rigid. As this is an uncommon category of polymer backbone rigidity, examples of semi-rigid and rigid polyzwitterions in the literature were reviewed as well as stilbene-containing semi-rigid polymers. Using a deprotection strategy, anionic polyelectrolytes and polyampholytes of stilbene-maleic anhydride copolymers were synthesized and characterized by first synthesizing organic-soluble polymer precursors. Solution shear rheology and statistical segment length measurements reveal that carboxylated polyanions containing stilbene and maleic acid remain semi-rigid in aqueous solutions. It was found that these semi-rigid polyanions exhibited excellent anti-HIV activity possibly due to their more extended polymer chains. This was the first time that intrinsic polymer rigidity was introduced as a possible design parameter for microbicidal applications. Reversible addition fragmentation chain transfer (RAFT) polymerization techniques were used to copolymerize 4-diethylaminostilbene with maleic anhydride. These new semi-rigid copolymers were incorporated into double hydrophilic block copolymers (DHBCS) containing semi-rigid and flexible segments. The subsequent solutions properties of these DHBCs were evaluated with respect to pH and salt responsiveness. Notably, the DHBCs

exhibited a “like-charge” attraction as ionic strength increased which was attributed to the semi-rigid character of the polyampholyte block copolymer.

Acknowledgements

First I would like to thank my advisor Dr. S. Richard Turner for all of his patience, time, effort, mentoring, and guidance throughout my graduate school career. I feel very fortunate to have worked with such a dedicated, enthusiastic, passionate scientist. I would also like to thank my committee members. Dr. Alan Esker, Dr. Richey Davis, and Dr. Tim Long, for always willing to help and guide me in research, class, and career opportunities. A special thanks goes to Dr. Richard Gandour for his patience, guidance, and collaboration.

I'd like to give a special thanks to Dr. Ryan Walczak, Dr. John Reynolds, and Ms. Sherri Vig. All three of you provided me with the tools, knowledge, drive, and passion for chemistry leading up to graduate school and your support was momentous.

I was fortunate to be adopted into a second family while in Virginia. I would like to thank the Hudsons, Beckners, Neighbors, and McCreary's for allowing me to join holiday dinners and for loving me when my biological family was so far away. You will forever be in my heart. I would not have made it through graduate school without Amanda and Kacey as they provided constant support, a home away from home, and put up with my shenanigans. Also, I'd like to thank my best friends Lauren and Charlotte for always making me feel like I was never too far away from home.

Finally, I would like to thank my family for supporting me through my graduate career. I was blessed to have two wonderful parents who made science fun and surrounded me with it everyday. Their constant support, love, and guidance shaped who I am as a person and a scientist. Thank you for always pushing me to be my best and

loving me more than words can describe! To my sisters, Amanda, Amelia, and Abigail, thank you for keeping me sane, grounded, and loved!

Table of Contents

List of Figures

List of Tables

Attribution

Several colleagues and coworkers aided in the writing and research behind several of the chapters of this dissertation. A brief description of their background and their contributions are included here.

Chapter 2: Alice Savage (graduate student, Department of Chemistry, Virginia Tech) provided the primary writing for this chapter. Xu Zhou (Ph.D., Department of Chemistry, Virginia Tech) and Jing Huang (graduate student, Department of Chemistry, Virginia Tech) contributed to the writing of this review chapter. S. Richard Turner (Ph.D., Department of Chemistry, and MII at Virginia Tech) is the advisor and committee chair. Professor Turner provided guidance, writing, and editing of this chapter.

Chapter 3: Yi Li, (Ph.D., Department of Chemistry, Virginia Tech) synthesized the polymers analyzed in this chapter. Alice Savage performed the physical solution characterization of these polyanions as well as writing and editing. Xu Zhou (Ph.D., Department of Chemistry, Virginia Tech) contributed to the titration results of this chapter. S. Richard Turner (Ph.D., Department of Chemistry, and MII at Virginia Tech) provided guidance and writing of this chapter. Professor Richey Davis (Ph.D., Department of Chemical Engineering, Virginia Tech) provided guidance, segment length calculations, and writing of this chapter.

Chapter 4: Alice Savage analyzed microbicide data. Yi Li, (Ph.D., Department of Chemistry, Virginia Tech) synthesized the polymers analyzed in this chapter. Lindsay Matolyak (undergraduate, Indiana University of Pennsylvania) contributed to the

polyanion synthesis. Gustavo Doncel (Ph.D., Eastern Virginia Medical School) preformed the antiviral assays. S. Richard Turner (Ph.D., Department of Chemistry, and MII at Virginia Tech) is the advisor. Professor Richard Gandour (Ph.D., Department of Chemistry, Virginia Tech) provided guidance, data analysis, and liaison with Dr. Doncel.

Chapter 6: Alice Savage synthesized and characterized polymers in this chapter. Elizabeth Ullrich (Virginia Tech), Zachary Kiernan (Virginia Tech), Stacey Chin (Carnegie Mellon), and Caitlyn Kost (Virginia Tech) were all undergraduate researchers that contributed to the synthesis of the polymers discussed in this chapter. S. Richard Turner (Ph.D., Department of Chemistry, and MII at Virginia Tech) is the advisor and provided guidance, data analysis, and writing.

Chapter 1: **Introduction to Rigid and Semi-rigid Polyzwitterions**

1.1 *Introduction*

Rigid polyelectrolytes and polyzwitterions frequently appear in nature, for example proteins[1,2]. The synthesis and properties of both synthetic and naturally occurring rigid polyelectrolytes are well documented and have been heavily investigated [1,3-5] due to their wide variety of applications.[4,6,7] Similarly, investigations into rigid polyzwitterions[8] increased in the recent decades to satisfy the need for synthetic analogs of biological polymers.[9] The synthesis and properties of semi-rigid and rigid polyzwitterions are the focus of this review.

Synthetic or naturally occurring polyelectrolytes and polyzwitterions contain charged functional groups located within the polymer backbone or as pendent functional groups. Polyzwitterions contain both positive (cationic) and negative (anionic) ionizable groups where as polyelectrolytes contain only anionic or cationic groups. Harris et al.[10] first reported the synthesis of a polyzwitterion (polymerized Vitamin B) in 1941. Likewise, Alfrey et al. synthesized the first flexible polyampholyte, based on the copolymerization of 2-vinylpyridine and methacrylic acid in 1950[11], and Mochel et al. reported one of the first synthetic polybetaines in 1956.[12] For this review, polymers with anionic and cationic groups on separate monomers are considered polyampholytes (Figure 1.1.1a)[11,13] while polymers with the anionic and cationic moieties located on the same monomers are considered polybetaines[12,14-16] (Figure 1.1.1b).[17] Herein, we review the synthesis and solution properties of rigid and semi-rigid polyzwitterions (polyampholytes and

polybetaines). We explore the effects of their physical and solution properties like polymer rigidity and ionic strength sensitivities as well as different synthetic strategies to afford the rigid polyzwitterions.

a) Polyampholyte **b) Polybetaine**

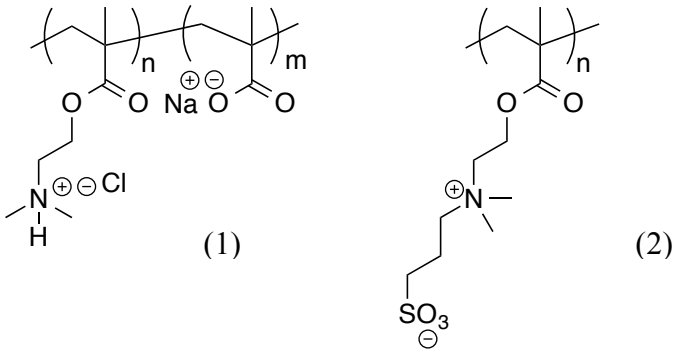

Figure 1.2.1. Structural examples of flexible a) polyampholytes (poly(dimethylaminoethyl methacrylate-*r*-methacrylic acid)[18] and b) polybetaines (poly(N,N′-dimethyl(methacryloylethyl)ammonium propanesulfonate))[19].

1.2 *Polymer Rigidity*

The intrinsic rigidity (stiffness) of a polymer directly influences solid and solution physical properties; yet, to a lesser extent than the side groups of a polymer.[20] The side groups tend to affect solubility, crystallinity, intermolecular interactions, and surface properties; whereas, the skeletal backbone affects strength, flexibility (rigidity), chain length, stability, etc.[20] In the case of polymer flexibility, the type of backbone bonds (C–C, C=C, C–O, C–N, etc.), pendent functional groups, and external factors like solvent, pH, and ionic strength can affect polymer rigidity.[20] Figure 1.2.1 depicts a range of

synthetic and naturally occurring polymers that contain flexible, semi-rigid, and rigid backbones organized by their increasing persistence lengths (defined below).

Numerous examples of polyzwitterions with flexible chains have been reported.[13,17] However, this review is focused on rigid (or semi-rigid) polyzwitterions which posses the combination of rigid polymer backbones with zwitterionic functional groups that promote coulombic inter– and intramolecular interactions. Both intrinsic polymer rigidity and zwitterionic character can contribute to the final physical and solution properties.

Traditionally, polymer rigidity is measured in solution by two physical polymer parameters: persistence length and Kuhn length (also called statistical segment length). The persistence length of a polymer describes the distance along the polymer backbone before the direction changes significantly (l_p).[21] The Kuhn Length (b) is defined as "how far one must travel along a chain until all "memory" of the starting direction is lost" where $b = 2l_p$.[22] Both parameters are used to evaluate the rigidity of a polymer backbone where more rigid polymers contain longer persistence lengths and longer Kuhn lengths. Typically for polymers to be considered a rigid-rod, the Contour length (the maximum end-to-end distance of a polymer chain) of a polymer must equal or approach its persistence length. For flexible polymers, the l_p is << Contour length, and for semi-rigid polymers, the l_p is < Contour length (typically 4 nm (poly(1-phenyl-1-propyne)) < l_p < 8 nm (poly(fluorene))).

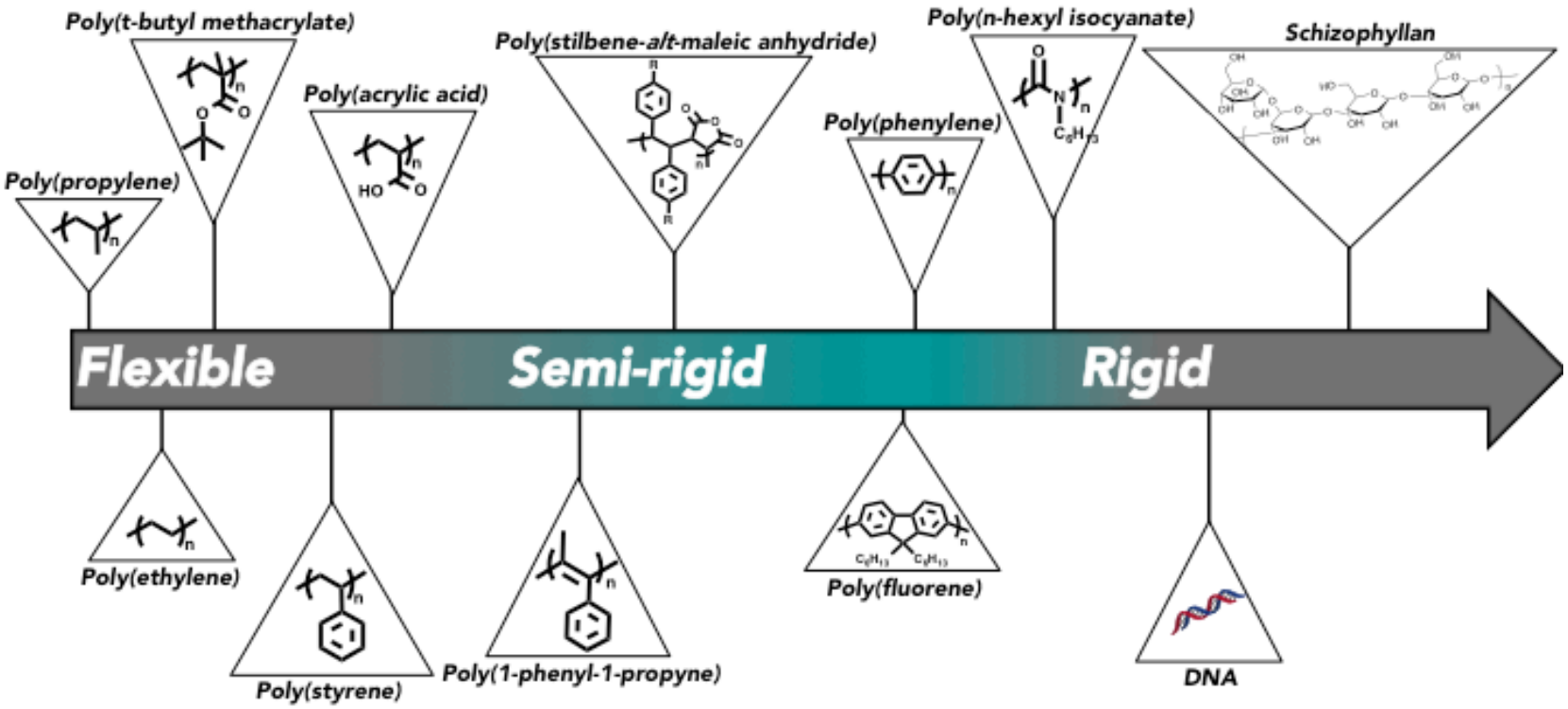
Poly(t-butyl methacrylate)
Poly(propylene)
Poly(acrylic acid)
Poly(stilbene-a/t-maleic anhydride)
Poly(n-hexyl isocyanate)
Poly(phenylene)
Schizophyllan
Flexible
Semi-rigid
Rigid
Poly(ethylene)
Poly(styrene)
Poly(1-phenyl-1-propyne)
Poly(fluorene)
DNA

Figure 1.2.1. A variety of different polymers arranged from left to right in ascending polymer rigidity (persistence lengths). Poly(propylene) (atactic) (0.56 nm)[23] < poly(ethylene) (0.69 nm)[23] < (poly(*t*-butyl methacrylate) (0.80 nm)[24] < poly(styrene) (0.90 nm) [23] < poly(acrylic acid) (in dioxane) (1.4 nm)[25] < poly(1-phenyl-1-propyne) (3.8 nm)[26] < poly(stilbene-*alt*-maleic anhydride) (3–6 nm)[27] < poly(fluorene) (8.0 nm)[28] < poly(phenylene) (12.6 nm)[29,30] < poly(N-hexyl isocyanate) (40 nm)[28,31] < DNA (double stranded) (50 nm)[32] < Schizophyllan (137 nm)[31].

1.3 *Synthesis of Semi-rigid and Rigid Polymers*

Both step-growth (polycondensation) and chain-growth polymerization techniques can afford polymers having more rigid backbones. Conjugated polymers are a significant class of rigid synthetic polymers typically synthesized through cross-coupling techniques like Suzuki-Miyaura[33], Stille,[34] or Mizoroki-Heck[35] polycondensation reactions. Significant effort has been made to synthesize these conjugated polymers with controlled molar mass and narrow dispersity (or narrow PDIs).[37] Recent advances in chain-growth polycondensation reactions controlled the molar mass by using catalysts that transfer intramolecularly.[36,37] Semi-rigid and rigid polymers can be synthesized by traditional chain-growth polymerization reactions with conventional radical and controlled radical polymerizations of sterically crowded monomers.[27,38,39] Decorating these semi-rigid and rigid polymers with ionic pendent groups produces rigid polyzwitterions or polyelectrolytes.

1.4 *Synthesis of Semi-rigid and Rigid Polyzwitterions*

Using an adaptation of the basic polymerization techniques described above for preparing rigid, neutral, organic-soluble polymers, the synthesis of rigid polyzwitterions can be easily achieved through the following three approaches. Non-charged precursor polymers can be converted to charged polymers by two approaches, in addition to preparing polyzwitterions via the direct polymerization of charged monomers.

1) The synthesis of organic-soluble polymer precursors without ionizable functional groups followed by the ionization of the polymer post-polymerization constitutes the first route. For example, the post-polymerization sulfonation of polystyrene provides a pathway to synthesize poly(styrene sulfonate)[40] or the synthesis of a polybetaine post-polymerization.[41]

2) The second method involves the polymerization of monomers with protected functional groups that are deprotected/cleaved after the polymerization reaction.[42,43] Both approaches (1 and 2) allow for the molar mass characterization of the polymer precursors by using traditional polymer characterization techniques like SEC (size exclusion chromatography) in organic solvents. For the second approach, the amount of functional groups and charged residues can be tailored by using different substituted monomers.[44]

3) Finally, the direct polymerization of water-soluble, ionized monomers affords many different polyelectrolytes and polyzwitterions.[45,46] This one-step process bypasses the precursor polymers and the resulting polyelectrolytes can be easily processed in aqueous solvents. Disadvantages arise when characterizing the molar mass of the resulting

polyzwitterions. Due to aggregation and polymer-column interactions, molar mass determination of these charged polymers has proved difficult but not impossible with SEC[47] or AF4 (asymmetric-flow field flow fractionation)[48]. Step-growth and chain-growth techniques mentioned above can easily be adapted to these approaches, which result in a variety of rigid zwitterionic polymers.[49,50]

1.5 *Common Solution Properties of Polyzwitterions*

Due to their ionic nature, polyzwitterions are soluble in aqueous solutions at a variety of pHs, ionic strengths, and temperatures. When measuring the solution properties of polyzwitterions, it is crucial to measure the degree of ionization, or the overall effective charge of the polymers to understand the coulombic inter– and intramolecular interactions. ζ-potential, and potentiometric titrations are often used to measure the overall charge of the polymer in solution at a given pH. Polyzwitterions often display an isoelectric point (IEP, *pI*) where the overall charge of the polymer is electrically neutral at a certain pH.[11] The IEP is intrinsic to each polymer and arises from the pK_a and pK_b of the zwitterionic groups, as well as the ratio of acidic to basic groups. At this point, the polymers are also the least soluble due to their reduced ionic nature and may precipitate from solution depending on the hydrophobicity of the polymer.[51] The IEP can theoretically be calculated by using the following acid-base equilibrium equations (Equations 1.5.1 and 1.5.2) determined by Patrickios[52] and Doty[53] et al. where pK_b = –log K_b, pK_a = –log K_a, and R = the ratio of acidic to basic functional groups. K_b and K_a are the equilibrium dissociation constants for basic and acidic functional groups, respectively.

$$pI = pK_a - \log\left[\left(\frac{R}{2}\right)\left[\frac{-(1-R)}{R} + \sqrt{\left(\frac{1-R}{R}\right)^2 + \left(\frac{4}{R}\right)10^{pK_a - pK_b}}\right]\right] \quad \text{(eq. 1.5.1)}$$

$$pI = pK_b + \log\left[\left(\frac{1}{2}\right)\left[\frac{(1-R)}{R} + \sqrt{\left(\frac{1-R}{R}\right)^2 + \left(\frac{4}{R}\right)10^{pK_a - pK_b}}\right]\right] \quad \text{(eq. 1.5.2)}$$

Typically equation 1.5.1 is used for polyzwitterions with excess basic functional groups (R<1), while equation 1.5.2 is used for polyzwitterions with excess acidic functional groups (R>1). At certain R ratios (R = ½, 1, and 2), equation 1.5.1 simplifies to equations 1.5.3, 1.5.4, and 1.5.5, respectively.

In equation 1, when R = ½, there are twice as many basic functional groups to acidic functional groups and equation 1.5.2 simplifies to the following equation 1.5.3.

$$pI = pK_b \quad \text{(eq. 1.5.3)}$$

When R =1, the amount of acidic functional groups is equal to the basic functional groups and equation 1 simplifies to the following equation 1.5.4.

$$pI = \frac{(pK_a + pK_b)}{2} \quad \text{(eq. 1.5.4)}$$

When R =2, there are twice as many acidic functional groups to basic functional groups and the equation 1.5.2 simplifies to the following equation 1.5.5.

$$pI = pK_a \qquad \text{(eq. 1.5.5)}$$

Ultimately, the IEP serves as a pH reference point for the solution properties of different zwitterions. In polymer solutions above (or below) the IEP pH, the polymers tend to behave as polyelectrolytes with a more negative (or positive) overall net charge. Whereas, polymers near their corresponding IEP demonstrate polyzwitterion character by containing positive and negative residues. This dynamic characteristic of polyzwitterions enables polymers to exhibit both the *polyelectrolyte* effect and *antipolyelectrolyte* effect (described in the next section). This broadens the response to external stimuli which increases the potential of the polyzwitterions for use in multiple applications.[54]

1.6 *Ionic Strength Response: Polyelectrolyte and Antipolyelectrolyte Effects*

It is of fundamental importance to calculate and evaluate the response of polyzwitterions to ionic strength. Because polyzwitterions contain a high concentration of both positive and negative charges, the ionic strength of the solution (the ionic strength of the polymer and of any added salt) can affect polymer solubility, polymer size (polymer chain extension or contraction), aggregation, thermal transitions (upper critical and lower critical solution temperatures), etc. This fundamental knowledge can be important in

biological applications,[55] wastewater treatment systems,[56] or battery systems[57] where the ionic strength varies drastically.

With respect to polymer size, aggregation, and solubility, there remain two typical effects that describe the response of a polyelectrolyte to ionic strength: *polyelectrolyte* and *antipolyelectrolyte* effect. The polyelectrolyte effect describes the decrease in polymer viscosity (or coil size) as the ionic strength increases (Figure 1.6.1a).[58] Conversely, an increase in viscosity (or coil size) upon an increase of ionic strength is the antipolyelectrolyte effect (Figure 1.6.1b).[13,17] Generally, polyelectrolytes containing only cationic or anionic functional groups exhibit the polyelectrolyte effect, independent of pH. This occurs due to a reduction of intramolecular electrostatic (coulombic) *repulsive* forces as the ionic strength increases. This is not the same with polyzwitterions, which are sensitive to pH.

There are certain characteristics or properties that polyzwitterions contain in dilute aqueous solutions that will be frequently discussed in this review.

1) Polyzwitterions can exhibit both the polyelectrolyte and antipolyelectrolyte effects depending on the pH of the system.[13]

2) When the ionic strength increases in a polymer solution near the IEP, polyzwitterions exhibit an antipolyelectrolyte effect with an increase in viscosity due to a reduction of intramolecular electrostatic (coulombic) *attractive* forces or salt screening.[59]

3) When polyzwitterions contain an overall positive or negative charge (pH deviated from that of the IEP), they also tend to exhibit the polyelectrolyte effect.[17]

4) In addition, the viscosity of polyampholytes with imbalanced charges tends to decrease when the ionic strength is first increased due to a reduction of electrostatic repulsive forces.[60-63] However, upon the addition of more salt (higher ionic strength), the viscosity increases.

5) Polybetaines are typically insoluble in salt-free aqueous solutions due to their intrinsically neutral (less ionic) nature. They exhibit a "salting in"[64] effect where upon the addition of a small amount of salt (small increase in ionic strength), the polybetaines dissolve in dilute aqueous solutions and then exhibit an antipolyelectrolyte effect.

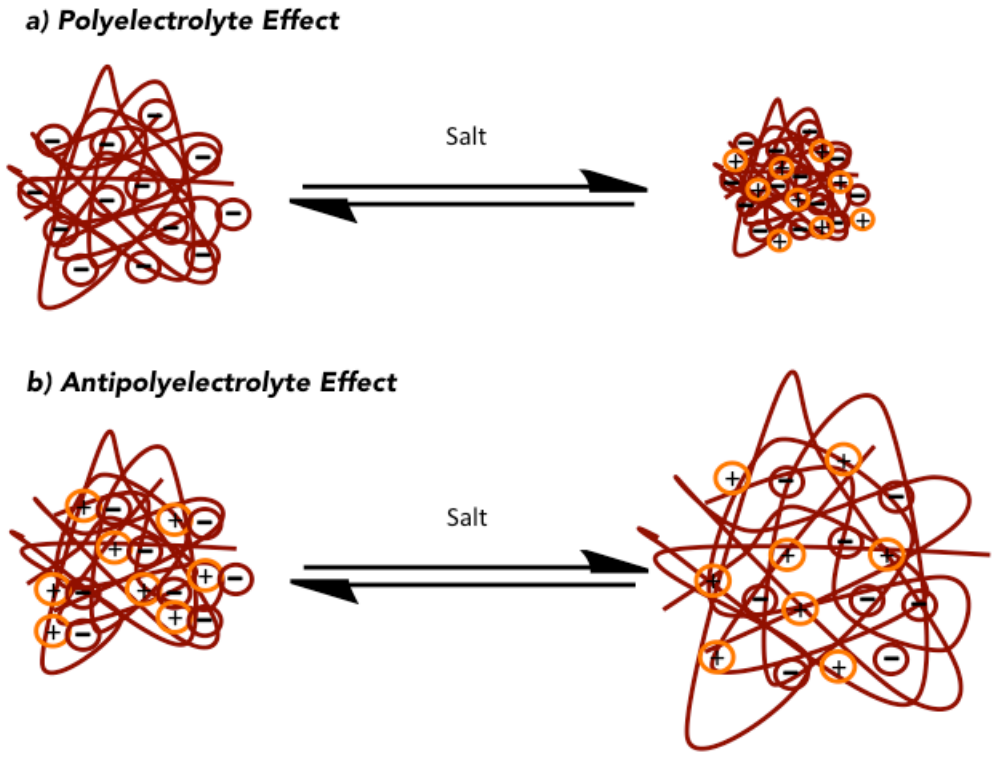

Figure 1.6.1. A schematic representing a) the polyelectrolyte effect[65] and b) the antipolyelectrolyte effect.[13] a) The polyelectrolyte effect: upon the addition of salt, a

polyelectrolyte polymer coil shrinks do to a reduction of coulombic intramolecular repulsive forces. b) The antipolyelectrolyte effect: upon the addition of salt, the polyelectrolyte polymer coil expands due to a reduction of coulombic intramolecular attractive forces.

1.7 *Semi-rigid and Rigid Polyampholytes and Applications*

The first flexible polyampholyte was synthesized by Alfrey et al. [11] in 1950. It was not until 1997 that Tour et al.[66] synthesized one of the first rigid polyampholytes. Rigid polyampholytes, such as proteins and polyamino acids,[1] occur naturally in many biological systems. Synthetic rigid polyampholytes proved difficult to synthesize possibly due to lengthy multi-step monomer synthesis. The following examples of rigid polyampholytes are categorized based on polymer backbone: conjugated polymers, bio-based polymers, cyclolinear polymers, and sterically congested linear polymers.

1.7.1 Rigid Conjugated Polyampholytes

As previously mentioned, rigid conjugated polyampholytes were typically synthesized by using aromatic cross-coupling reactions.[37] This affords many conjugated polymers with a variety of heterocyclic polymer backbones like polythiophene, polypyrrole, poly(fluorene), polysquaraine, etc.

Tour et al.[67] synthesized one of the first rigid polyampholytes with a polythiophene backbone (Figure 1.7.1.1). This polythiophene contained nitro and amino groups on separate monomers polymerized with Stille cross-coupling[68] reactions. Its zwitterionic character was confirmed with an optical spectral shift between the protected neutral precursor and the water-soluble rigid polyampholyte.[67] By extending the π-conjugation with donor and acceptor monomers, the resulting low optical bandgap copolymers were declared to show potential in optoelectronics.

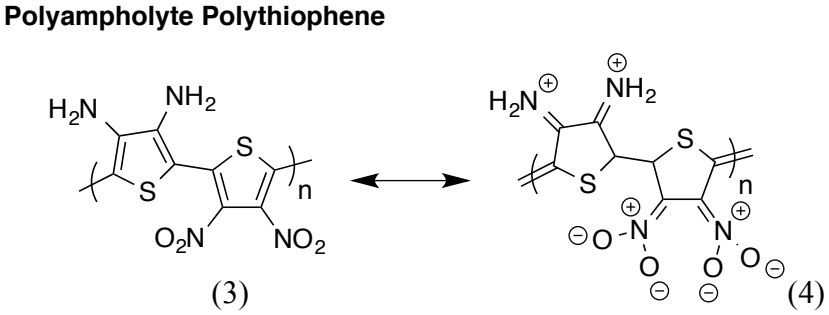

Figure 1.7.1.1. The structure of the rigid polyampholyte with a polythiophene backbone synthesized by Tour et al.[67]

An uncommon conjugated polymer, polysquaraine, has been synthesized by incorporating the organic dye, squaric acid, into a polymer backbone. These polysquaraines gathered considerable interest and attention due to their rigid polyelectrolyte backbone.[5] Eldo et al.[69] and Lu et al.[70] synthesized fully conjugated, polyampholyte polysquaraines via a nonoxidative donor-acceptor polymerization of squaric acid with bispyrroles (Figure 1.7.1.2a)[69] and the polycondensation reaction of

squaric acid and 3-octylpyrrole (Figure 1.7.1.2b)[70], respectively. The positive charges of both polymers remain on the pyrrole moieties while the negative charges remains on the squaric acid repeat unit. The zwitterionic form still appears conjugated with a low optical bandgap and intense near-infrared absorption.[69] These rigid conjugated polyampholytes were processed into thin films on the metal substrates in linear and folded conformations of the polysquaraines. Identified by a shift in absorbance from 544 nm to 514 nm, the folded conformation was promoted by introducing an active metal plate (Ag, Cu, Fe, Zn, Rh, Pt, and Pb) to a solution of the polysquaraine polyzwitterion (6) in Figure 1.7.1.2, which induced this more compact (folded) conformation through intramolecular hydrogen bonding.[70]

a) **Polyampholyte Polysquaraines**

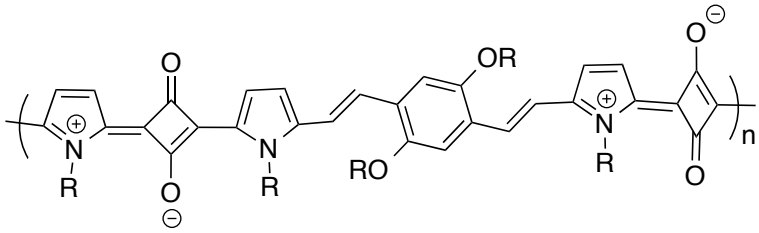

(5)

b) **Polyampholyte Polysquaraines**

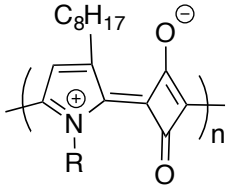

(6)

Figure 1.7.1.2. Examples of rigid polysquaraine in the literature with both positive and negative charges located on separate monomers.[69,70]

1.7.2 Rigid Polyampholytes Synthesized with Biomaterials

In recent years, interest in polymers from monomers from renewable resources has intensified due to the high cost of petroleum and concern about sustainability. As a result, many bio-based polymers were studied as possible replacements for petroleum-based polymers in plastics, elastomers, and in various charged polyelectrolytes and polyampholytes.

A biodegradable rigid polyampholyte (poly(α,β-$_L$-aspartic acid)) was synthesized in 2012 as an anti-biofouling material.[71] $_L$-aspartic acid was polymerized by using a thermal polycondensation reaction to produce a polysuccinimide[72] which was then converted to the polyampholyte by randomly functionalizing succinic acids with $_L$-histidinate and carboxylic acids (Figure 1.7.2.1).[71] The resulting poly(α,β-$_L$-aspartic acid) polyampholyte was pH responsive and tended to precipitate or cloud around its IEP. It showed potential as an anti-biofouling material for biomedical devices due to its biodegradability and zwitterionic character.

Polyampholyte Poly(α, β–$_L$-aspartic acid)

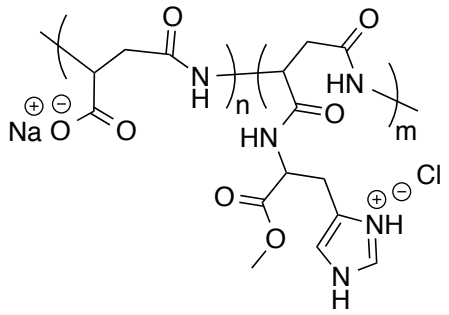

(7)

Figure 1.7.2.1. The structure of the poly(α,β-$_L$-aspartic acid) polyampholyte synthesized by Wang et al. [71]

Recently, Zhou et al.[8] synthesized another rigid polyampholyte by randomly functionalizing cellulose with amino and carboxyl groups. The resulting rigid polyampholyte was pH responsive and salt-resistant. An increased salt-solubility can be critical for many biological applications with high ionic strength, as many polyelectrolytes flocculate upon an increased ionic strength. Zhou et al. reported that these rigid polyampholytes exhibited an antipolyelectrolyte effect[13] where the intrinsic viscosity of the polyampholytes increased as the salt (NaCl) concentration increased, and the viscosity increased as the pH approached the IEP. These characteristics have significant potential for applications in the food, pharmaceutical, and cosmetics industries.[8]

1.7.3 Cyclolinear and Sterically Congested Polyampholytes

Intrinsic polymer rigidity not only increases with the type of backbone bond (C–C, to C=C), but also the steric congestion (crowding) of the enchained pendent groups along

the backbone may cause more extended (or more rigid) polymer chains with limited rotational freedom. Examples of semi-rigid or rigid polyampholytes resulting from highly functionalized or highly congested polymer backbones are given below.

Patrickios et al.[73] synthesized a rigid polyampholyte, cyclolinear, block copolymer by using the RAFT cyclopolymerization of a tertiary-butyl α-(hydroxymethyl)acrylate ether dimer (TBHMA) followed by chain-extension with 2-(dimethylamino)ethyl methacrylate (DMAEMA) and deprotection of the *tert*-butyl groups. Due to the steric hindrance and the enchained ring structure of the cyclolinear ether repeat unit,[74] the resulting polyampholyte block copolymer contains an anionic rigid TBHMA segment and a cationic flexible DMAEMA segment (Figure 1.7.3.1). Researchers measured the pK_as of the acid residues.

Polyampholyte poly(α-(hydroxymethyl)acrylate)

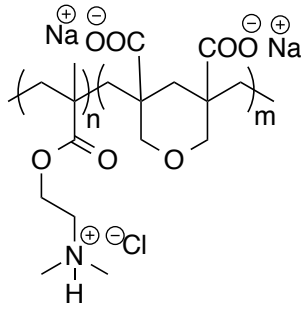

(8)

Figure 1.7.3.1. The structure of the rigid, cyclolinear, block polyampholyte poly(α-(hydroxymethyl)acrylate ether dimer)-*b*-(dimethylamino ethyl methacrylate) synthesized by Patrickios et al.[73]

Recently, our group studied the alternating copolymerizations of a family of 1,2-diphenylethylenes (stilbene) monomers with maleic anhydride and *N*-substituted maleimides.[42-44,75,76] The vicinal phenyl groups in the backbone and the cyclic anhydride units afforded semi-rigid copolymers[27] and semi-rigid polyampholytes (Figure 1.7.3.2).[42,43] Due to limited solubility of the semi-rigid copolymers in salt solutions, block copolymers were synthesized to promote the solubility. The resulting block copolymers exhibited a pH and salt responsiveness attributed to the semi-rigid ampholytic segments.

To synthesize these block copolymers that contain semi-rigid and flexible segments, the semi-rigid segments were chain extended with a non-charged, amphiphilic, acrylamide, homopolymer by using RAFT polymerization techiniques. After deprotection, the resulting block copolymers, which then contained ampholytic semi-rigid segments and amphiphilic flexible segments, formed polyion complexes (PICs) in water, Figure 1.7.3.2 (9).[42,43] These block polyampholytes exhibited an antipolyelectrolyte effect and increased solubility in salt solutions.[42] As the ionic strength increased, the size of the double hydrophilic block copolymers systematically increased which was attributed to the "like-charge" attraction of the semi-rigid chains. This "like-charge" attraction was attributed to Manning's counterion condensation theory[77] and to the counterion mediated attraction of like-charged rods.[78] Accordingly, when the ionic strength is increased by the addition of a low molar mass salt, the counterions can condense along the polymer chains, which induces dipoles along the polymer chains (Figure 1.7.3.3). The more-extended semi-rigid polymer chains aggregated (increased PIC size) due to the electrostatic (coulombic) intermolecular *attractive* forces of induced dipoles as shown in poly((oligo-(ethylene

glycol)methacrylate)-*b*-(N,N,N′,N′-tetraethyl-4,4′-diamino-(*E*)-stilbene-*alt*-maleic anhydride)).[42]

Polyampholyte Poly((diethylaminostilbene-*alt*-maleic acid)-*b*-acryloylmorpholine)

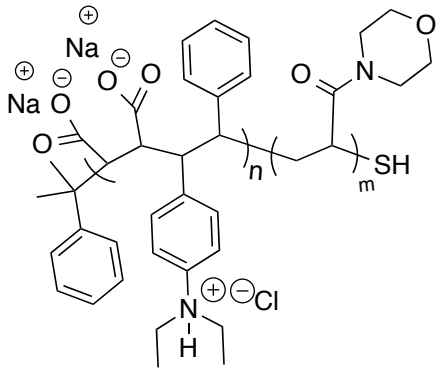

(9)

Figure 1.7.3.2. The structure of the semi-rigid polyampholyte poly(4-diethtylaminostilbene-*alt*-maleic acid)-*b*-acryloylmorpholine.[43]

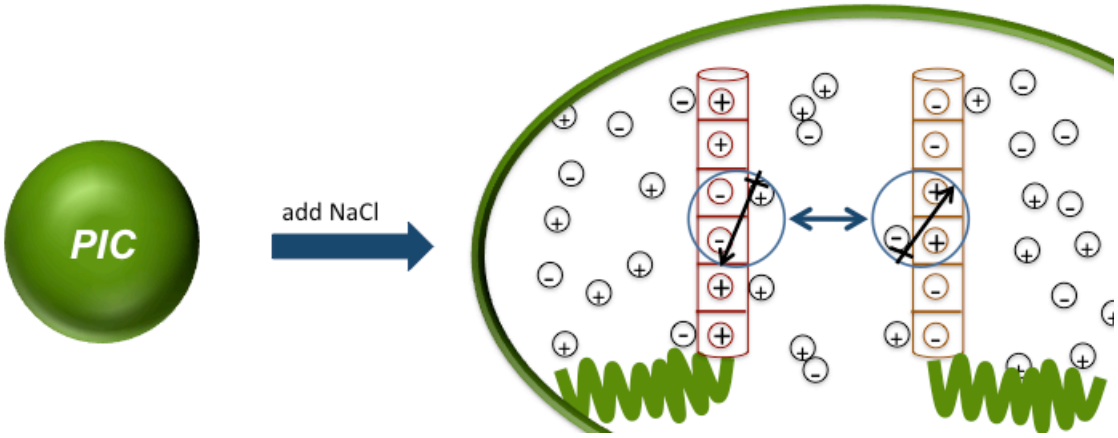

Figure 1.7.3.3. A diagram depicting the condensation of sodium chloride counterions on the backbone of a rigid (or semi-rigid) polyampholyte within a PIC.[77] The induced dipoles increase intermolecular attractions between the polymer chains of the same charge ("like-charge" attraction).

Similarly, polymer rigidity increases by incorporating ringed structures into the polymer backbone. Chen et al.[45,46] synthesized a polyampholyte poly(arylene ether sulfone) based on the polycondensation reaction of sulfonated dichlorodiphenylsulfone and *N*-aminoethyl-3,3-bis(4-hydroxyphenyl)-1-isobenzopyrrolidone ((10), Figure 1.7.3.4). The resulting semi-rigid polyampholyte contained alternating amino and sulfonate groups in a ratio of 1:2. By cross-linking the polyampholyte with *m*-phenylenediamine and trimesoyl chloride in an interfacial polymerization, the semi-rigid polyampholyte was used in thin-film composite membranes for reverse-osmosis water-purification.[79,80] The combination of increased polymer rigidity and zwitterionic functionality resulted in high salt rejection while still maintaining the structural integrity of the membrane. Chen et al.[46] were also able to incorporate these semi-rigid polyampholytes in a multi-layer film by conventional

layer-by-layer assembly. 1-Butyl-3-methylimidazolium chloride ([BMIM]) (a positive, single-charged species) was added after the deposition of the polyampholyte layer to metathesize the inner negatively charged sulfonate groups. This resulted in an overall positive charge ((11), Figure 1.7.3.4) followed by the successful deposition of the anionic layer.[46]

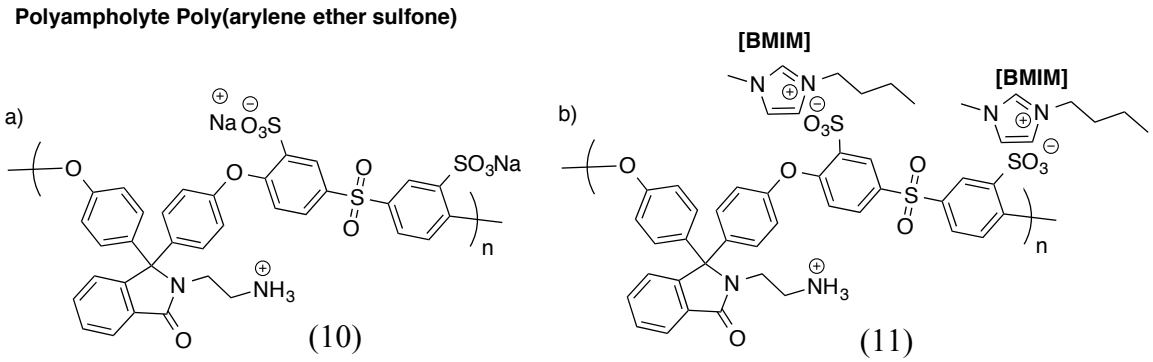

Figure 1.7.3.4. The structure of the rigid, polyampholyte poly(arylene ether sulfone)[45] (a) and the structure of the postive polymer layer that contains "metathesized sulfonate groups"[46] (b) synthesized by Chen et al.

1.8 *Synthesis of Semi-rigid and Rigid Polybetaines and Applications*

Mochel et al.[12] functionalized polyvinyl acetals with betaine functional groups in 1956 to report one of the first flexible polybetaines. While it wasn't until 1989 that the first rigid polybetaine was reported by Terbojevich et al. (described in Section 1.8.2).[81] Semi-rigid and rigid polybetaines are more prevalent in the literature than rigid polyampholytes possibly due to the need for only one monomer that contains the zwitterionic functionality. Particularly in the conjugated polymer field, multi-step synthesis is required for many aromatic monomers. Synthesizing one monomer with both cationic

and anionic functionality (polybetaines) requires less time and money than synthesizing two monomers with different functionalities. However, examples of flexible polybetaines greatly outnumber their rigid counterparts. Examples of rigid polybetaines based on conjugated rigid heterocyclic polymers, bio-based polymers, cyclolinear polymers, and sterically congested linear polymers are described below.

1.8.1 Rigid Conjugated Polybetaines

Chan et al.[82] synthesized one of the first rigid, conjugated polybetaines by polycondensation reactions of *o*-aminobenzylphosphonic acid in acid medium (Figure 1.8.1.1). The resulting fully-conjugated polyaniline contained both positive (amino) and negative (phosphonic acid) functional groups on the same monomer which was water-soluble in its conjugated, doped form. These rigid polybetaines were potentially advantageous in applications like antistatic agents and biosensors due to their water-processability of the polybetaines in the self-doped conducting form.[82] The water-processability, enhances environmentally friendly processing, broadens application windows, and decreases cost.

Polybetaine poly(*o*-aminobenzylphosphonic acid)

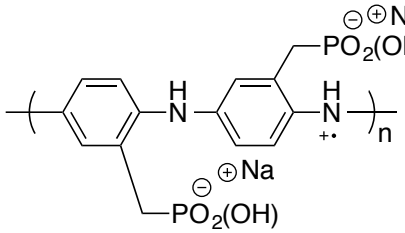

(12)

Figure 1.8.1.1. The conjugated, rigid, polybetaine poly(*o*-aminobenzylphosphonic acid) synthesized by Chan et al. [82]

Other conjugated rigid polybetaines were synthesized by polymerizing a thiophene monomer with a chiral amino acid functionalized side-chain (Figure 1.8.1.2)[83-85] or a betaine (a neutral molecule containing both positive and negative functional groups).[86-88] The pH responsive rigid polybetaine containing a chiral amino acid functionalized side-chain demonstrated different optical transitions when interacting with synthetic peptides.[84,85] The zwitterionic character of the polybetaines allowed for these polymers to complex to both cationic and anionic polypeptides, and the different optical transitions of the polythiophene backbone were monitored after complexation.[84] The polythiophene with a betaine side-chain was polymerized using an air-stable Suzuki-coupling polymerization in ionic liquids and used as cathode modification layers in solar cells.[88] This rigid polybetaine exhibited the "salting-in" and antipolyelectrolyte effect in NaBr solutions.[86,87] The electrostatic intermolecular attractive forces of the polybetaines were exploited by attaching peptides or surfaces, and the optical transitions of the rigid polymer backbone were monitored. The recognition properties of these polybetaines remain highly desirable.

Polybetaine poly(thiophene)

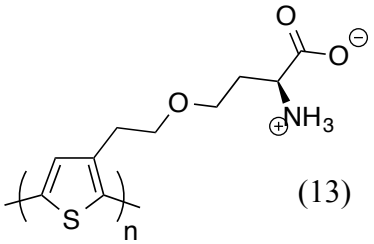

(13)

Figure 1.8.1.2. A structural example of a polythiophene containing a betaine pendent group.[84,85]

Poly(fluorene)s are another class of conjugated polymers, and interest in poly(fluorene) copolymers with betaine pendent functional groups has recently increased.[41,89-93] Functionalization at the 9-position of 2,7-dibromo-fluorene resulted in a betaine-containing monomer (Figure 1.8.1.3). Derivatives of this betaine monomer were copolymerized with other aromatic monomers (1,4-bis(4,4,5,5-tetramethyl-1,3,2-dioxaborolan-2-yl)benzene,[92] 2,7-bis-(1,3,2-dioxaborolan-2-yl)-9,9-dioctylfluorene,[41] 2,7-dibromo-9,9-bis[3′-(N,N-dimethylamino)propyl]fluorene, [89] and 4,7-dibromo-2,1,3-benzothiazole).[90] The resulting rigid polybetaines were used for many different property studies or potential applications, where the coulombic interactions of the pendent groups and physical and optical properties of the rigid backbone were exploited simultaneously. For example, Xu et. al. [92] used a polybetaine poly(fluorene) as a sensor for sugar detection. Fang et al.[41] and Duan et al.[89,90] used a polybetaine poly(fluorene) copolymer as efficient electron injection layers in polymer light-emitting diodes. Elmalem et al.[91] used a polybetaine poly(fluorene phenylene) as a single component, mechanically strong hydrogel. Again, these rigid polybetaines exhibited a "salting in" effect and were pH responsive.

Polybetaine poly(fluorene)

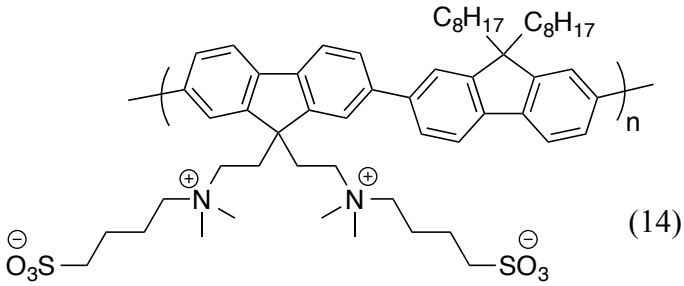

(14)

Figure 1.8.1.3. The structure of a rigid poly(fluorene) containing a betaine pendent group.[41]

1.8.2 Rigid Polybetaines Synthesized with Biomaterials

Early reports of rigid polybetaines, like those made by Terbojevich, relied on the modification of bio-based polymers such as chitosan.[81] The functionalized-chitosan polybetaines exhibited more salt resistance (antipolyelectrolyte effect) than the fully cationic chitosan that remained very insoluble in salt solutions and exhibited a polyelectrolyte effect. More recently, Elschner et al.[94] synthesized a cellulose-based polybetaine with amino and carboxyl pendent groups. The resulting polybetaines were pH responsive at physiologically relevant pHs with possible use in drug delivery applications.[94]

1.8.3 Cyclolinear and Sterically Congested Polybetaines

As previously mentioned, the steric congestions of pendent groups along a polymer backbone typically increase polymer rigidity. Enchained bulky groups like ring structures can increase polymer rigidity.[27] Bieglé et al.[95,96] synthesized semi-rigid polybetaines consisting of isocyanide polymer backbones and betaine pendent groups. Poly(isocyanide)s typically result from acid-catalyzed, chain-growth polymerization techniques[97] and contain one pendent group per backbone carbon. The steric crowding of the pendent groups affords the semi-rigid polymer backbone, and the zwitterionic character arises from the derivatization of the pendent groups.[98,99] Poly(isocyanides) tend to develop hierarchal structures, such as helices and to exhibit lyoptropic behavior when in concentrated solutions.[96] Two types of polybetaines were synthesized (amino with a sulfonate or dicyanoethenoloate) and showed unique thermal and salt responses. The

poly(isocyanide) with an amino–sulfonate betaine groups ((15), Figure 1.8.3.1a) exhibits both an UCST (upper-critical solution temperature), while the poly(isocyanide) with an amino–dicyanoethenolate betaine exhibited a LCST (lower-critical solution temperature) ((16), Figure 1.8.3.1b). Each phase transition temperature was dependent upon the type and concentration of salt added. Also, both semi-rigid betaines exhibited a "salting-in"[13,17,61] effect and after further increasing the ionic strength, proceeded to exhibit an antipolyelectrolyte effect.

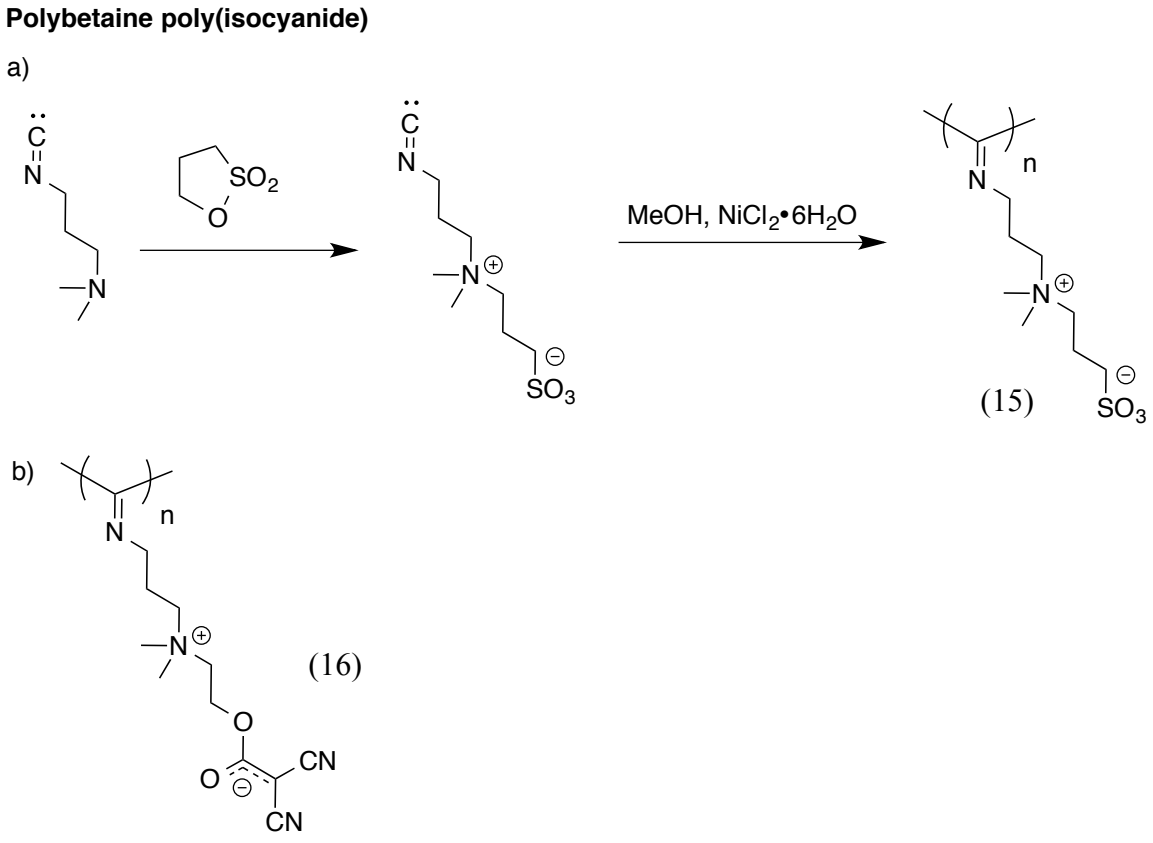

Figure 1.8.3.1. The synthetic scheme for poly(isocyanides) containing betaine pendent groups (a)[95,96] and a poly(isocyanide) with an amino–dicyanoethenolate betaine (b).

Like polyampholytes, polybetaines were synthesized by the cyclopolymerization of allyic monomers to produce semi-rigid, cyclolinear polybetaines. Favresse[100] et al., Al-Hamouz[101] et al., and Avci[102] et al. synthesized cyclolinear polybetaines with the radical polymerization of *N,N*-diallyl-*N*-pentyl-ammonioacetate monomers (Figure 1.8.3.2). While still maintaining their semi-rigid character, these semi-rigid polybetaines exhibited the "salting-in" effect followed by the anti-polyelectrolyte effect. These cyclolinear polybetaines formed homogeneous blends with inorganic salts and produced organic-inorganic hybrid materials.[100]

Polybetaine poly(*N,N*-diallyl-*N*-pentyl-ammonioacetate)

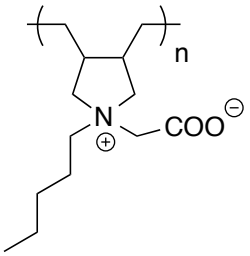

(17)

Figure 1.8.3.2. The structure of the cyclolinear, semi-rigid, poly(*N,N*-dialkyl-*N*-2-(alkoxycarbonyl)allyl allyl) polybetaine synthesized by Favresse et al. [100]

As mentioned in the Section 1.7.3, poly(styrene-*alt*-maleic anhydride) copolymers appeared semi-rigid. [27] Semi-rigid polybetaines consisting of functionalized poly(styrene-*alt*-maleic anhydride) copolymers were synthesized by using conventional radical polymerization followed by the post-polymerization functionalization of the anhydride

units.[103] The semi-rigid polybetaines (Figure 1.8.3.3) showed the same "salting-in" effect, followed by an antipolyelectrolyte effect[13] and were used to reveal the effects of different counterions upon the solution properties of these polybetaines.

Polybetaine poly(styrene-*alt*-(*N,N*-dimethyl maleamidic acid) propyl ammonium propane sulfonate)

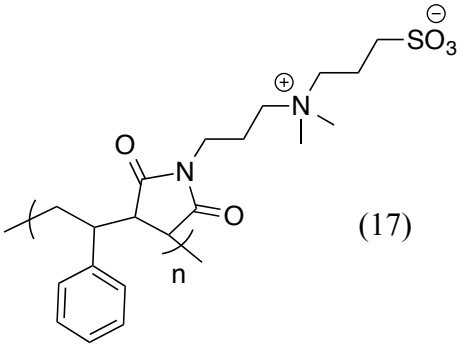

(17)

Figure 1.8.3.3. The structure of the semi-rigid poly(styrene-*alt*-maleimide) containing a betaine pendent group synthesized by Lee et al. [103]

1.9 *Conclusions*

This review highlights the synthesis, solution properties, and applications of semi-rigid and rigid polyzwitterions. This includes synthetic protocols of semi-rigid and rigid polyampholytes and polybetaines that combine the zwitterionic character of pendent groups with a more rigid polymer backbone. At present, there are few examples of block copolymers containing statistical rigid polyampholytes or polybetaines. The paucity of examples may result from the difficult and lengthy multi-step synthesis of monomers and polymers (i.e. post-polymerization functionalization). Combining modern different

polymerization techniques, such as polycondensation and controlled radical polymerizations, would result in controlled block polyzwitterions.

1.10 *References*

(1) Conway, B. E.; Butler, J. A. V. Effect of salts on the interaction of nucleic acid particles, *J. Polym. Sci.* **1954**, *12*, 199–208.

(2) Fuoss, R. M.; Cathers, G. I. Polyelectrolytes. I. Picrates of 4-vinylpyridine-styrene copolymers, *J. Polym. Sci.* **1947**, *2*, 12–15.

(3) Fujita, H. Counterion distribution in dilute solutions of rigid spherical macromolecular ions in the absence of added salt, *J. Chem. Phys.* **1955**, *23*, 837–846.

(4) Holm, C.; Rehahn, M.; Oppermann, W.; Ballauff, M. Stiff-chain polyelectrolytes, *Adv. Polym. Sci.* **2004**, *166*, 1–27.

(5) Duarte, A.; Pu, K. Y.; Liu, B.; Bazan, G. C. Recent advances in conjugated polyelectrolytes for emerging optoelectronic applications, *Chem. Mater.* **2011**, *23*, 501–515.

(6) Cabane, E.; Zhang, X. Y.; Langowska, K.; Palivan, C. G.; Meier, W. Stimuli-responsive polymers and their applications in nanomedicine, *Biointerphases* **2012**, *7*, 1–27.

(7) Singh, P. K.; Singh, V. K.; Singh, M. Zwitterionic polyelectrolytes: A review, *E-Polymers* **2007**, 1618–7229.

(8) You, J.; Hu, H. Z.; Zhou, J. P. Synthesis, structure and solution properties of the novel polyampholytes based on cellulose, *Cellulose* **2013**, *20*, 1175–1185.

(9) Palermo, E. F.; Vemparala, S.; Kuroda, K. In *Tailored Polymer Architectures for Pharmaceutical and Biomedical Applications*, **2013**; Vol. 1135, pp 319–330.

(10) Harris, S. A. Chemistry of vitamin B6. IV. Reactions in solutions at elevated temperatures, *J. Am. Chem. Soc.* **1941**, *63*, 3363–3367.

(11) Alfrey, T.; Morawetz, H.; Fitzgerald, E. B.; Fuoss, R. M. Synthetic electrical analog of proteins *J. Am. Chem. Soc.* **1950**, *72*, 1864–1864.

(12) Mochel, W. E.; Weaver, C. Silver halide emulsions of poly(vinyl acetal) polymers; US Patent 2,753,264, July 3, 1956.

(13) Dobrynin, A. V.; Colby, R. H.; Rubinstein, M. Polyampholytes, *J. Polym. Sci. Pol. Phys.* **2004**, *42*, 3513–3538.

(14) Ladenheim, H.; Morawetz, H. A new type of polyampholyte: poly(4-vinylpyridine betaine), *J. Polym. Sci.* **1957**, *26*, 251–254.

(15) Schuster, C.; Gehm, R. Poly(vinyl betaines); DE Patent 1009809, June 6, 1957.

(16) Hart, R.; Timmerman, D. New polyampholytes: poly(sulfo betaines), *J. Polym. Sci.* **1958**, *28*, 638–640.

(17) Lowe, A. B.; McCormick, C. L. Synthesis and solution properties of zwitterionic polymers, *Chem. Rev.* **2002**, *102*, 4177–4189.

(18) Mori, H.; Müller, A. H. E. New polymeric architectures with (meth)acrylic acid segments, *Prog. Polym. Sci.* **2003**, *28*, 1403–1439.

(19) Willcock, H.; Lu, A.; Hansell, C. F.; Chapman, E.; Collins, I. R.; O'Reilly, R. K. One-pot synthesis of responsive sulfobetaine nanoparticles by RAFT polymerisation: the effect of branching on the UCST cloud point, *Polym. Chem.* **2014**, *5*, 1023–1030.

(20) a) Milstien, J. B.; Charney, E. The rigidity of polymer molecules in solution. Electric dichroism of poly(butyl isocyanates), *Macromolecules* **1969**, *2*, 678–679. b) Allcock, H. R.; Lampe, F. W. In *Contemporary Polymer Chemistry*; Prentice-Hall, Inc: Englewood Cliffs, New Jersey, **1990**; 2nd Ed.; pp 536–542.

(21) Erman, B.; Flory, P. J.; Hummel, J. P. Moments of the end-to-end vectors for p-phenylene polyamides and polyesters, *Macromolecules* **1980**, *13*, 484–491.

(22) Sperling, L. H. In *Introduction to Physical Polymer Science*; John Wiley & Sons Inc: Hoboken, New Jersey, **2006**, pp 213.

(23) Fetters, L.; Lohse, D.; Colby, R. Physical Properties of Polymers Handbook; Mark, J. E., Ed.; Springer: New York, 2007, p 447.

(24) Muroga, Y.; Sakuragi, I.; Noda, I.; Nagasawa, M. Effect of β-substitution on chain flexibility, *Macromolecules* **1984**, *17*, 1844–1847.

(25) Taylor, T. J.; Stivala, S. S. Small-angle X-ray scattering of poly(acrylic acid) in solution, *Polymer* **1996**, *37*, 715–719.

(26) Hirao, T.; Teramoto, A.; Sato, T.; Norisuye, T.; Masuda, T.; Higashimura, T. Stiff-chain nature of poly(1-phenyl-1-propyne) in dilute solution, *Polym. J.* **1991**, *23*, 925–932.

(27) Li, Y.; Zhang, M.; Mao, M.; Turner, S. R.; Moore, R. B.; Mourey, T. H.; Slater, L. A.; Hauenstein, J. R. Chain stiffness of stilbene containing alternating copolymers by SAXS and SEC, *Macromolecules* **2012**, *45*, 1595–1601.

(28) Mourey, T.; Le, K.; Bryan, T.; Zheng, S.; Bennett, G. Determining persistence length by size-exclusion chromatography, *Polymer* **2005**, *46*, 9033–9042.

(29) Guilleaume, B.; Blaul, J.; Ballauff, M.; Wittemann, M.; Rehahn, M.; Goerigk, G. The distribution of counterions around synthetic rod-like polyelectrolytes in solution, *Eur. Phys. J. E: Soft Matter Biol. Phys.* **2002**, *8*, 299–309.

(30) Vanhee, S.; Rulkens, R.; Lehmann, U.; Rosenauer, C.; Schulze, M.; Köhler, W.; Wegner, G. Synthesis and characterization of rigid rod poly(p-phenylenes), *Macromolecules* **1996**, *29*, 5136–5142.

(31) Bohdanecky, M. New method for estimating the parameters of the wormlike chain model from the intrinsic viscosity of stiff-chain polymers, *Macromolecules* **1983**, *16*, 1483–1492.

(32) Wang, L.; Bloomfield, V. A. Small-angle x-ray scattering of semidilute rodlike DNA solutions: polyelectrolyte behavior, *Macromolecules* **1991**, *24*, 5791–5795.

(33) Suzuki, A. Recent advances in the cross-coupling reactions of organoboron derivatives with organic electrophiles, 1995–1998, *J. Organomet. Chem.* **1999**, *576*, 147–168.

(34) Bao, Z.; Chan, W.; Yu, L. Synthesis of conjugated polymer by the Stille Coupling Reaction, *Chem. Mater.* **1993**, *5*, 2–3.

(35) Sato, T.; Takata, T. Synthesis and Characterization of Poly[3]rotaxane through the Mizoroki-Heck Coupling Polymerization of Divinyl-functionalized [3]Rotaxane, *Polym. J* **2009**, *41*, 470–476.

(36) Zhang, Q. T.; Tour, J. M. Low optical bandgap polythiophenes by an alternating donor/acceptor repeat unit strategy, *J. Am. Chem. Soc.* **1997**, *119*, 5065–5066.

(37) Yokoyama, A.; Suzuki, H.; Kubota, Y.; Ohuchi, K.; Higashimura, H.; Yokozawa, T. Chain-growth polymerization for the synthesis of polyfluorene via Suzuki−Miyaura coupling reaction from an externally added initiator unit, *J. Am. Chem. Soc.* **2007**, *129*, 7236–7237.

(38) Ebdon, J. R.; Hunt, B. J.; Hussein, S.; Radical copolymerization of maleic anhydride with *trans*-stilbene, *Brit. Polym. J.* **1987**, *19*, 333–337.

(39) Masuda, T.; Takahashi, T.; Higashimura, T. Polymerization of 1-phenyl-1-alkynes by halides of niobium and tantalum, *Macromolecules* **1985**, *18*, 311–317.

(40) Biswas, M.; Chatterjee, S. Chemical modification of polystyrene. II. A cation exchange resin from polystyrene electrophilically substituted with pyromellitic dianhydride, *J. Appl. Polym. Sci.* **1982**, *27*, 4645–4653.

(41) Fang, J. F.; Wallikewitz, B. H.; Gao, F.; Tu, G. L.; Muller, C.; Pace, G.; Friend, R. H.; Huck, W. T. S. Conjugated zwitterionic polyelectrolyte as the charge injection layer for high-performance polymer light-emitting diodes, *J. Am. Chem. Soc.* **2011**, *133*, 683–685.

(42) Mao, M.; Turner, S. R. Aggregation of rod-coil block copolymers containing rigid polyampholyte blocks in aqueous solution, *J. Am. Chem. Soc.* **2007**, *129*, 3832–3833.

(43) Savage, A. M.; Ullrich, E.; Chin, M. S.; Kiernan, Z.; Kost, C.; Turner, S. R. Synthesis and characterization of double hydrophilic block copolymers containing semi-rigid and flexible segments, *J. Polym. Sci. Pol. Chem.* **2014**.

(44) Li, Y.; Mao, M.; Matolyak, L. E.; Turner, S. R. Sterically crowded anionic polyelectrolytes with tunable charge densities based on stilbene-containing copolymers, *ACS Macro Lett.* **2012**, *1*, 257–260.

(45) Chen, G.; Li, S. H.; Zhang, X. S.; Zhang, S. B. Novel thin-film composite membranes with improved water flux from sulfonated cardo poly(arylene ether sulfone) bearing pendant amino groups, *J. Membr. Sci.* **2008**, *310*, 102–109.

(46) Chen, G.; Wu, G. J.; Wang, L. M.; Zhang, S. B.; Su, Z. H. Layer-by-layer assembly of single-charged ions with a rigid polyampholyte, *Chem. Commun.* **2008**, 1741–1743.

(47) Bruessau, R. J. Size exclusion chromatography of polyelectrolytes with aqueous elution solvents, *Makromol. Chem-M Symp.* **1992**, *61*, 199–218.

(48) Wahlund, K. G.; Litzen, A. Application of an asymmetrical flow field-flow fractionation channel to the separation and characterization of proteins, plasmids,

plasmid fragments, polysaccharides and unicellular algae, *J. Chromatogr.* **1989**, *461*, 73-87.

(49) Yamamoto, T.; Kimura, T.; Komura, M.; Suzuki, Y.; Iyoda, T.; Asaoka, S.; Nakanishi, H. Block copolymer permeable membrane with visualized high-density straight channels of poly(ethylene oxide), *Adv. Funct. Mater.* **2011**, *21*, 918–926.

(50) Osada, Y.; Katsumura, E.; Inoue, K. Photomechanochemical energy conversion in a polyamide containing a stilbene structure in the backbone, *Makromol. Chem., Rapid Commun.* **1981**, *2*, 411–415.

(51) Bekturov, E.; Bimendina, L. Interpolymer complexes In *Speciality Polymers*; Advances in Polymer Science, Springer Berlin Heidelberg: 1981; Vol. 41, p 99–147.

(52) Patrickios, C. S. Polypeptide amino-acid-composition and iosoelectric point. 1. A closed-form approximation, *J. Colloid Interface Sci.* **1995**, *175*, 256–260.

(53) Ehrlich, G.; Doty, P. Macro-ions. III. The solution behavior of a polymeric ampholyte., *J. Am. Chem. Soc.* **1954**, *76*, 3764–3777.

(54) Ali, S. A.; Haladu, S. A. A novel cross-linked polyzwitterion/anion having pH-responsive carboxylate and sulfonate groups for the removal of Sr2+ from aqueous solution at low concentrations, *React. Funct. Polym.* **2013**, *73*, 796–804.

(55) Owen, D. H.; Katz, D. F. A vaginal fluid simulant, *Contraception* **1999**, *59*, 91–95.

(56) Goldblatt, M. Wastewater treatment, *Chem. Eng. Prog.* **2008**, *104*, 35–36.

(57) Rong, J.; Ge, M.; Fang, X.; Zhou, C. Solution ionic strength engineering as a generic strategy to coat graphene oxide (GO) on various functional particles and its application in high-performance lithium–sulfur (Li–S) batteries, *Nano Letters* **2013**, *14*, 473–479.

(58) Beer, M.; Schmidt, M.; Muthukumar, M. The electrostatic expansion of linear polyelectrolytes: Effects of gegenions, co-ions, and hydrophobicity, *Macromolecules* **1997**, *30*, 8375–8385.

(59) McCormick, C. L.; Johnson, C. B. Water-soluble copolymers. 29. Ampholytic copolymers of sodium 2-acrylamido-2-methylpropanesulfonate with (2-acrylamido-2-methylpropyl)dimethylammonium chloride: solution properties, *Macromolecules* **1988**, *21*, 694–699.

(60) Lee, W. F.; Chen, C. F. Poly(2-hydroxyethyl methacrylate-co-sulfobetaine)s hydrogels: 3. Synthesis and swelling behaviors of the [2-hydroxyethyl methacrylate-co-N,N'-dimethyl (acrylamido propyl) ammonium propane sulfonate] hydrogels, *Polymer Gels and Networks* **1998**, *6*, 493–511.

(61) McCormick, C. L.; Johnson, C. B. Water-soluble polymers. 33. ampholytic terpolymers of sodium 2-acrylamido-2-methylpropanesulfonate with 2-acrylamido-2 methylpropanedimethylammonium chloride and acrylamide - synthesis and aqueous-solution behavior, *Polymer* **1990**, *31*, 1100–1107.

(62) McCormick, C. L.; Salazar, L. C. Water-soluble copolymers. 44. Ampholytic terpolymers of acrylamide with sodium 2-acrylamido-2-methylpropanesulfonate and 2-acrylamido-2-methylpropanetrimethylammonium chloride, *Polymer* **1992**, *33*, 4384–4387.

(63) Wielema, T. A.; Engberts, J. B. F. N. Zwitterionic polymers 4. pyrene as a photophysical probe for coulombic interactions in poly(vinylsulphobetaines), *Eur. Polym. J.* **1990**, *26*, 1065–1070.

(64) Wielema, T. A.; Engberts, J. B. F. N. Zwitterionic polymers 3. salt effects on the solubility of poly(vinyl sulfobetaines) and poly(vinyl betaines) in aqueous-solution, *Eur. Polym. J.* **1990**, *26*, 639–642.

(65) Fernandes, A. L. P.; Martins, R. R.; da Trindade Neto, C. G.; Pereira, M. R.; Fonseca, J. L. C. Characterization of polyelectrolyte effect in poly(acrylic acid) solutions, *J. Appl. Polym. Sci.* **2003**, *89*, 191–196.

(66) Florjanczyk, Z.; Bzducha, W.; Wieczorek, W.; Zygadlo-Monikowska, E.; Krawiec, W. l.; Chung, S. H. Highly conducting lithium polyelectrolytes based on maleic anhydride-styrene copolymers, *J. Phys. Chem. B* **1998**, *102*, 8409–8416.

(67) Zhang, Q. T.; Tour, J. M. Low optical bandgap polythiophenes by an alternating donor/acceptor repeat unit strategy, *J. Am. Chem. Soc.* **1997**, *119*, 5065–5066.

(68) Ciferri, A.; Kudaibergenov, S. Natural and synthetic polyampholytes. 1. Theory and basic structures, *Macromol. Rapid Commun.* **2007**, *28*, 1953–1968.

(69) Eldo, J.; Ajayaghosh, A. New low band gap polymers: Control of optical and electronic properties in near infrared absorbing pi-conjugated polysquaraines, *Chem. Mater.* **2002**, *14*, 410–418.

(70) Lu, H.-C.; Lin, M.-Y.; Chou, S.-L.; Peng, Y.-C.; Lo, J.-I.; Shiu, H. W.; Chen, C.-H.; Cheng, B.-M. Linear and folded films of a zwitterionic polysquaraine, *RSC Advances* **2013**, *3*, 21294–21297.

(71) Wang, X. J.; Wu, G. L.; Lu, C. C.; Wang, Y. N.; Fan, Y. G.; Gao, H.; Ma, J. B. Synthesis of a novel zwitterionic biodegradable poly (α,β-L-aspartic acid) derivative with some L-histidine side-residues and its resistance to non-specific protein adsorption, *Colloids and Surfaces B-Biointerfaces* **2011**, *86*, 237–241.

(72) Wang, Y.; Wang, Y.; Wu, G.; Fan, Y.; Ma, J. pH-responsive self-assembly and conformational transition of partially propyl-esterified poly(α,β-l-aspartic acid) as amphiphilic biodegradable polyanion, *Colloids and Surfaces B-Biointerfaces* **2009**, *68*, 13–19.

(73) Rikkou-Kalourkoti, M.; Kassi, E.; Patrickios, C. S. Synthesis and characterization of rigid functional anionic polyelectrolytes: Block copolymers and star homopolymers, *J. Polym. Sci. Pol. Chem.* **2012**, *50*, 665–674.

(74) Mathias, L. J.; Kusefoglu, S. H.; Ingram, J. E. Cyclopolymerization of the ether of methyl α-(hydroxymethyl)acrylate, *Macromolecules* **1988**, *21*, 545–546.

(75) Mao, M.; Kim, C.; Wi, S.; Turner, S. R. Chain structure of substituted stilbene-maleic anhydride alternating copolymer probed by solid-state NMR, *Macromolecules* **2008**, *41*, 387–389.

(76) Mao, M.; Turner, S. R. Synthesis and characterization of highly functionalized polymers based on N,N,N',N'-tetraalkyl-4,4'-diaminostilbene and maleic anhydride, *Polymer* **2006**, *47*, 8101–8105.

(77) Manning, G. S. Limiting laws and counterion condensation in polyelectroyte solutions. I. Colligative properties, *J. Chem. Phys.* **1969**, *51*, 924–933.

(78) Ha, B. Y.; Liu, A. J. Counterion-mediated attraction between two like-charged rods, *Phys. Rev. Lett.* **1997**, *79*, 1289–1292.

(79) Cadotte, J. E. Reverse osmosis membrane; U.S. Patent 4,039,440 A, Aug 2, 1977.

(80) Petersen, R. J. Composite reverse osmosis and nanofiltration membranes, *J. Membr. Sci.* **1993**, *83*, 81–150.

(81) Terbojevich, M.; Carraro, C.; Cosani, A.; Focher, B.; Naggi, A. M.; Torri, G. Solution studies of chitosan 6-O-sulfate, *Makromol. Chem.* **1989**, *190*, 2847–2855.

(82) Chan, H. S. O.; Ho, P. K. H.; Ng, S. C.; Tan, B. T. G.; Tan, K. L. A new water-soluble, self-doping conducting polyaniline from poly(O-aminobenzylphosphonic acid) and its sodium-salts - synthesis and characterization, *J. Am. Chem. Soc.* **1995**, *117*, 8517–8523.

(83) Andersson, M.; Ekeblad, P. O.; Hjertberg, T.; Wennerstroem, O.; Inganaes, O. Polythiophene with a free amino acid side chain, *Polym. Commun.* **1991**, *32*, 546–548.

(84) Nilsson, K. P. R.; Rydberg, J.; Baltzer, L.; Inganas, O. Self-assembly of synthetic peptides control conformation and optical properties of a zwitterionic polythiophene derivative, *P Natl Acad Sci USA* **2003**, *100*, 10170–10174.

(85) Bjork, P.; Nilsson, K. P. R.; Lenner, L.; Kagedal, B.; Persson, B.; Inganas, O.; Jonasson, J. Conjugated polythiophene probes target lysosome-related acidic vacuoles in cultured primary cells, *Mol. Cell. Probe.* **2007**, *21*, 329–337.

(86) Page, Z. A.; Duzhko, V. V.; Emrick, T. Conjugated thiophene-containing polymer zwitterions: Direct synthesis and thin film electronic properties, *Macromolecules* **2013**, *46*, 344–351.

(87) Page, Z. A.; Liu, F.; Russell, T. P.; Emrick, T. Rapid, facile synthesis of conjugated polymer zwitterions in ionic liquids, *Chem. Sci.* **2014**, *5*, 2368–2373.

(88) Liu, F.; Page, Z. A.; Duzhko, V. V.; Russell, T. P.; Emrick, T. Conjugated polymeric zwitterions as efficient interlayers in organic solar cells, *Adv. Mater.* **2013**, *25*, 6868–6873.

(89) Duan, C. H.; Wang, L.; Zhang, K.; Guan, X.; Huang, F. Conjugated zwitterionic polyelectrolytes and their neutral precursor as electron injection layer for high-performance polymer light-emitting diodes, *Adv. Mater.* **2011**, *23*, 1665–1669.

(90) Duan, C. H.; Zhang, K.; Guan, X.; Zhong, C. M.; Xie, H. M.; Huang, F.; Chen, J. W.; Peng, J. B.; Cao, Y. Conjugated zwitterionic polyelectrolyte-based interface modification materials for high performance polymer optoelectronic devices, *Chem. Sci.* **2013**, *4*, 1298–1307.

(91) Elmalem, E.; Biedermann, F.; Scherer Maik, R. J.; Koutsioubas, A.; Toprakcioglu, C.; Biffi, G.; Huck Wilhelm, T. S. Mechanically strong, fluorescent hydrogels from zwitterionic, fully π-conjugated polymers, *Chem. Commun.* **2014**, 1–4.

(92) Xu, Q. L.; An, L. L.; Yu, M. H.; Wang, S. Design and synthesis of a new conjugated polyelectrolyte as a reversible pH sensor, *Macromol. Rapid Commun.* **2008**, *29*, 390–395.

(93) Kumar, A.; Pace, G.; Bakulin, A. A.; Fang, J. F.; Ho, P. K. H.; Huck, W. T. S.; Friend, R. H.; Greenham, N. C. Donor-acceptor interface modification by zwitterionic conjugated polyelectrolytes in polymer photovoltaics, *Energy & Environmental Science* **2013**, *6*, 1589–1596.

(94) Elschner, T.; Heinze, T. A promising cellulose-based polyzwitterion with pH-sensitive charges, *Beilstein J. Org. Chem* **2014**, *10*, 1549–1556.

(95) Biegle, A.; Mathis, A.; Galin, J. C. Towards highly functionalized and semi-rigid polyzwitterions, 1-Poly(dizwitterionic methacrylates): synthesis and specific properties, *Macromol. Chem. Physic.* **1999**, *200*, 1393–1406.

(96) Biegle, A.; Mathis, A.; Galin, J. C. Towards highly functionalized and semi-rigid polyzwitterions. 2. Poly(zwitterionic isocyanides): synthesis and specific properties, *Macromol. Chem. Physic.* **2000**, *201*, 113–125.

(97) Millich, F. Polymerization of isocyanides, *Chem. Rev.* **1972**, *72*, 101–113.

(98) van der Eijk, J. M.; Nolte, R. J. M.; Drenth, W. Polyisocyanides 5. Synthesis and polymerization of carbylhistidine and carbylhistamine, *Recueil des Travaux Chimiques des Pays-Bas* **1978**, *97*, 46–49.

(99) van der Eijk, J. M.; Nolte, R. J. M.; Drenth, W.; Hezemans, A. M. F. Optically active polyampholytes derived from L- and D-carbylanayl-L-histidine, *Macromolecules* **1980**, *13*, 1391–1397.

(100) Favresse, P.; Laschewsky, A. Synthesis and investigation of new amphiphilic poly(carbobetaine)s made from diallylammonium monomers, *Polymer* **2001**, *42*, 2755–2766.

(101) Al-Hamouz, O. C. S.; Ali, S. A. pH-responsive polyphosphonates using butler's cyclopolymerization, *J. Polym. Sci. Pol. Chem.* **2012**, *50*, 3580–3591.

(102) Avci, D.; Lemopulo, K.; Mathias, L. J. Cyclocopolymerization of allyl-acrylate quaternary ammonium salts with diallyldimethylammonium chloride, *J. Polym. Sci. Pol. Chem.* **2001**, *39*, 640–649.

(103) Lee, W. F.; Chen, Y. M. Poly(sulfobetaine)s and corresponding cationic polymers. X. Viscous properties of zwitterionic poly(sulfobetaine) derived from styrene-(N,N-dimethylaminopropyI maleamidic acid) copolymer in aqueous salt solutions, *J. Appl. Polym. Sci.* **2004**, *91*, 726–734.

Chapter 2: **A Review of Semi-rigid, Stilbene-containing Alternating Copolymers**

2.1 *Authors*

Alice M. Savage,[†] Xu Zhou,[†] Jing Huang,[†] and S. R. Turner[†]

[†]Department of Chemistry MC0212 and Macromolecules and Interfaces Institute MC0344, Virginia Tech, Blacksburg, Virginia 24061, United States

2.2 *Abstract*

The synthesis and properties of alternating, sterically congested, stilbene-containing alternating copolymers is reviewed. Persistence lengths (2-6 nm) determined by size exclusion chromatography (SEC) and small angle x-ray scattering (SAXS) techniques show that these are semi-rigid copolymers. Fully characterized polyanions and polyampholytes, prepared from organic-soluble precursors were studied, along with their respective salt and pH response behavior resulting from the semi-rigid polymer backbone. The solid state characterization from these studies reveals a high degree of hindered rotation along the polymer backbone. The contorted structure and the hindered rotation of the polymer backbone generate inefficient chain packing, which leads to an increase of nanoporosity and higher surface areas. The semi-rigid stilbene-containing copolymers are

a new class of copolymers where the increased polymer backbone rigidity leads to a wide range of polymer properties not attained with flexible polymers.

2.3 *Keywords*

stilbene, alternating copolymers, copolymerization, maleic anhydride, maleimides

2.4 *Introduction*

Substituted stilbenes (1, 2-diphenylethylenes) are widely studied and used organic compounds for the optical properties arising from their conjugated ethylene structure, e.g. optical brighteners, dyes, etc..[7,8] The many applications of stilbene derivatives have resulted in a large library of substituted stilbene small molecules and facile synthetic techniques to enable synthesis of a variety of derivatives many of which can serve as copolymerizable monomers. However, the addition polymerization and copolymerization of this family of 1,2-disubstituted olefins, like all 1,2-substituted ethylene structures, is difficult due to the steric constraints of the 1,2-structure. Homopolymerization of stilbene and substituted stilbenes to the corresponding poly (benzyl) backbone has not been achieved; however alternating copolymerization of stilbene both anionically [10] and radically [11] is well documented. In alternating copolymerizations, the cross-propagation step is greatly favored since the steric interactions in the cross propagation step are depressed compared to those required for a successful self-propagation of the stilbene monomers. In addition the electronic effects resulting from electron rich and electron poor comonomers cross-propagating with an electron rich or electron poor terminal radical favor fast cross-propagation. Stilbene copolymers have been claimed in the

patent literature to be useful in lubricants,[12] lubricating oil additives,[13,14] thermal stability additives for photoresists, [15] and improved stain resistant polyamide textiles, [16] although successful commercialization of these potential applications is not known.

The radical alternating copolymerization of unsubstituted stilbene is the most studied stilbene polymerization.[17-19] It was found in 1930 that stilbene copolymerized with maleic anhydride.[11] Since neither monomer can undergo radical homopolymerization, these are strictly alternating copolymers with no stilbene-stilbene or maleic anhydride-maleic anhydride dyads present.[20] This study attracted many groups to study the comonomer reactivity ratios,[20] monomer sequences,[18] thermal stability,[21] and copolymerization mechanism.[22-24] However, surprisingly limited solubilities and uninteresting brittle materials have slowed detailed investigations of the copolymerizations and the properties of the resulting copolymers.[25]

N-substituted maleimides readily radically polymerize with stilbene into predominately alternating copolymer structures—maleimides can radically homopolymerize so some maleimide-maleimide dyads can be present in these copolymers.[19,26,27] Many of these copolymers have limited solubilities in common organic solvents so solution studies are limited.

Our recent work involves the design and synthesis of new stilbene comonomers with specifically chosen functional groups for effecting the copolymerization with maleic

anhydride or N-substituted maleimides. Radical polymerization processes are compatible with many functional groups [28] and the alternating nature of the copolymerization enables precise placement of functionality into the copolymer backbones for study of the structure/property relationships of these novel sterically congested backbone polymers in both solution and the solid state.

2.5 *Monomer Substituent Effect on Copolymerization*

The type and position of substituents on the aromatic groups of stilbene were found to have a significant effect on both the overall copolymerization rates as well as the solubility of the copolymers.[5] Several methyl-substituted stilbene monomers were prepared by using the Wittig-Horner reaction and the resulting monomers were copolymerized with maleic anhydride. Feed ratio/composition studies and ^{13}C NMR confirmed the strictly alternating sequences in the backbone.[5] The methyl-substitution increased the solubility of the copolymers in organic solvents by disrupting copolymer aggregation. This allowed for thorough characterization of these copolymers via SEC, NMR and DLS (dynamic light scattering). We note that with unsubstituted stilbene and maleic anhydride copolymers, strong aggregation in DLS was observed which likely accounts for the "insolubility" of these copolymers as reported in the literature. The location of the methyl groups on the phenyl rings was found to have a strong influence on the overall rate of copolymerization. Methyl groups in the para position led to increase copolymerization rates due to the inductively electron donating characteristics which lead to a more reactive stilbene radical to cross propagate with the electron deficient double bond of maleic anhydride. The ortho methyl stilbene monomers (Figure 2.5.1a) were

found to copolymerize at significantly slower rates due to the loss of conjugation of the aromatic groups with the radical due to steric interactions of the methyl groups forcing the phenyl groups out-of-plane. DLS measurements showed that the para-substituted stilbene copolymers formed higher molecular mass aggregates in solution, where little aggregation was observed in the ortho substituted samples.[5]

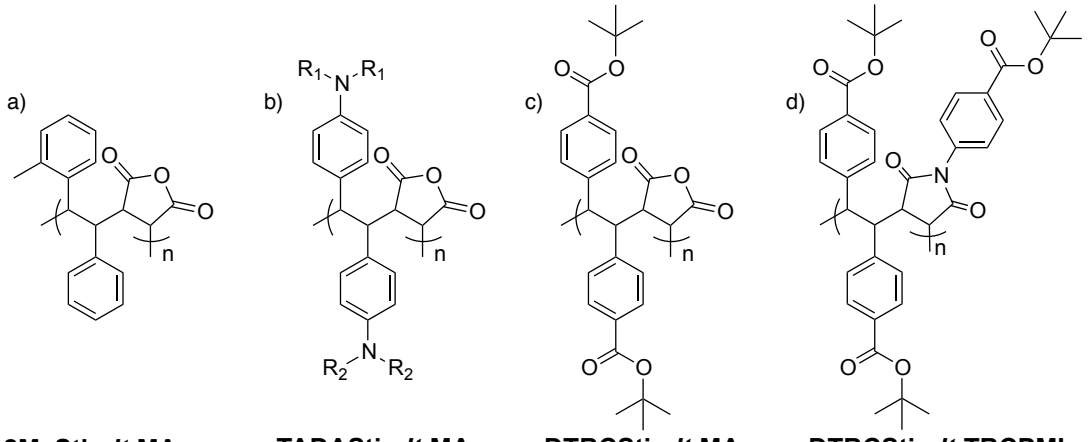

Figure 2.5.1 Structures of organic-soluble, main-chain stilbene-containing copolymer precursors. a) poly((*E)*-2-methylstilbene-*alt*-maleic anhydride) (2MeSti-*alt*-MAn) [5], b) poly(N,N,N′,N′-tetraalkyl-4,4′-diaminostilbene-*alt*-maleic anhydride) (TADASti-*alt*-MAn)[6], c) poly((*E*)-di-*tert*-butyl-4,4′-stilbenedicarboxylate-*alt*-maleic anhydride) (DTBCSti-*alt*-MAn) [9], and d) poly((*E*)-di-*tert*-butyl-4,4′-stilbenedicarboxylate-*alt*-*tert*-butyl 4-maleimidobenzoate) (DTBCSti-*alt*-TBCPMI) [9].

Strong electron donating groups, such as dialkyl amino substituents in the para position of stilbene showed extremely high copolymerization rates (Figure 2.5.1b).[6] Unsymmetrical alkyl substituents on the stilbene comonomers were employed to obtain soluble copolymers. For all of the stilbene copolymers thermal analyses by DSC showed no observable T_g at temperatures less than 250 °C.[6]

With the goal of synthesizing a family of precisely functionalized polyanions, both styrene and stilbene monomers were synthesized with *tert*-butyl ester groups in the para positions.[9] Higher temperatures were required to obtain efficient copolymerizations because of the electron withdrawing nature of the para ester groups. The use of the *tert*-butyl ester copolymers (Figure 2.5.1c-d), as precursors to the polyanions, enabled the accurate determination of the molar mass and molar mass distributions by SEC avoiding the known SEC analysis problems of polyelectrolytes. The *tert*-butyl ester groups were found to cleanly thermally decompose as determined by the expected weight loss for extrusion of isobutylene in thermal gravimetric analyses.[9] For study of the polyanions, deprotection with trifluoroacetic acid followed by neutralization with base and dialysis yielded the pure, well-characterized polyanions. The solution properties of the precursor *tert*-butyl ester copolymers and the polyanions were studied in detail.[2]

2.6 *Polymer Rigidity*

The early investigation of main-chain stilbene copolymers suggested that they possessed characteristics consistent with rigid rod like structures. This lead to further investigation into the chain stiffness of the copolymer backbone.[1,6,29] When examining the ^{1}H NMR spectra of any of these copolymers, the backbone and aromatic peaks appeared very broad.[5] When associated with rigid polymers and high molecular mass materials, broad peaks develop due to strong homonuclear dipolar couplings and slow ^{1}H relaxation rates.[30] With no observed T_g below 250 °C, evidence of hindered rotation and limited movement of the polymer backbone pointed to a more rigid polymer backbone with a sterically-crowded configuration. In the case of poly (N,N,N′,N′-tetraethyl-4,4′-

diaminostilbene-*alt*-maleic anhydride) (TEDASti-*alt*-MAn), the copolymer backbone likely conformed into a contorted, sterically-crowded conformation with the maleic anhydride units existing predominately in the cis configuration.[29]

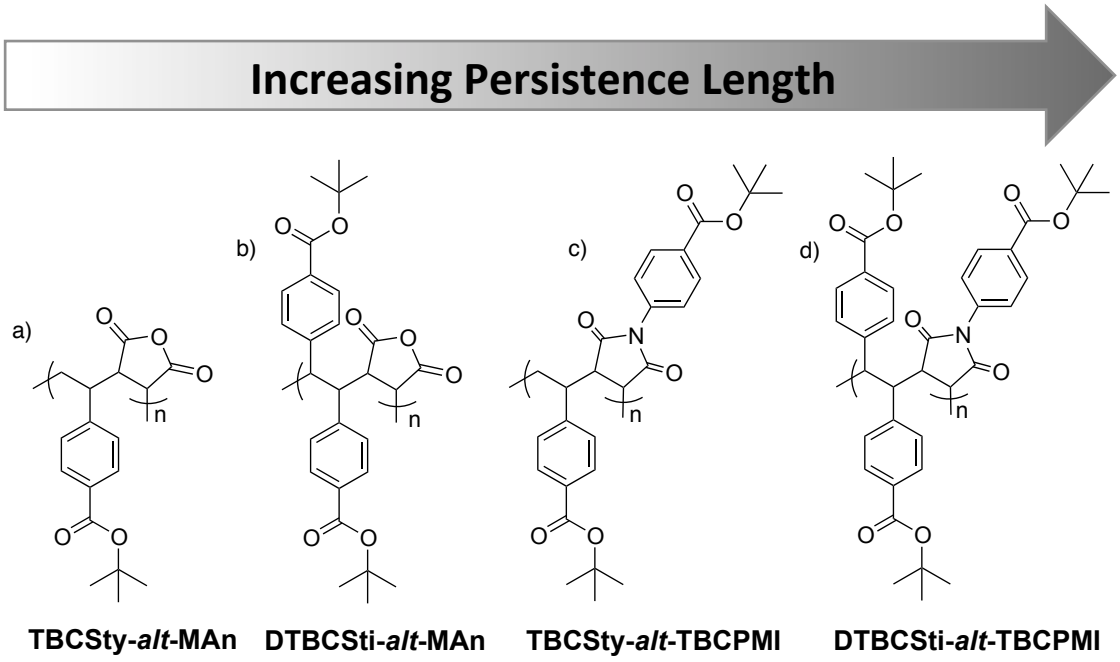

Figure 2.6.1 A series of *tert*-butyl protected stilbene and styrene containing alternating copolymer precursors in order of increasing rigidity (increases left to right). a) poly((*tert*-butyl 4-vinyl benzoate-*alt*-maleic anhydride) (CSty-*alt*-MAn), b) poly((*E*)-di-*tert*-butyl 4,4′-stilbenedicarboxylate-*alt*-maleic anhydride) (DTBCSti-*alt*-MAn), c) poly(*tert*-butyl 4-vinyl benzoate-*alt*-*tert*-butyl 4-maleimidobenzoate) (CSty-*alt*-TBCPMI) and d) poly((*E*)-di-*tert*-butyl 4,4′-stilbenedicarboxylate-*alt*-*tert*-butyl 4-maleimidobenzoate) (DTBCSti-*alt*-TBCPMI) [3].

To confirm the rigidity or chain stiffness of the stilbene alternating copolymers, SEC and SAXS were use to directly measure the chain stiffness (persistence length, l_p).[3] Defined as a measure of chain stiffness or rigidity, persistence lengths provides a direct

comparison of intrinsic polymer chain stiffness with other flexible and rigid polymers. **(***E*)-di-*tert*-butyl 4,4′-stilbenedicarboxylate and the styrene analog (*tert*-butyl 4-vinyl benzoate**)** were copolymerized with MAn and *tert*-butyl 4-maleimidobenzoate, respectively. This copolymer series was studied to investigate the effects of the added extra phenyl ring of stilbene monomer and cyclic monomer structure (MAn versus maleimide) on the persistence lengths.[3,9] Based on SEC and SAXS methods,[31-34] this copolymers series exhibited the persistence lengths between 2–6 nm (Figure 2.6.1). From this direct comparison and measurement, stilbene-alternating copolymers are classified as semi-rigid polymers. For example, a typical flexible copolymer, polystyrene, exhibits a persistence length of 0.9 nm [35] and a rigid copolymer, polyphenylene with sulfonate ester side groups, exhibits a persistence length of 13 nm.[36,37] Accordingly, the stilbene-containing copolymers appear 20% more rigid than the styrene analogs and the maleimide-containing copolymers appear 50% more rigid than MAn-containing copolymers of the same comonomer. The polymer physical properties that arise from these semi-rigid and sterically-crowded copolymers involve unique solution and solid-state properties.

2.7 *Solution Properties*

Using the same deprotection strategy above, a family of polyanion and polyampholyte copolymers were prepared with stilbene comonomers and the solution properties arising from the semi-rigid copolymer backbone were studied.[1,2,9]

2.7.1 Polyanions

As mentioned above, carboxylated polyanions [3,9] were synthesized from the deprotection

of the precursor copolymers, and fully characterized with respect to molar mass, composition, and intrinsic polymer rigidity. Further physical aqueous solution properties evaluated by using steady-state solution shear rheology, dynamic light scattering (DLS), and titration studies proved critical to understanding effects of polymer rigidity and conformation in aqueous solutions.[2]

Using steady-state solution shear rheology, reduced viscosity plotted against polymer concentration revealed a prominent polyelectrolyte effect in deionized water for DCSti-*alt*-MA, CSty-*alt*-MA, and Sti-*alt*-MA shown in Figure 2.7.1.1.[2] Increasing the sodium chloride (NaCl) concentration suppressed the polyelectrolyte effect by decreasing the Debye Length and electrostatic repulsions as the polymer concentration decreased. These results were consistent with semi-rigid polymers.

The statistical segment length (L_k) for each copolymer with or without NaCl was measured by adding the intrinsic statistical segment length (L_0) to the electrostatic statistical segment length (L_{ke}).[38-40] In deionized water, the carboxylated copolymers behaved like rigid-rods due to strong electrostatic repulsions and the statistical segment lengths decreased as NaCl concentration increased. Thus, the polyanions behaved like semi-rigid copolymers in NaCl solutions and followed the same rigidity trends established for the intrinsic statistical segments lengths above.[3]

To further characterize the polymer properties in aqueous solutions, pH titration were used to evaluate the dissociation behavior of the polyanions. Titration results revealed

multiple inflection points arising from the two vicinal carboxylic acid groups. Due to the close proximity of the diacids, each carboxylic acid has a distinct pKa and dissociates at different pH. This is consistent with poly(styrene-*alt*-maleic acid) (Sty-*alt*-MA) titration results.[41]

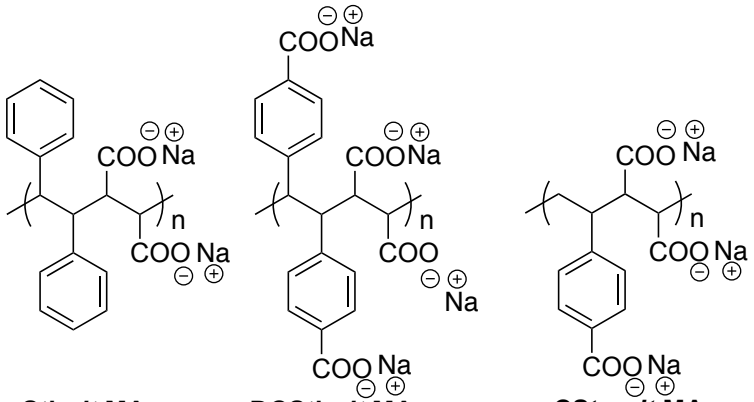

Figure 2.7.1.1 Structures of carboxylated stilbene-containing polyanions: poly(stilbene-*alt*-maleic acid) (Sti-*alt*-MA), poly((4,4′-stilbenedicarboxylate)-*alt*-maleic acid) (DCSti-*alt*-MA), and poly((4-vinyl benzoic acid)-*alt*-maleic acid) (CSty-*alt*-MA) [2].

2.7.2 Polyampholytes

The first stilbene-containing polyampholyte diblock copolymers were prepared using RAFT (reversible addition fragmentation chain transfer) polymerization techniques.[1] The diblock copolymer, poly(OEGMA-*b*-(TADASti-*alt*-MAn)), consisted of a polymerized methoxy-capped oligo-(ethylene glycol)methacrylate) (OEGMA) block chain extended with N,N,N′,N′-tetraethyl-4,4′-diaminostilbene and MAn.[1] After molar mass determination in organic solvent, the block copolymer converted to its subsequent polyampholyte (Figure 2.7.2.1) via simple acid hydrolysis. The resulting water-soluble polyampholyte ((OEGMA-*b*-(TADASti-*alt*-MA))) formed polyion complexes (PICs) and

exhibited a pH and salt responsiveness atypical of polyampholytes.

To evaluate the PIC aggregate response to pH and salt concentration, DLS was used to monitor the aggregate size. The aggregate size increased as the pH approached the isoelectric point (IEP) of the polyampholyte. For more flexible and non-flexible polyampholytes, as the pH neared the IEP, the copolymer chains expand as the electrostatic attractive forces decrease.[42,43] Atypical for polyampholytes, adding NaCl to the ((OEGMA-*b*-(TADASti-*alt*-MA))) copolymer solution increased the PIC size even as the electrostatic repulsions decrease. The "like-charge" attraction of the polymer chains causes polymer chains to aggregate and increase PIC size.[44-46] The semi-rigid polymer backbone of the TADASti-*alt*-MA block facilitated dipole-dipole interactions of condensed counter-ions and induced the "like-charge" attraction.[44,46] Ongoing work involves investigating the effects of charge density, molar mass, and linear, water-soluble homopolymers blocks.[47]

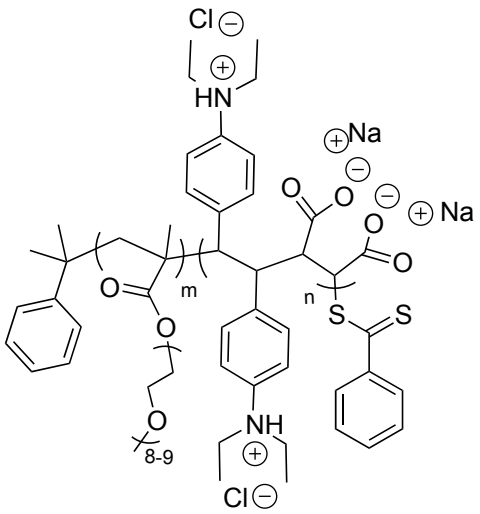

OEGMA-b-(TEDASti-*alt*-MA)

Figure 2.7.2.1 Polyampholyte structure of poly(oligo-(ethylene glycol)methacrylate)-*b*-((N,N,N′,N′-tetraethyl-4,4′-diaminostilbene)-*alt*-maleic acid)) ((OEGMA-*b*-(TADASti-*alt*-MA))) [1]

2.7.3 Solid-State Properties

Forming brittle films when cast from solution, the semi-rigid copolymers offer unique solid-state properties like birefringence and nanoporosity as a result of the sterically-crowded copolymer backbones. Hindered rotations and inefficient chain packing of the copolymer backbone significantly affects and enhances the solid-state properties.

A series of methyl-substituted maleimide copolymers with stilbene and styrene analogs films exhibited large negative birefringence up to 0.02 for Sti-*alt*-2MePMI (Figure 2.7.3.1).[4] During casting of the film, the ortho-methyl forced the phenyl groups to align normal to the imide plane. Due to the anisotropy of the benzene ring, the alignment of the

phenyl rings, and the restricted rotation induced a negative birefringence.[48] The same effect did not appear in Sti-*alt*-NPMI (Figure 2.7.3.1b)) without the ortho-methyl substituent; thus, the phenyl rings freely rotated. The less sterically-crowded Sty-*alt*-2MePMI (Figure 2.7.3.1 a)) showed a low negative birefringence of 0.002 which indicated the sterically crowded polymer backbone influences the free rotation of the phenyl rings.

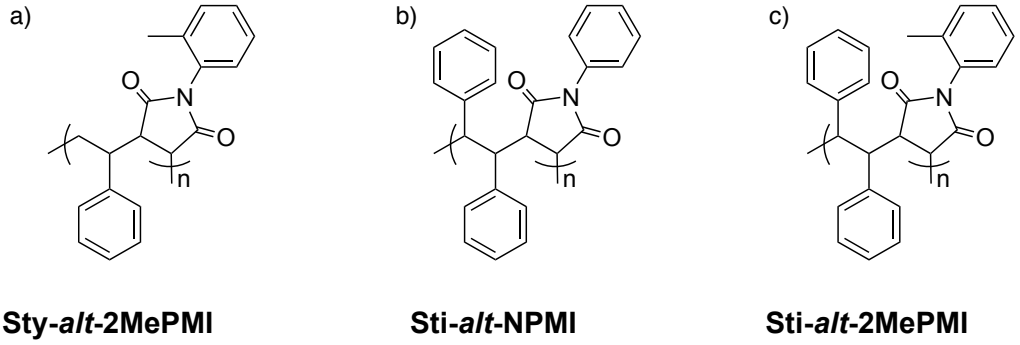

Figure 2.7.3.1 Structures of maleimide copolymers with stilbene and styrene analogs. a) poly(styrene-*alt*-N-(2-methylphenyl) maleimide) (Sty-*alt*-2MePMI); b) poly(stilbene-*alt*-N-phenyl maleimide) (Sti-*alt*-NPMI); c) poly(stilbene-*alt*-N-(2-methylphenyl) maleimide) (Sti-*alt*-2MePMI) [4].

The nanoporous characteristics of the same series of *tert*-butyl carboxylate functionalized alternating copolymers using nitrogen adsorption/desorption isotherms and atomistic molecular simulations were studied (Figure 2.6.1).[49] These alternating copolymers showed a nanoporosity with Brunauer-Emmett-Teller (BET) surface area of 20-40 m^2/g. This is likely due to the insufficient chain packing of these semi-rigid polymer chains and

the increase in the internal free volume leads to an increased surface area. Also, as the chain rigidity increased, then the BET surface areas increased for this copolymer series.[49]

2.8 *Conclusions*

This review highlights the synthesis and properties of sterically crowded stilbene-containing copolymers. The alternating copolymerization gives precise control over monomer sequence, which affords precise placement of functional groups along the polymer backbone. With precise control over monomer sequence, stilbene-containing alternating copolymers afford semi-rigid copolymers. Both the solution and solid-state properties confirm the semi-rigid nature of the backbone. Continued research on stilbene-containing copolymers and block copolymers is focused on new polymeric derivatives to explore the wide range of solid state and solution properties that result from the semi-rigid backbone characteristics.

2.9 *References*

(1) Mao, M.; Turner, S. R. Aggregation of rod-coil block copolymers containing rigid polyampholyte blocks in aqueous solution, *J. Am. Chem. Soc.* **2007**, *129*, 3832–3833.

(2) Li, Y.; Savage, A. M.; Zhou, X.; Richard Turner, S.; Davis, R. M. Solution properties of stilbene-containing sterically crowded alternating polyanions, *J. Polym. Sci. Poly. Phys.* **2013**, *51*, 1565–1570.

(3) Li, Y.; Zhang, M.; Mao, M.; Turner, S. R.; Moore, R. B.; Mourey, T. H.; Slater, L. A.; Hauenstein, J. R. Chain stiffness of stilbene containing alternating copolymers by SAXS and SEC, *Macromolecules* **2012**, *45*, 1595–1601.

(4) Mao, M.; England, J.; Turner, S. R. Alternating stilbene copolymers with negative birefringence, *Polymer* **2011**, *52*, 4498–4502.

(5) Li, Y.; Turner, S. R. Free radical copolymerization of methyl substituted stilbenes with maleic anhydride, *Eur. Polym. J.* **2010**, *46*, 821–828.

(6) Mao, M.; Turner, S. R. Synthesis and characterization of highly functionalized polymers based on N,N,N',N'-tetraalkyl-4,4'-diaminostilbene and maleic anhydride, *Polymer* **2006**, *47*, 8101–8105.

(7) Stilbene dyes. *Kirk-Othmer Encyclopedia of Chemical Technology*, 4th ed.; John Wiley & Sons, Inc.: Vol. 27, pp 1–11.

(8) Aktiebolaget Henkel-Helios Detergent compositions; United Kingdom Patent 810,151, March 11, 1959.

(9) Li, Y.; Mao, M.; Matolyak, L. E.; Turner, S. R. Sterically crowded anionic polyelectrolytes with tunable charge densities based on stilbene-containing copolymers, *ACS Macro Lett.* **2012**, *1*, 257–260.

(10) Yuki, H.; Okamoto, Y.; Tsubota, K.; Kosai, K. Anionic copolymerizations of trans-stilbene with butadiene, isoprene, and 2,3-dimethylbutadiene, *Polym. J.* **1970**, *1*, 147–154.

(11) Wagner-Jauregg, T. Additive heteropolymerization, *Ber. Dtsch. Chem. Ges. B* **1930**, *63B*, 3213–3224.

(12) Schaschel, E. T. Reaction products of silicon monoxide and olefins; U.S. Patent 3,907,750, July 19, 1971.

(13) Anderson, W. S. Copolymers of ethylene and stilbene for use as lubricant additives; U.S. Patent 3,338,877, Aug. 29, 1967.

(14) Marvel, C. S.; Anderson, W. S. Copolymerization of 1,3-butadiene with some polynuclear aromatic hydrocarbons, *J. Am. Chem. Soc.* **1954**, *76*, 5434–5435.

(15) Turner, S. R.; Arcus, R.; Houle, C.; Schleigh, W. High-Tg base-soluble copolymers as novolac replacements for positive photoresists, *Polymer Science and Engineering* **1986**, *26*, 1096–1100.

(16) Fitzgerald, P. H.; Rao, N. S.; Vinod, Y. V.; Henry, G. K.; Prowse, K. S. Stain-resistant aromatic/maleic anhydride polymers; EP Patent 0,329,899, August 30, 1989.

(17) Chu, Q.; Lu, H.; He, T.; Ding, M. Synthesis and thermal polymerization of a novel stilbene-maleimide AB-monomer, *Polym. Bull.* **2000**, *43*, 471–475.

(18) Ha, N. T. H. Determination of triad sequence distribution of copolymers of maleic anhydride and its derivatives with donor monomers by ^{13}C NMR spectroscopy, *Polymer* **1998**, *40*, 1081–1086.

(19) Rzaev, Z. M. O.; Milli, H.; Akovali, G. Complex-radical alternating copolymerization of trans-stilbene with *N*-substituted maleimides, *Polym. Int.* **1996**, *41*, 259–265.

(20) Lewis, F. M.; Mayo, F. R. Copolymerization. IX. Comparison of some cis and trans isomers, *J. Am. Chem. Soc.* **1948**, *70*, 1533–1536.

(21) McNeill, I. C.; Polishchuk, A. Y.; Zaikov, G. E. Thermal degradation studies of alternating copolymers. III. The copolymer of maleic anhydride with trans-stilbene, *Polym. Degrad. Stab.* **1995**, *47*, 319–329.

(22) Ebdon, J. R.; Hunt, B. J.; Hussein, S. Radical copolymerization of maleic-anhydride with trans-stilbene, *British Polymer Journal* **1987**, *19*, 333–337.

(23) Hallensleben, M. L. Electron donor-acceptor complexes and polymerization. V. Copolymerization of maleicanhydride and trans-stilbene under ultraviolet irradiation, *Eur. Polym. J.* **1973**, *9*, 227–231.

(24) Rzaev, Z. M.; Zeinalov, I. P.; Medyakova, L. V.; Babaev, A. I.; Agaev, M. M. Mechanism of radical copolymerization of maleic anhydride with trans-stilbene, *Vysokomol. Soedin., Ser. A* **1981**, *23*, 614–618.

(25) Tanaka, T.; Vogl, O. Head-to-head poly(methyl cinnamate) from alternating stilbene-maleic anhydride copolymer - {poly[1,2-bis(methoxycarbonyl)-3,4-diphenyltetramethylene]}, *Macromol. Synth.* **1982**, *8*, 21–24.

(26) Hayakawa, K.; Kawase, K.; Yamakita, H. On the reaction mechanism of gamma-ray solid-state copolymerization, *J. Polym. Sci., Poly. Chem. Ed.* **1985**, *23*, 2739–2746.

(27) Yamakita, H.; Hayakawa, K. Copolymerization of N-ethylmaleimide with stilbenes, *J. Polym. Sci. Pol. Chem.* **1972**, *10*, 2223–2235.

(28) Braunecker, W. A.; Matyjaszewski, K. Controlled/living radical polymerization: Features, developments, and perspectives, *Prog. Polym. Sci.* **2007**, *32*, 93–146.

(29) Mao, M.; Kim, C.; Wi, S.; Turner, S. R. Chain structure of substituted stilbene-maleic anhydride alternating copolymer probed by solid-state NMR, *Macromolecules* **2008**, *41*, 387–389.

(30) Weigand, F.; Fulber, C.; Blumich, B.; Spiess, H. W. Spatially resolved NMR of rigid polymers and elastomers, *Magn. Reson. Imaging* **1994**, *12*, 301–304.

(31) Beaucage, G.; Rane, S.; Sukumaran, S.; Satkowski, M. M.; Schechtman, L. A.; Doi, Y. Persistence length of isotactic poly(hydroxy butyrate), *Macromolecules* **1997**, *30*, 4158–4162.

(32) Bohdanecky, M. New method for estimating the parameters of the wormlike chain model from the intrinsic viscosity of stiff-chain polymers, *Macromolecules* **1983**, *16*, 1483–1492.

(33) Schmid, C. W.; Rinehart, F. P.; Hearst, J. E. Statistical length of DNA from light scattering, *Biopolymers* **1971**, *10*, 883–893.

(34) Sharp, P.; Bloomfield, V. A. Light scattering from wormlike chains with excluded volume effects, *Biopolymers* **1968**, *6*, 1201–1211.

(35) Fetters, L.; Lohse, D.; Colby, R. Physical Properties of Polymers Handbook; Mark, J. E., Ed.; Springer: New York, 2007, p 447.

(36) Vanhee, S.; Rulkens, R.; Lehmann, U.; Rosenauer, C.; Schulze, M.; Koehler, W.; Wegner, G. Synthesis and characterization of rigid rod poly(p-phenylenes), *Macromolecules* **1996**, *29*, 5136–5142.

(37) Guilleaume, B.; Blaul, J.; Ballauff, M.; Wittemann, M.; Rehahn, M.; Goerigk, G. The distribution of counterions around synthetic rod-like polyelectrolytes in

solution, a study by small-angle X-ray scattering and by anomalous small-angle X-ray scattering, *Eur. Phys. J. E* **2002**, *8*, 299–309.

(38) Davis, R. M.; Russel, W. B. On the theory of dilute polyelectrolyte solutions: extensions, refinements, and experimental tests, *J. Polym. Sci. Pol. Phys.* **1986**, *24*, 511–533.

(39) Davis, R. M.; Russel, W. B. Intrinsic viscosity and Huggins coefficients for potassium poly(styrenesulfonate) solutions, *Macromolecules* **1987**, *20*, 518–525.

(40) Yamazaki, S.; Muroga, Y.; Noda, I. Persistence lengths of ionenes in methanol, *Langmuir* **1999**, *15*, 4147–4149.

(41) Garrett, E. R.; Guile, R. L. Potentiometric titrations of a polydicarboxylic acid: maleic acid-styrene copolymer, *J. Am. Chem. Soc.* **1951**, *73*, 4533–4535.

(42) Lowe, A. B.; McCormick, C. L. Synthesis and solution properties of zwitterionic polymers, *Chem. Rev.* **2002**, *102*, 4177–4189.

(43) Gotzamanis, G.; Tsitsilianis, C. Stimuli-responsive A-*b*-(B-*co*-C) diblock terpolymers bearing polyampholyte sequences, *Macromol. Rapid Commun.* **2006**, *27*, 1757–1763.

(44) Lee, K.-C.; Borukhov, I.; Gelbart William, M.; Liu Andrea, J.; Stevens Mark, J. Effect of mono- and multivalent salts on angle-dependent attractions between charged rods, *Phys Rev Lett* **2004**, *93*, 128101.

(45) Ha, B. Y.; Liu, A. J. Counterion-mediated attraction between two like-charged rods, *Phys. Rev. Lett.* **1997**, *79*, 1289–1292.

(46) Hampton, K. W., Jr.; Ford, W. T. Styrylmethyl(trimethyl)ammonium methacrylate polyampholyte latexes, *Macromolecules* **2000**, *33*, 7292–7299.

(47) Savage, A. M.; Turner, S. R. *unpublished work* **2014**.

(48) Riande, E.; Sáiz, E. In *Dipole moments and birefringence of polymers*; Prentice Hall: Michigan, U.S., **1992**, pp 1–341.

(49) Zhou, X.; Li, Y.; Hart, K. E.; Abbott, L. J.; Lin, Z. X.; Svec, F.; Colina, C. M.; Turner, S. R. Nanoporous structure of semirigid alternating copolymers via nitrogen sorption and molecular simulation, *Macromolecules* **2013**, *46*, 5968–5973.

Chapter 3:**Solution Properties of Stilbene-containing Sterically Crowded Alternating Polyanions**

3.1 *Authors*

Yi Li, Alice M. Savage, Xu Zhou, S. Richard Turner*†, Richey M. Davis*‡

†Department of Chemistry and Macromolecules and Interfaces Institute, Virginia Tech Blacksburg, Virginia 24061-0344, United States

‡Department of Chemical Engineering, Virginia Tech Blacksburg, Virginia 24061-0344, United States

Fax: +1-540-231-3971; E-mail address: srturner@vt.edu (S.R.T.), rmdavis@vt.edu (R.M.D)

3.2 *Abstract*

Sterically crowded stilbene-containing alternating polyanions were prepared via an indirect strategy of synthesizing "protected" monomers followed by deprotection and neutralization of the polyanion precursors. The solution properties of these new sterically crowded polyelectrolytes were studied. Steady state solution shear rheology showed a pronounced polyelectrolyte effect. The persistence lengths of these polyelectrolytes were

determined. The dissociation behavior of the polyanions was investigated by pH titration with HCl and multi-step dissociation behavior was observed. Chain size and aggregation was studied by using DLS at varying ionic stre*n*gths. Polyelectrolytes behaved like rigid-rods and formed concentrated solutions at the polymer concentration of 1.0 mg/mL.

3.3 *Introduction*

Stilbene containing alternating copolymers constitute a new family of sterically crowded copolymers which possess important properties manifested by a congested copolymer backbone.[1-6] Our previous studies from solid-state NMR torsional angle measurements showed that the maleic anhydride units in a *N,N,N′,N′*-tetraethyl 4, 4′-diaminostilbene (TDAS)-maleic anhydride (MAH) alternating copolymer were incorporated by copolymerization in a predominantly *cis* configuration.[1] The copolymer with these *cis* configurations of the anhydride units in the chain results in a highly kinked copolymer backbone.. We recently reported the synthesis of new anionic polymers and their precursors based on *tert*-butyl carboxylated stilbenes and styrenes.[2] SAXS and SEC measurements quantified the chain stiffness by determining the persistence lengths of these polyanion precursors.[3] It was concluded that stilbene-containing copolymers are a new class of semi-rigid polymers. It was also observed that a block copolymer containing a TDAS-MAH polyampholyte block and a poly(methoxy-capped oligo-(ethylene glycol)methacrylate) block exhibited polyion complexes (PICs) with unusual pH and salt responsive properties similar to the "like-charge" attraction effects in rigid polyelectrolytes.[4] In addition, bimodal peaks were observed in SEC measurements with the copolymer of 4-methylstilbene and maleic anhydride. DLS measurements indicated

interchain aggregation as the origin of the apparent high molecular mass fraction.[5] Films of the alternating copolymer of stilbene and *N*-(2-methylphenyl)maleimide) were found to have a very strong negative birefringence.[6]

For polyelectrolytes if it important to understand the dependence of the polymer solution viscosity η on solution parameters such as the polymer concentration C and the ionic strength I. For example, hydrolyzed and neutralized maleic anhydride-containing copolymers form an important class of polyelectrolytes with many industrial applications. The solution properties of these copolymers have been intensively studied.[7-13] The dissociation behavior of a series of maleic anhydride-derived copolymers was studied by Colby and coworkers.[12] A two-step dissociation process corresponding to the dissociation of the two adjacent carboxylic acids from enchained maleic anhydride units was observed in aqueous $CaCl_2$ (0.02 N) solution for most of the maleic acid-containing copolymers.[12] The dilute solution behavior of these maleic acid-containing copolymers has also been characterized by static and dynamic light scattering, intrinsic viscosity, and pulsed-gradient spin-echo NMR spectroscopy.[13] Therefore, it is of significant scientific interest to understand the solution properties of these stilbene-containing copolymers.

As discussed earlier, the "precursor" approach with organic soluble "blocked" functional group monomers that can be copolymerized and the non-charged copolymers characterized in normal organic solvents has been reported previously.[2] This avoids the well-known problems that are often encountered with characterizing the molar mass and molecular weight distributions in charged macromolecules. Our approach enables us to

prepare new polyelectrolytes with tunable charges and charge densities.[2] Analogous styrenic copolymers, for comparison to the stilbene structures, have also been prepared.[2] The study in this paper is focused on the characterization of solution properties of these carboxylate stilbene- and styrene-containing alternating polyanions.

3.4 *Experimental*

3.4.1 Materials

Synthesis of (*E*)-di-*tert*-butyl 4, 4′-stilbenedicarboxylate (DTBSC) and *tert*-butyl 4-vinylbenzoate (TBVB) monomers was described previously.[2]

Stilbene and styrenic copolymers were synthesized via free radical polymerization. In Figure 3.4.1.1, copolymer I was synthesized from (*E*)-stilbene (STB) and maleic anhydride (MAH). Copolymer II was composed alternating units from (*E*)-di-*tert*-butyl 4,4′-stilbenedicarboxylate (DTBSC) and maleic anhydride (MAH). Copolymer III was based on *tert*-butyl 4-vinylbenzoate (TBVB) and maleic anhydride (MAH).. The specific procedures for preparing copolymers I, II, and III were previously reported.[2,5] The structures of copolymers I, II, and III are shown in Figure 3.4.1.1. Copolymer II had M_n 40.0 kg/mol and M_w 47.2 kg/mol and M_n 21.6 kg/mol and M_w 31.7 kg/mol for the polyelectrolyte effect study, determined by SEC in THF. Copolymer III had M_n 41.1 kg/mol and M_w 64.6 kg/mol determined in DMF containing 0.1 M lithium nitrate and 1% formic acid as SEC eluent and had M_n 30.0 kg/mol and M_w 54.4 kg/mol for the polyelectrolyte effect study. Copolymer I was not soluble in organic solvents available

for SEC measurement and its corresponding polyanion I formed aggregates in the solvents used for aqueous SEC. As a result, it was not possible to measure the molar mass of copolymer I.

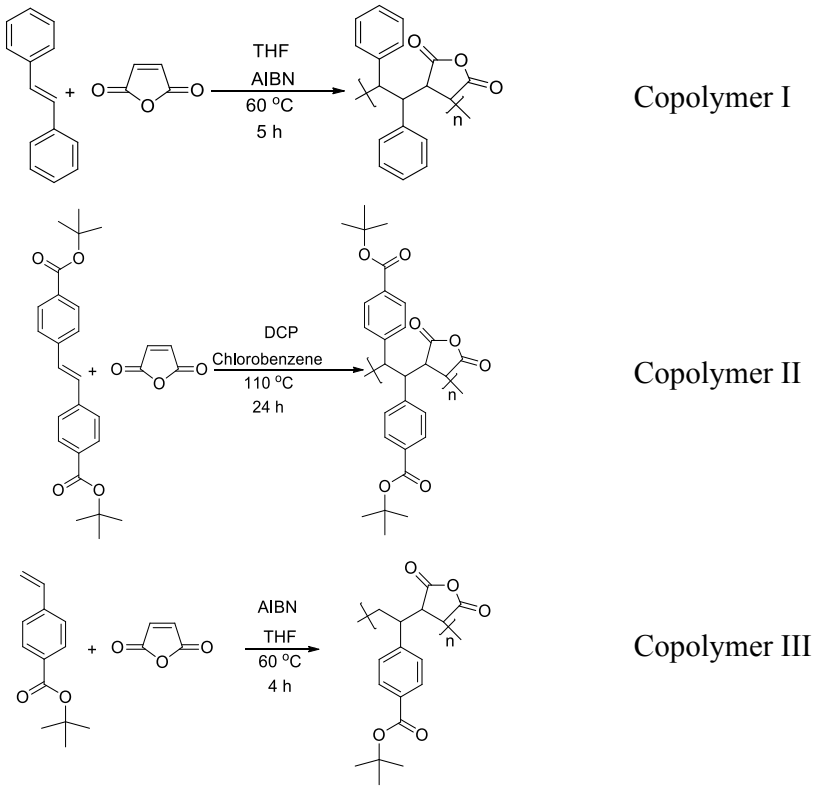

Figure 3.4.1.1 The structures of copolymers I, II and III

Conversion of polyelectrolyte precursors to their corresponding polyanions was also reported.[2] Structures of the resulting polyanions are shown in Figure 3.4.1.2. After copolymers II and III were deblocked by TFA (trifluoroacetic acid) and neutralized in an excess of NaOH solution at 50 °C for 24 h, polyanions II and III. Polyanion I was obtained by neutralization in an excess of NaOH solution at 50 °C for 24 h. Each

polyanion solution in 40 mL of water was dialyzed for 48 h against 1000 mL of deionized water. The DI water was changed every 4-6 hours. The polyanion solutions were frozen by immersion of sample vials in liquid nitrogen. The frozen samples were freeze-dried for 24 h on a Virtis lyophilizer to yield white fluffy solids.

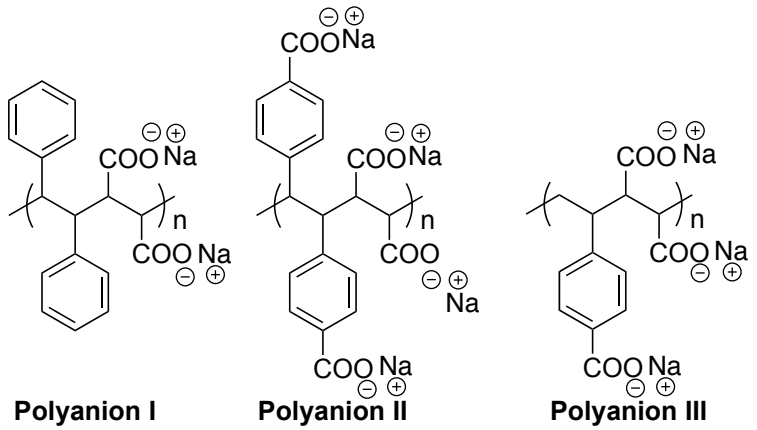

Figure 3.4.1.2 The structures of polyanions I, II and III.

3.5 *Characterization*

Molar masses of the copolymers II, and III were determined using a Waters size exclusion chromatograph equipped with a Waters 1515 isocratic HPLC pump, a Viscotek 270 viscosity detector, and a Waters 2414 differential refractive index detector operating at 880 nm and 35 ^{o}C and a Waters 717 plus autosampler, a Wyatt miniDAWN multiangle laser light scattering (MALLS) detector operating a He-Ne laser at 690 nm. The *dn*/*dc* values were determined using the Wyatt Astra V software package. SEC measurements were performed at 35 °C in THF or DMF containing 0.1 M lithium nitrate and 1% formic

acid at a flow rate of 1.0 mL/min. A Virtis lyophilizer (Gardiner, NY) equipped with a drum manifold and a condenser was used at a pressure of <30 mTorr.

Steady-state solution shear rheological experiments were performed with a TA Instruments AR-G2 rheometer at 25 ^{o}C using concentric cylinder geometry. Polyanions II and III in deionized water with different amounts of NaCl as added salt were analyzed using shear rate sweeps from 0.01 to 1000 s^{-1}.

All pH titrations were carried out with a pH glass electrode in conjunction with a pH meter at room temperature. The polyanion used for each titration was ~25 mg with the concentration in a range of 1.1~1.4 mg/mL in $CaCl_2$ solution. The concentration of $CaCl_2$ solution used for each titration was 0.02 M. The aqueous HCl titrant (0.0075 M) was delivered into the stirred polymer solution from a 50 mL burette. The pH readings for the solution were stable and accurate to 0.01 pH unit. Dissociation behavior of polyanions I, II, III was studied by backward titration procedures (i.e., from pH 11 titrate with HCl). Titration was performed with HCl as the titrant for hydrolyzed samples that contain sodium carboxylate groups.

Cloud point concentrations were measured using dynamic light scattering with a Malvern Zetasizer NanoZS particle analyzer equipped with a He-Ne linear polarized laser (**λ**= 632.8 nm) at a scattering angle of 173 and at 25 °C. All experiments were conducted in 12 mm square disposable polystyrene cuvettes. Salt concentrations were adjusted by the addition of concentrated NaCl solutions (2 M and 5 M) directly to the cuvette containing

1 mL of a 1 mg/mL polymer solution in DI water. After each addition, the polymer-salt solution was stirred and allowed to sit for 15 mins before measurement.

3.6 *Results and Discussion*

3.6.1 Polyelectrolyte Effect

The reduced viscosity (η_{sp}/C) vs. concentration of the polymer solution (C) plots for polyanion II (Figure 3.6.1.1) show a strong polyelectrolyte effect in deionized water that was increasingly suppressed by adding NaCl.[14,15] The concentration of added NaCl was 0.1 mg/mL and 5.0 mg/mL of the polymer solution, respectively. The reduced viscosity is defined as $\eta_{sp}/C = (\eta - \eta_0)/\eta_0 C$, where η is the Newtonian solution viscosity and η_s is the solvent viscosity. The counterions from the polyelectrolyte chains that are free to dissociate contribute to the ionic strength along with the contribution from the added salt, I_s, so that the effective ionic strength (moles/volume) I is given by[16]

$$I = I_s + \frac{1}{2}\left(\frac{L_B}{L_c}\right)_{eff}\frac{L_{RU}C}{L_B M_{RU}} \qquad \text{eq (3.6.1.1)}$$

where L_B is the Bjerrum length (0.71 nm in water at room temperature[16]), L_c is the average spacing between charges along the polymer backbone and is defined as the length per repeat unit L_{Ru} divided by the number of ionizable groups per repeat unit, L is the contour length, M_{RU} is the molecular weight of the repeat unit, and C is the concentration of the polymer solution (mass/volume). The factor of ½ arises because only the counterions from the polyelectrolyte contributes to the ionic strength. The fraction of

counterions that are free to dissociate from the polyion backbone can be estimated from Manning's counterion condensation theory[16]

$$\left(\frac{L_B}{L_c}\right)_{eff} = \frac{L_B}{L_c} \quad \text{when} \quad \frac{L_B}{L_c} < 1$$

$$\left(\frac{L_B}{L_c}\right)_{eff} = 1 \text{ when} \quad \frac{L_B}{L_c} > 1 \qquad \text{(eq. 3.6.1.2)}$$

The length per repeat unit of polyanion II, L_{Ru}, is 0.504 nm. The number of ionizable groups per repeat unit of polyanion II is 4. Therefore L_c = (0.504/4) = 0.126 nm/charge. L_B/L_c = 0.71/0.126 = 5.6 > 1. Thus, equation 3.6.1.1 reduces to

$$I = I_s + \frac{1}{2}\frac{L_{RU}C}{L_B M_{RU}} \qquad \text{(eq. 3.6.1.3)}$$

The Debye length κ^{-1}, the electrostatic screening length in ionic solutions, in water at 25 ^{o}C is given by[17,18]

$$\kappa^{-1} = \left(8\pi L_B N_A I\right)^{-1/2} \qquad \text{(eq. 3.6.1.4)}$$

where N_A is Avogadro's number.

Using equations 3.6.1.3 and 3.6.1.4, it is shown in Table 3.6.1.1 how the ionic strength and Debye length can change with polymer concentration as the polyanion II solution was diluted. When the solution was diluted with deionized water, the reduced viscosity increased markedly as seen in Figure 3.6.1.1 due to the 2.5-fold increase in the Debye length κ^{-1} over the concentration range probed. The increase in electrostatic repulsion

between ionized segments in the polymer coils resulted in coil expansion due to increased chain stiffness and excluded volume effects. When the solution was diluted with NaCl at 0.1 mg/mL (0.0017 M), the added salt resulted in increased screening of the backbone charges compared to the deionized water case, so that the reduced viscosity did not increase as much. However, since the effective ionic strength of the polymer solution at the beginning of the dilution process – 0.0094 M when the polymer concentration was 1.02 g/dL - was higher than the ionic strength of the diluent NaCl solution (0.0017 M), κ^{-1} increased by ~ 1.8-fold over the concentration range probed and so the reduced viscosity increased. For dilutions made with NaCl at 5 mg/mL, aggregation of the polymer occurred which limited the concentration range that could be probed from 0.16 to 0.59 g/dL. When the solution was diluted with NaCl at 5 mg/mL, the reduced viscosity decreased with concentration and the curvature was largely suppressed because κ^{-1} decreased which resulted in decreased electrostatic repulsion with decreasing concentration.

Table 3.6.1.1 Ionic Strengths and Debye Lengths of Polyanion II

[NaCl] (mg/mL)	C (g/dL)	I x 10^{-3} (mol/L)*	κ^{-1} (nm)**
0	0.16	1.2	8.8
0	1.02	7.7	3.5
0.1	0.16	2.9	5.7
0.1	1.02	9.4	3.2
5.0	0.16	87	1.04
5.0	0.59	90	1.02

* calculated by using eq. 3.6.1.3. **calculated by using eq. 3.6.1.4.

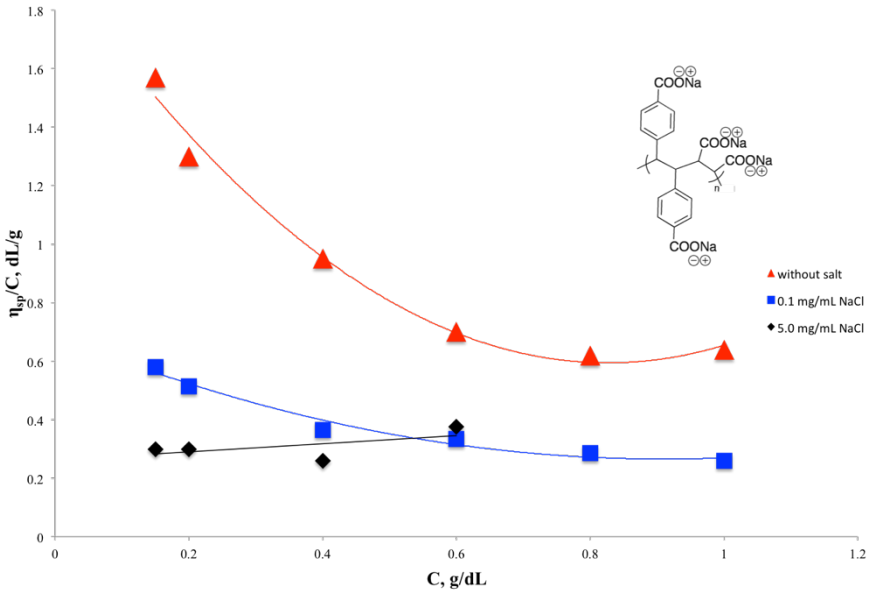

Figure 3.6.1.1 Plots of the reduced viscosity vs. concentration for polyanion II (the stilbene copolymer).

A similar polyelectrolyte effect was also observed for polyanion III (the styrene control copolymers). These results are consistent for polymers with a semi-rigid backbone characterized by chain stiffening and excluded volume effects driven by electrostatic interactions mediated by the effective ionic strength.

Chain stiffness is characterized by the statistical segment length[21] L_k, which, for a polyelectrolyte, depends on the intrinsic stiffness of the uncharged backbone due to steric hindrance and on charge repulsions between adjacent ionized groups along the backbone according to[17,19,20]

$$L_k = L_{k0} + L_{ke} \qquad \text{(eq. 3.6.1.5)}$$

where L_{k0} is the intrinsic or unperturbed statistical segment length and L_{ke} is the electrostatic statistical segment length. While a theory for L_{ke} has not been definitively tested, we employ below the line charge model of Odijk which predicts that L_{ke} increases with the square of the Debye length. A competing theory by de Gennes, *et al*.[22,23] predicts that L_{ke} increases with the Debye length. The data in the present study are not sufficient to provide a definitive test of these theories and so the results from the line charge theory are used to provide a qualitative explanation of the reduced viscosity trends. A model for L_{ke} that is consistent with the Manning's line-charge counterion condensation theory results in[24]

$$L_{ke} = \frac{\kappa^{-2}}{2L_B} \qquad \text{(eq. 3.6.1.6)}$$

The number of statistical segments per chain N_k is given by

$$N_K = \frac{L}{L_K} \qquad \text{(eq. 3.6.1.7)}$$

Values of L_k and N_k for polyanions II and III were calculated from equations 3.6.1.5–3.6.1.7 and the results are shown in Tables 3.6.1.2 and 3.6.1.3, respectively. For polyanion II at a concentration of 0.16 g/dL in deionized water, L_k is greater than 60 nm and the polymer contains approximately 0.38 statistical segments and so the polymer chain should behave like a rigid-rod. Addition of NaCl of 5.0 mg/mL led to a dramatic decrease of the Debye length (Table 3.6.1.1) and, thus, a decrease of the statistical segment length of the polymer backbone. Table 3.6.1.2 shows that, at 5.0 mg/mL of added NaCl, chain stiffening due to electrostatic repulsion has been greatly suppressed,

resulting in L_k being close to the value of the intrinsic statistical segment length L_{k0} of the corresponding uncharged polymer chain in tetrahydrofuran (THF).

In comparison to polyanion II (the stilbene copolymer), polyanion III (the styrene control) exhibited less chain stiffness due to the smaller value of L_{k0}, as shown in Table 3.6.1.3. It is observed the statistical lengths in deionized water with no added NaCl for polyanion III are smaller than those for polyanion II by 25~30%. As with polyanion II, a NaCl concentration of 5.0 mg/mL resulted in a value of L_k very close to that of the intrinsic statistical segment length L_{k0} of the corresponding uncharged polymer chain obtained in THF.

Table 3.6.1.2 Statistical Segment Lengths and Number of Statistical Segments for Polyanion II.

[NaCl] (mg/mL)	C (g/dL)	L_{ke} (nm)*	L_k (nm)	N_k**
0	0.16	55	61	0.38
0	1.02	8.6	15	1.6
5.0	0.16	0.76	6.8	3.4
5.0	0.59	0.73	6.7	3.4

* Calculated from equation 3.6.1.6. The intrinsic statistical segment length of the uncharged polyanion II backbone, 6.0 nm, was obtained by SEC and SAXS.[3] ** The contour length L for polyanion II is 23 nm.

Table 3.6.1.3 Statistical Segment Lengths and Number of Statistical Segments for Polyanion III.

[NaCl] (mg/mL)	C (g/dL)	L_{ke} (nm)*	L_k (nm)	N_k**
0	0.16	38	43.3	1.2
0	1.02	6.0	11.2	4.5
5.0	0.16	0.75	6.0	8.4
5.0	0.77	0.70	5.9	8.5

* Calculated from equation 3.6.1.6. The intrinsic statistical segment length of the uncharged polyanion III backbone, 5.2 nm, was obtained by SEC and SAXS.[2] ** The contour length L for polyanion III is 50 nm.

3.6.2 Cloud Point Determination

In the cloud point measurements, the scattering intensities were plotted as a function of the total ionic strength I (eq. 3.6.1.1) consisting of the contributions from the added salt and the polyelectrolytes. A representative cloud point curve is shown in Figure 3.6.2.1, for polyanion II where, for pH 6.3, the scattering intensity rose sharply for Polyanion I in the range 1-1.2 M. The ionic strength at which the cloud point was reached increased by at least 3-fold when the pH was increased from 6.3 to 6.8 due to increasing ionization of the carboxylate groups (Table 3.6.2.1)

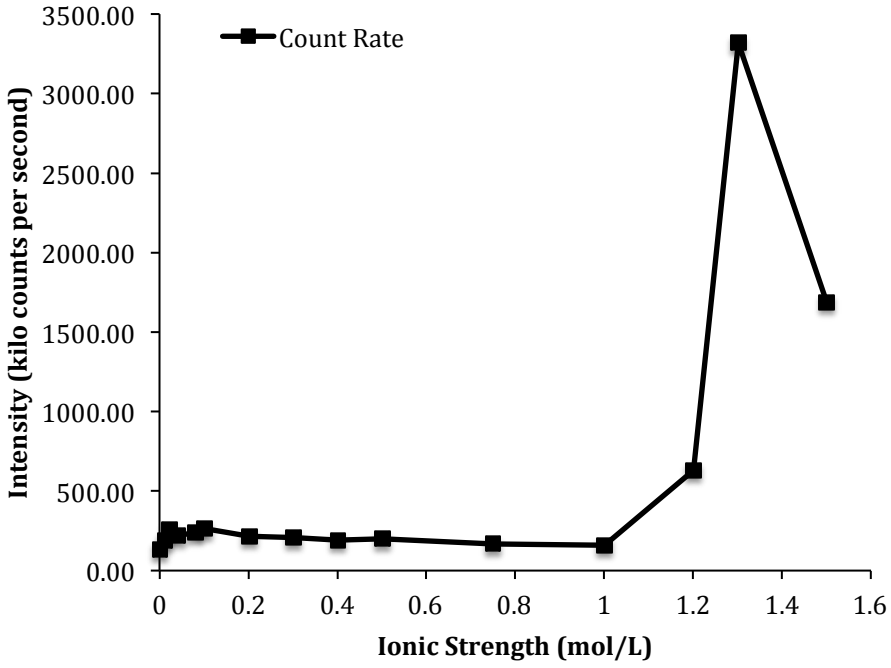

Figure 3.6.2.1 Plot of the intensity vs total ionic strength for the cloud point determination of polyanion II at a pH of 6.3.

Table 3.6.2.1 Cloud Point Ionic Strength Results for Polyanions I, II, and III.

	Polyanion I	Polyanion II	Polyanion II	Polyanion III
Charges/RU*	2	4	4	3
Charges/C atom	1/9	1/5	1/5	~1/4
pH	7.6	6.3	6.8	7.3
Cloud Point Ionic Strength, I (mol L^{-1})	3.0	1.1	>4.5***	>5.0***
L_{k0} (nm)-**	--	6 ± 0.6	6 ± 0.6	5.2 ± 0.5

* repeat unit. ** the intrinsic statistical segment length of uncharged polyanion. ***not detectable .

Polyanion I has a lower cloud point ionic strength than polyanion II at pH > 6.8 which is consistent with the former having a lower number of charges per repeat unit, particularly

if the bare statistical segment length L_{k0} was the same for both polymers. However, prior work has shown that the uncharged version of polyanion I was markedly less soluble than the uncharged version of polyanion II.[25] While this does not prove that $L_{k0,I} > L_{k0,II}$, it is at least consistent with the present findings that suggest polyanion I is less soluble than polyanion II.

There was not a significant difference in the cloud point ionic strengths for polyanion III and polyanion II. This is not surprising in view of their similarities in the number of charges per carbon atom and their values of L_{k0}.

3.6.3 Titration Results

The pH titration curve for polyanions I from the dissociated ions to the acid form is shown in Figure 5. To convert freeze-dried polyanion I into the dissociated form, excess NaOH was added to adjust the polymer solution pH value reading ~11 initially. In Figure 5, the pH titration in deionized water for polyanion I is shown as curve (1) with only one inflection point. In the presence of 0.02 M $CaCl_2$, two distinct inflection points for this sample can be identified in the curve, corresponding to the dissociation of the two carboxylic acid groups in the maleic acid comonomer.

A brief review of several model dicarboxylic acids may facilitate characterizing and evaluating the dissociation behavior of polyanions I, II and III. As shown in Table 3.6.3.1, model dicarboxylic acid compounds including succinic acid (4.16, 5.61), maleic acid (1.83, 6.07) and fumaric acid (3.03, 4.42) were previously studied using the pH titration method.[13] pK_1 and pK_2 values of maleic acid are far apart from each other while

those for fumaric acid and succinic acid are close to each other. On the corresponding titration curves maleic acid (*cis*-configuration) exhibited two-step dissociation behavior while fumaric acid (*trans*-configuration) only showed a single dissociation. It was stated by Colby et al. that the absence of the two-step titration curve is attributed to the closeness of two pKs that is caused by the *trans*-configuration of the two acids.[13] Colby et al. also studied the dissociation behavior of a series of maleic acid-containing copolymers.[13] This two-step behavior corresponds to the dissociation of the two carboxylic acid groups in the maleic acid comonomer. The dissociation behavior of copoly(isobutylene-*alt*-maleic acid sodium salt) (IBMA-Na) was sharpened by addition of $CaCl_2$ to the polymer solution.

In Figure 3.6.3.1 (Curve 1), two distinct inflection points were observed in the titration. This indicates that the two carboxylic acid groups from the succinic acid like units in the chain influence each other. As the first carboxylic acid group is neutralized this carboxylate anion influences the ionization of the second carboxylic acid group electrostatically since the negative charges in close proximity will cause some rotation of the groups away from each other.[13]

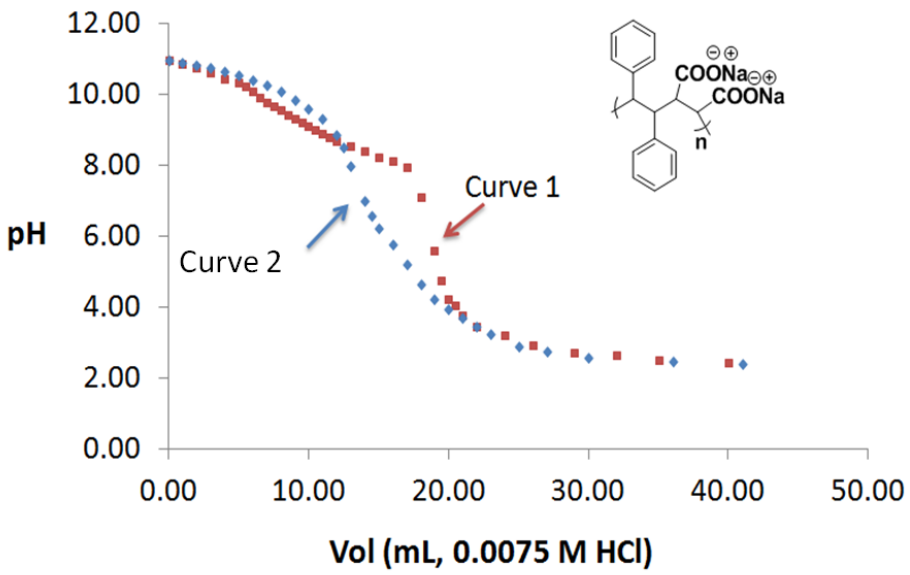

Figure 3.6.3.1 Titration curves of polyanion I (25.5 mg) with excess NaOH (0.1 M, 1.1 mL) in $CaCl_2$ solution (18 mL, 0.020 M) (Curve 1) and in deionized water (18 mL, 0.020 M) (Curve 2).

Table 3.6.3.1 pK_1 and pK_2 for Dicarboxylic Acids.

	(pK_1, pK_2)
succinic acid	(4.16, 5.61)
maleic acid	(1.83, 6.07)
fumaric acid	(3.03 4.42)

Similar two-step dissociation behavior of the two carboxylic acid groups in the maleic acid comonomer was also observed for polyanions II and III, shown in Figures 3.6.3.2 and 3.6.3.3 respectively. In addition a third inflection point was also observed for polyanions II and III, corresponding to the dissociation of benzoic acid groups. The

aromatic carboxylic acid neutralizations in Figure 3.6.3.2 show only one peak since the two carboxylic acids have identical chemical environments. These occur at the lower pH values as a result of the greater acidity of the aromatic carboxylic acids compared to the aliphatic ones on the chain. The succinic acid units show two peaks because of the electrostatic effects described above. A similar titration curve was observed for the styrene carboxylic acid based alternating copolymer in Figure 3.6.3.3.

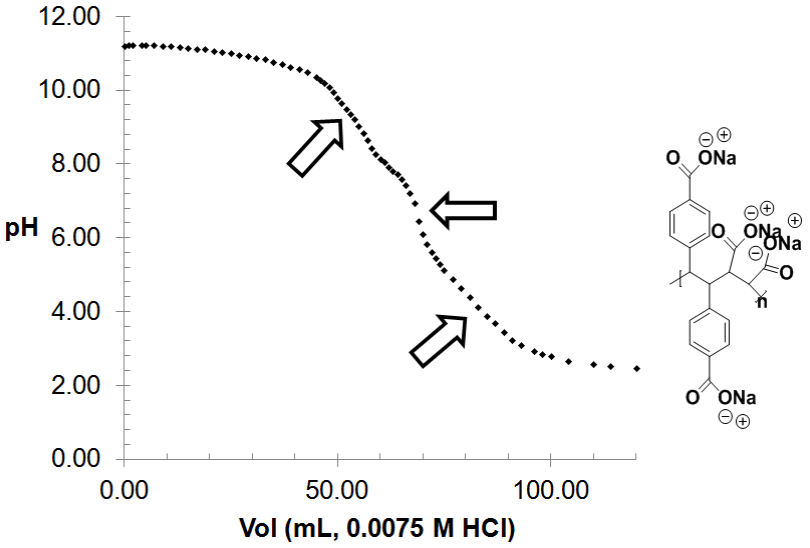

Figure 3.6.3.2 Titration curve of polyanion II (25.5 mg) in $CaCl_2$ solution (24 mL, 0.020 M) with excess NaOH (0.1 M, 6.8 mL).

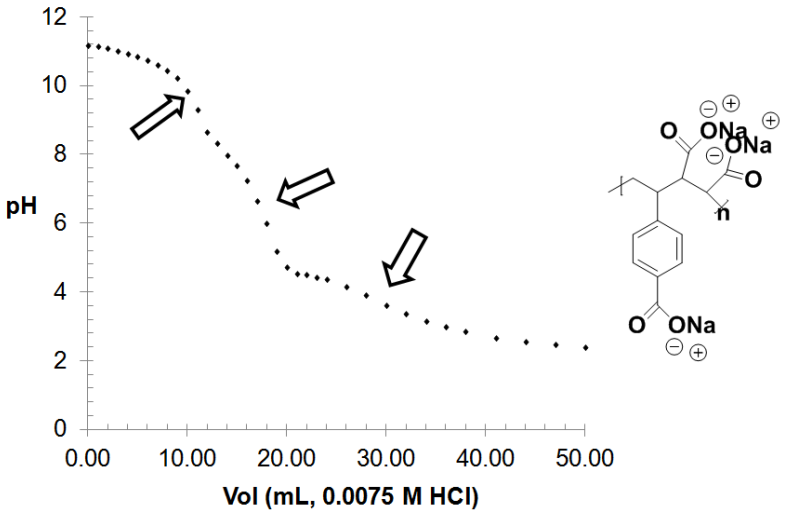

Figure 3.6.3.3 Titration curve of polyanion III (24.3 mg) in $CaCl_2$ solution (18 mL, 0.020 M) with excess NaOH (0.1 M, 1.3 mL).

3.7 *Summary*

Copolymers I, II and III were readily converted into their corresponding anionic polyelectrolytes via deprotection reactions. From dilute solution viscosity study, a pronounced "polyelectrolyte effect" was observed due to the chain collapse in the presence of added salt and chain expansion on dilution which is in a good agreement with the backbone of a flexible or semi-rigid polyelectrolyte. The statistical segment lengths of polyanions II and III in deionized water with and without additional salt were calculated and compared. In deionized water, both polyanions behave like rigid-rods. The statistical segment lengths of polyanion III with no added NaCl at solution concentrations of 0.16 and 1.02 g/dL are smaller than those of polyanions II by 25~30%, which is consistent with L_k value differences previously measured on the uncharged polyelectrolyte precursors, copolymers II and III. A two-step dissociation behavior was observed for the two carboxylic acids from maleic acid comonomer of polyanion I, II and III. This

indicated that two acid groups are in close proximity to exert influence on each other. It was found that polyanions I, II and III exhibited large R_h values in deionized water with no added salt. The separation distance was determined and compared to the Debye length. The results indicated the polymer solution is in concentrated regime at the polymer concentration of 1 mg/mL.

3.8 *References*

(1) Mao, M.; Kim, C.; Wi, S.; Turner, S. R. Chain structure of substituted stilbene−maleic anhydride alternating copolymer probed by solid-state NMR, *Macromolecules* **2007**, *41*, 387–389.

(2) Li, Y.; Mao, M.; Matolyak, L. E.; Turner, S. R. Sterically crowded anionic polyelectrolytes with tunable charge densities based on stilbene-containing copolymers, *ACS Macro Letters* **2012**, *1*, 257–260.

(3) Li, Y.; Zhang, M.; Mao, M.; Turner, S. R.; Moore, R. B.; Mourey, T. H.; Slater, L. A.; Hauenstein, J. R. Chain stiffness of stilbene containing alternating copolymers by SAXS and SEC, *Macromolecules* **2012**, *45*, 1595–1601.

(4) Mao, M.; Turner, S. R. Aggregation of rod−coil block copolymers containing rigid polyampholyte blocks in aqueous solution, *J. Am. Chem. Soc.* **2007**, *129*, 3832–3833.

(5) Li, Y.; Turner, S. R. Free radical copolymerization of methyl substituted stilbenes with maleic anhydride, *Eur. Polym. J.* **2010**, *46*, 821–828.

(6) Mao, M.; England, J.; Turner, S. R. Alternating stilbene copolymers with negative birefringence, *Polymer* **2011**, *52*, 4498–4502.

(7) Dubin, P.; Strauss, U. P. Hydrophobic hypercoiling in copolymers of maleic acid and alkyl vinyl ethers, *J. Phys. Chem.* **1967**, *71*, 2757–2759.

(8) Dubin, P. L.; Strauss, U. P. Hydrophobic bonding in alternating copolymers of maleic acid and alkyl vinyl ethers, *J. Phys. Chem.* **1970**, *74*, 2842–2847.

(9) Briššová, M.; Štaudner, E. Behaviour of MAn-based polyelectrolytes in water solutions: Influence of pH and ionic strength, *Eur. Polym. J.* **1996**, *32*, 529–533.

(10) Reinhardt, S.; Steinert, V.; Werner, K. Investigations on the dissociation behaviour of hydrolyzed alternating copolymers of maleic anhydride and propene—I. Potentiometric titrations, *Eur. Polym. J.* **1996**, *32*, 935–938.

(11) Kitano, T.; Kawaguchi, S.; Anazawa, N.; Minakata, A. Dissociation behavior of an alternating copolymer of isobutylene and maleic acid by potentiometric titration and intrinsic viscosity, *Macromolecules* **1987**, *20*, 2498–2506.

(12) Sauvage, E.; Plucktaveesak, N.; Colby, R. H.; Amos, D. A.; Antalek, B.; Schroeder, K. M.; Tan, J. S. Amphiphilic maleic acid-containing alternating copolymers—2. Dilute solution characterization by light scattering, intrinsic viscosity, and PGSE NMR spectroscopy, *J. Polym. Sci. Pol. Phys.* **2004**, *42*, 3584–3597.

(13) Sauvage, E.; Amos, D. A.; Antalek, B.; Schroeder, K. M.; Tan, J. S.; Plucktaveesak, N.; Colby, R. H. Amphiphilic maleic acid-containing alternating copolymers—1. Dissociation behavior and compositions, *J. Polym. Sci. Pol. Phys.* **2004**, *42*, 3571–3583.

(14) Fernandes, A. L. P.; Martins, R. R.; da Trindade Neto, C. G.; Pereira, M. R.; Fonseca, J. L. C. Characterization of polyelectrolyte effect in poly(acrylic acid) solutions, *J. Appl. Polym. Sci.* **2003**, *89*, 191–196.

(15) Turner, S. R.; Wardle, R.; Thaler, W. A. Poly(sodium styrene sulfonate-*alt*-sodium-*N*(4-sulfophenyl)maleimide): A new water-soluble alternating copolymer, , *J. Polym. Sci. Pol. Chem. Ed.* **1984**, *22*, 2281–2285.

(16) Manning, G. S. Limiting Laws and Counterion Condensation in Polyelectrolyte Solutions I. Colligative Properties, *J. Chem. Phys.* **1969**, *51*, 924–933.

(17) Davis, R. M.; Russel, W. B. On the theory of dilute polyelectrolyte solutions: Extensions, refinements, and experimental tests, *J. Polym. Sci. Pol. Phys.* **1986**, *24*, 511–533.

(18) Davis, R. M. Analysis of dilute solutions of (carboxymethyl)cellulose with the electrostatic wormlike chain theory, *Macromolecules* **1991**, *24*, 1149–1155.

(19) Davis, R. M.; Russel, W. B. Intrinsic viscosity and Huggins coefficients for potassium poly(styrenesulfonate) solutions, *Macromolecules* **1987**, *20*, 518–525.

(20) Yamazaki, S.; Muroga, Y.; Noda, I. Persistence lengths of ionenes in methanol, *Langmuir* **1999**, *15*, 4147–4149.

3.9 *Appendix*

3.9.1 Bjerrum Length Calculations

The Bjerrum length is the interaction distance between two elementary charges and is defined by the following equation.[1]

$$L_B = \frac{e^2}{\varepsilon_r k_B T} \quad (1)$$

e is the elementary charge (1.602 $X10^{-12}$ coulombs), ε_r is the realative dielectric constant of water (80 Fm^{-1}), T is temperature in kelvin (300 K), and k_B is the Boltzman constant (1.3806$X10^{-23}$ m^2 kg s^{-2} K^{-1}). For these conditions, the Bjerrum length is equal to 0.71 nm.

Ha, B.-Y.; Thirumalai, D.; *Macromolecules* 1995, 28, 577-581.

3.9.2 Persistence Length Measurement By Using SEC

The following persistence length calculations and measurements for copolymer III were previously described by Li et al. in *Macromolecules* 2012, 45, 1595, and Mourey, T.; Le, K.; Bryan, T.; Zheng, S.; Bennett, G. *Polymer* **2005**, 46, 9033.

The copolymer was dissolved in DMF containing 0.1 M lithium nitrate and 1% formic acid at 1 mg/mL concentration. SEC was used to measure the molar mass of the copolymer and the Instrumentation consisted of a Agilent 1100 series isocratic pump,

autosampler and UV−visible absorption detector, Agilent PD2020 (formerly Precision Detectors) 15 and 90 deg elastic light scattering detector, Malvern 270 (formerly Viscotek) differential viscometry detector, and a Waters 410 differential refractive index detector plumbed in parallel with the differential viscometry detector.

Using the Bohdaneckỳ linear approximation, the persistence length was approximated by plotting the $M_w^2/[\eta]$ versus $M_w^{1/2}$. The slope (B_η) and intercept (A_η) are directly related to the persistence length of the polymer by the following equations.

$$\left(\frac{M_W{}^2}{[\eta]}\right)^{\frac{1}{3}} = A_\eta + B_\eta M_W{}^{\frac{1}{2}} \qquad (1)$$

$$A_\eta = \frac{A_o M_L}{\phi_\infty{}^{\frac{1}{3}}} \qquad (2)$$

$$B_\eta = \frac{B_o}{\phi_\infty{}^{\frac{1}{3}}}\left(\frac{2l_p}{M_L}\right)^{\frac{-1}{2}} \qquad (3)$$

The Φ_∞ is the limit of the viscosity function (2.86×10^{23}), B_o is constant (1.05) when the slope is linear (at low molar mass fractions), and M_L is the mass per unit Contour Length (610 g/nm for copolymer III). After plotting $M_w^2/[\eta]$ versus $M_w^{1/2}$, the slope ($B\eta$) was equal to 1.74 $g^{1/2}mol^{-1/6}mL^{-1/3}$. Using equation (3), the persistence length for copolymer polymer III equals 2.57 nm. This theory neglects excluded volume on molecular dimensions effects. At high molar mass, the viscosity expansion factor may not be negligible; therefore, the initial slope was taken.

Chapter 4: **Anti-HIV Activities of Precisely Defined, Semi-rigid, Carboxylated Alternating Copolymers**

4.1 *Authors*

Alice M. Savage[†], Yi Li[†], Lindsay E. Matolyak[†], Gustavo F. Doncel[§], S. Richard Turner[†], Richard D. Gandour*[†‡]

[†]Department of Chemistry MC0212 and Macromolecules and Interfaces Institute MC0344,

Virginia Tech, Blacksburg, Virginia 24061, United States

[§]CONRAD, Eastern Virginia Medical School, 601 Colley Ave., Norfolk, Virginia 23507, United States

[‡]Virginia Tech Center for Drug Discovery, Virginia Tech, Blacksburg, Virginia 24061, United States

4.2 *Keywords*

anti-HIV, microbicides, alternating copolymers, semi-rigid

4.3 *Abstract*

Di-*tert*-butyl (*E*)-4,4′-stilbenedicarboxylate and *tert*-butyl 4-vinylbenzoate were copolymerized with maleic anhydride and *tert*-butyl 4-maleimidobenzoate, individually and respectively. After conversion into polyanions, these four copolymers exhibited activity against four HIV-1 strains: IIIb, BaL, JR-CSF, and 92UG037. For both the IIIb and BaL HIV-1 strains, the lowest IC_{50} (0.095 and 0.23 μg/mL, respectively) values were obtained with poly(4,4′-stilbenedicarboxylate-*alt*-maleic acid) (DCSti-*alt*-MA). For JR-CSF and 92UG037, both tier 2 clinical isolates but different clades, DCSti-*alt*-MA exhibited the lowest IC_{50} (0.76 and 0.75 μg/mL, respectively). Although DCSti-*alt*-MA had the lowest IC_{50} in μg/mL for each strain, the other copolymers had IC_{50}s less than twofold higher. Further, these copolymers achieved high selectivity indices (>100) for these clinical isolates. Polymer rigidity, as measured by the statistical segment length, emerged as a key property when comparing anti-HIV activities with those of other polyanions. A speculative illustration was proposed for possible modes of inhibition.

4.4 *Introduction*

As of 2013, over 35.3 million people worldwide are living with HIV-1 and 2.3 million people are newly infected each year.[1] Developed as effective entry inhibitors to help prevent the spread of infection by HIV-1, polyanionic microbicides have a checkered

history.[2-4] At very low concentrations, polyanions effectively block the adsorption of virus to the surface of the host cell membrane through electrostatic interactions with the V3 loop of the HIV-1 glycoprotein 120 (gp120) or the glycoprotein 41 (gp41) complex[4-7] or both. Primarily comprising sulfonated and sulfated polymers, a library of polyanionic microbicides have shown anti-HIV activity in vitro at very low concentrations.[8,9] In spite of excellent in-vitro potencies, three sulfonated polyanions have failed Phase III clinical trials due to low efficacies, and, perhaps, enhanced infection.[8,10-13] Although many have abandoned polyanions as viable microbicides, others believe that polyanions are lead compounds that can be improved in terms of efficacy and safety to succeed ultimately in clinical trials. Pirrone et al.[8] state that efforts to develop microbicidal polyanions should proceed cautiously and be informed by the past. Romano et al.[14] conclude that products with a broad spectrum of activity, low toxicity, low risk of emerging resistance, and *low cost* are critical to the HIV prevention field. In addition, polyanions generally display antimicrobial activity against other sexually transmitted pathogens such as HSV-2,[15,16] HPV,[17] *Neisseria gonorrhoeae*[18] and *Chlamydia trachomatis*;[19] thus, they may be suitable ingredients for multipurpose prevention products.[15,18-21]

Concurrent with the development of other microbicidal polyanions,[9] poly(sodium 4-styrenesulfonate) (PSS) exhibited contraceptive abilities by being active against HIV-1 and other sexually transmitted pathogens in vitro.[22-24] Due to the inexpensive synthesis and broad antiviral activity, PSS was pursued as a microbicide candidate despite the relatively low activity.[22,25] Synthesized by radical polymerization techniques or through the sulfonation of polystyrene, PSS's robust history[26] in medical applications promised a

great rival to previously synthesized microbicides. In fact, a 2001 patent[25] claimed PSS as a viable method for the treating HIV infected cells. Anti-HIV activity improved with lower molar mass; an IC_{90} of 1.3 μg/mL or 282.6 nM for PSS of 4600 g/mol was reported.[25] Like PSS, dextran sulfate (DS) also exhibited increased anti-HIV activity against the IIIb strain with lower molar mass (e.g. IC_{50} of 0.2 μg/mL or 20 nM for DS of 10,000 g/mol).[15] Unfortunately, like the other polyanions in clinical trials, PSS and DS enhanced HIV infection in vitro after removal or washout of the microbicide.[8,27] Although only demonstrated in vitro on cell-based systems, the possibility of enhancing infection at low concentrations has been raised as a possible failure of some clinical trials.[8,27] However, enhanced HIV-1 infection after washout was not intrinsic to all polyanions.[27]

Several carboxylated copolymers made from maleic anhydride (MAn) and subsequently hydrolyzed to maleic acid (MA) showed potential as microbicides.[25,28-31] Poly(styrene-*alt*-maleic acid) (Figure 4.4.1, Sty-*alt*-MA), one of the most potent inhibitors against HIV-1 infection,[8,30] displayed no enhancement of infection after washout, and very low cytotoxicity in vitro.[27,29] This copolymer exhibited anti-HIV activity against several strains. Researchers[29,30] suggested that (a) the alternation of carboxylate ions (instead of sulfonate ions) with a hydrophobic phenyl group, (b) the location of the negative charge on the polymer backbone (instead of on the phenyl ring), and (c) two charges per repeat unit (RU) led to the improved microbicidal properties. A carboxylate- and sulfonate-containing copolymer, sulfonated poly(styrene-*stat*-maleic acid) (Sty-*stat*-MA), had outstanding anti-HIV activity (unidentified strain).[25] Similar to PSS, lower molar mass of

sulfonated Sty-*stat*-MA, with various comonomers ratios, improved antiviral activity (e.g., IC_{90} of 0.07 μg/mL or 11.5 nM for a copolymer of 6100 g/mol).[25] Another MA-containing copolymer, formed by polymerizing divinyl ether and MAn (DIVEMA), exhibited antiviral activity against the HIV-1 virus with an IC_{50} of 8 μg/mL.[31] All these MA-containing copolymers had very low cytotoxicity and potential to be viable microbicides.

From the drug-design perspective, the synthetic protocol controls the placement of functional groups along the polymer backbone. Comonomer reactivity ratios dictate the comonomer sequence distribution in radical copolymerizations. The sulfonated Sty-*stat*-MA described in Bellettini and Bellettini's patent[25] contains dyad sequences with adjacent sulfonate groups similar to those in PSS. It also contains unsulfonated dyad sequences similar to those in Sty-*alt*-MA and sulfonated dyad sequences that consist of a SS alternating with MA, poly(sodium 4-styrenesulfonate-*alt*-MA). Stilbene, a monomer related to styrene, readily copolymerizes with acceptor comonomers like MAn.[32] Because stilbene cannot homopolymerize (unlike styrene), any resulting copolymer contains *only* alternating sequences independent of monomer feed ratios. Ultimately, controlling the comonomer sequence distribution in a precise manner may lead to more potent, safer microbicides.

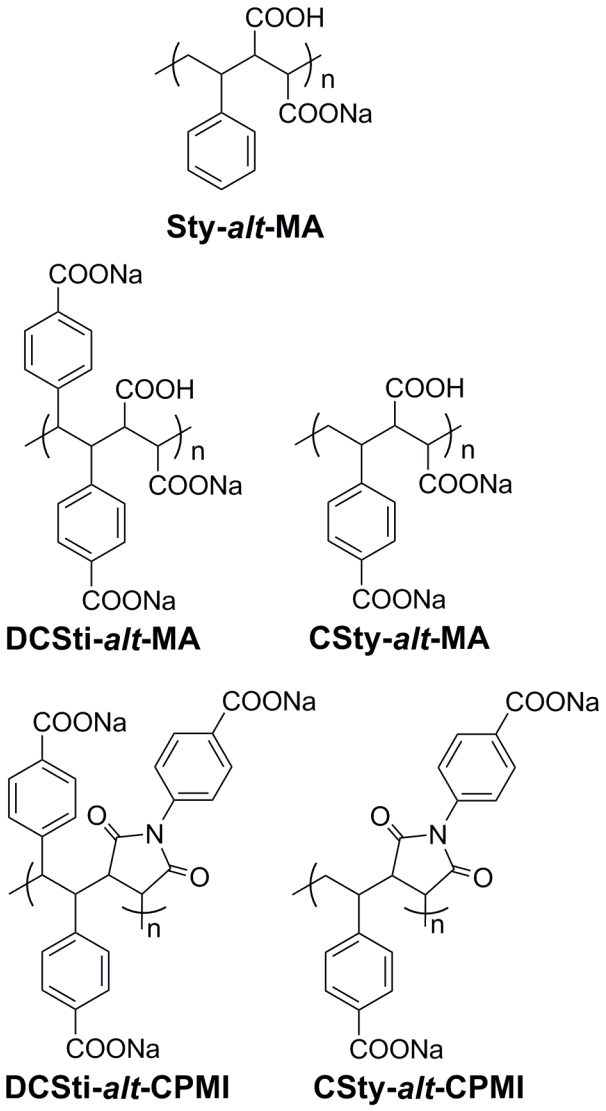

Figure 4.4.1 The structures of the alternating polyanions with antiviral properties at pH 7: Sty-*alt*-MA (poly(styrene-*alt*-maleic acid)), DCSti-*alt*-MA (poly(4,4′-stilbenedicarboxylate-*alt*-maleic acid)), CSty-*alt*-MA (poly(4-vinylbenzoate-*alt*-maleic acid)), DCSti-*alt*-CPMI (poly(4,4′-stilbenedicarboxylate-*alt*-4-maleimidobenzoate)), and CSty-*alt*-CPMI (poly(4-vinylbenzoate-*alt*-4-maleimidobenzoate)).

New classes of stilbene and styrene polyanions (Figure 4.4.1) synthesized by the Turner laboratory[33-35] offer an opportunity to develop new microbicides with precisely defined dyad sequences and molar masses. These copolymers are made from polymerizing relatively electron-rich comonomers, di-*tert*-butyl (*E*)-4,4′-stilbenedicarboxylate (DTBCSti) and *tert*-butyl 4-vinylbenzoate (TBCSty), with electron-poor comonomers, MAn and *tert*-butyl 4-maleimidobenzoate (TBCPMI), individually and respectively. The organic soluble copolymers, which are precursors to polyanions, enable complete characterization with respect to molar mass, degree of polymerization (DP), and polymer rigidity by circumventing difficulties in evaluating polyelectrolytes with traditional techniques like size exclusion chromatography (SEC). After deprotection, the resulting semi-rigid polyanions (Figure 4.4.1) comprise tunable, by pH, charge densities per RU with a similar alternating copolymer backbone to Sty-*alt*-MA. This strategy provides new, fully characterized copolymers for evaluation as anti-HIV microbicides.

Herein, we report anti-HIV and cytotoxicity assays of these copolymers against four viral strains. We explore whether the chemical structure, the DP, or physical properties (e.g., statistical segment length[35]) of the copolymers in Figure 4.4.1 contribute to the excellent anti-HIV activities of these copolymers. We have also adopted a similar approach to Rando et al.,[36] who studied phenyl carboxylates attached to cellulose acetate and suggested three criteria—(a) overall pK_a of the acids, (b) number of carboxyl groups per RU, and (c) DP—to improve microbicidal properties. Varying comonomer composition probes how the chemical structure (pK_a, number of carboxyl groups per RU, distance from the backbone) affect activity. Changing the DP probes how the length of the

molecules affects activity. Changing the statistical segment length of the copolymers probes how rigidity affects activity. Of these, finding an ideal statistical segment length and DP for the polyanion to interact with gp120 or gp41 might optimize microbicidal properties.

4.5 *Results*

Table 4.5.1. Copolymers: Synthesis and Properties

Copolymer	M_n (kg mol^{-1})	DP	PDI
	Initiated with BPO		
DTBCSti-*alt*-MAn	4.7[a]	10	1.04
	40	84	1.08
	Initiated with DCP		
DTBCSti-*alt*-MAn	20	42	1.47
	110	230	1.50
DTBCSti-*alt*-TBCPMI	80	122	2.16
	Initiated with AIBN		
TBCSty-*alt*-MAn	30	99	1.95
	41	136	1.22
TBCsty-*alt*-TBCPMI	11	22	1.29
	94	197	1.94

[a] DP controlled with addition of CPDTC—RAFT chain transfer agent.

A series of *tert*-butyl-protected copolymers (Table 4.5.1, Figure 4.5.1) was synthesized by using both conventional radical and RAFT polymerization techniques. This protection

strategy enabled polymer characterization in common organic solvents, thus, reducing the typical difficulties in analyzing water soluble polyanions. The resulting number average molar masses (M_n), DP, and polydispersity index (PDI) were measured by SEC in THF. Initiator concentration roughly regulated DP in the conventional radical polymerizations with little control over their respective PDIs. To synthesize lower molar mass copolymers, the RAFT agent, 2-cyano-2-propyl dodecyl trithiocarbonate (CPDTC), was added to the reaction mixture. Further characterization of similar copolymers was reported.[33,35]

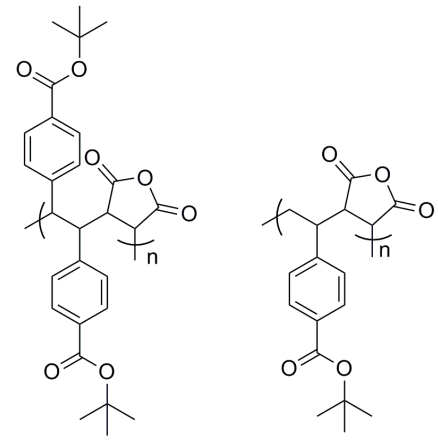

DTBCSti-*alt*-MAn **TBCSty-*alt*-MAn**

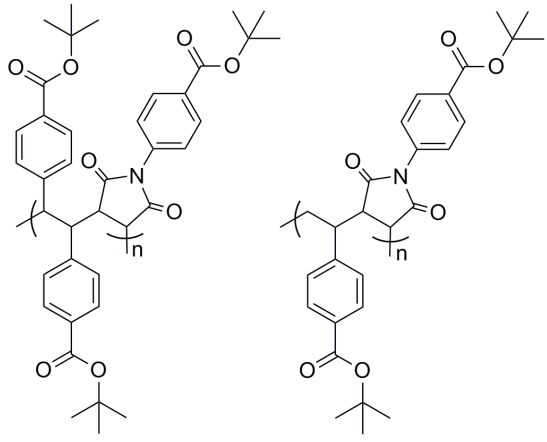

DTBCSti-*alt*-TBCPMI **TBCSty-*alt*-TBCPMI**

Figure 4.5.1 Alternating *tert*-butyl-protected precursor copolymers**.**

Treating *tert*-butyl-protected copolymers with TFA followed by neutralization gave carboxylates. Alkaline hydrolysis of the MAn-containing copolymers afforded the final polyanions (Figure 4.5.1, Tables 4.5.1–4.5.2). Complete conversion of the protected copolymers was confirmed by FTIR spectroscopy after dialysis of the four polyanions—DCSti-*alt*-MA, CSty-*alt*-MA, DCSti-*alt*-CPMI, CSty-*alt*-CPMI.

Table 4.5.2. Initial Assays of Antiviral Activity of Carboxylated Polyanions in Single-round Infection against HIV-1_{BaL} and HIV-1_{IIIB}

Copolymer	carboxyl/RU[a]	DP	IC_{50} (μg/mL)		IC_{50} (nM)[b]		Selectivity Index[c]	
			IIIb	BaL	IIIb	BaL	IIIb	BaL
DCSti-*alt*-MA	4	10	0.099	0.30	22	67	>1000	>330
	4	42	0.095	0.23	5.0	12	>1100	>440
	4	84	0.20	1.6	5.3	42	>500	>60
	4	230	0.52	1.3	5.0	13	>190	>80
CSty-*alt*-MA	3	99	0.47	0.80	15	26	>210	>130
	3	136	0.66	0.45	16	11	>150	>220
DCSti-*alt*-CPMI	3	122	0.76	1.2	11	18	>130	>80
CSty-*alt*-CPMI	2	197	0.23	1.0	2.9	12	>440	>100

[a]repeat unit. [b]molar mass estimated for CPMI-containing copolymers by presuming complete conversion into polyanion with sodium counterions and for MA-containing copolymers by presuming complete conversion of the carboxylphenyls and conversion of MA into a carboxyl and a carboxylate with a sodium counterion. [c]CC_{50}(cytotoxicity)/IC_{50}, where CC_{50}(cytotoxicity) >100 μg/mL for all polyanions.

Table 4.5.3. Repeat Assays of Antiviral Activity of Carboxylated Polyanions in Single-round Infection against HIV-1_{BaL} and HIV-1_{IIIB}

Copolymer	carboxyl/ RU[a]	DP	IC_{50} (μg/mL)		IC_{50} (nM)		Selectivity Index[b]	
			IIIb	BaL	IIIb	BaL	IIIb	BaL
DCSti-*alt*-MA	4	10	<0.32	<0.32	<68	<68	>320	>320
	4	42	<0.32	1.22	<16	60	>320	>82
CSty-*alt*-MA	3	136	<0.32	0.56	<8	14	>320	>180
DCSti-*alt*-CPMI	3	122	<0.32	1.81	<4	23	>320	>55
CSty-*alt*-CPMI	2	22	<0.32	0.55	<30	52	>320	>180

[a]repeat unit. [b]CC_{50}(cytotoxicity)/IC_{50}, where CC_{50}(cytotoxicity) >100 μg/mL for all polyanions.

Table 4.5.4. Antiviral Activity of Carboxylated Polyanions in PBMCs against HIV-$1_{JR\text{-}CSF}$ and HIV-$1_{92UG037}$

Copolymer	DP	IC_{50} (μg/mL)		IC_{50} (nM)		Selectivity Index[b]	
		JR-CSF	92UG037	JR-CSF	92UG037	JR-CSF	92UG037
DCSti-*alt*-MA	10	1.17	2.27	250	480	>86	>44
	42	0.76	0.75	37	37	>130	>130
CSty-*alt*-MA	136	0.86	1.01	21	25	>120	>99
DCSti-*alt*-CPMI	122	1.04	1.26	13	16	>97	>79
CSty-*alt*-CPMI	22	0.97	0.99	92	94	>100	>100

[a]repeat unit. [b]CC_{50}(cytotoxicity)/IC_{50}, where CC_{50}(cytotoxicity) >100 μg/mL for all polyanions.

4.5.1 Biological Activity

Polyanions were assayed initially (Table 4.5.2) against infection in HeLa cells by two lab-adapted viral strains: IIIb (X4), which uses the α-chemokine receptor, CXCR4, and BaL (R5), which uses the β-chemokine receptor, CCR5.[37,38] In response to a recommendation to assay these copolymers against additional strains, polyanions were recently prepared from original stocks of *tert*-butyl-protected copolymers. We prepared only the two DCSti-*alt*-MA copolymers (DP = 10 and 42) with the best activity for further testing. Based on limited supplies, we prepared CSty-*alt*-MA (DP = 136), DCSti-*alt*-CPMI (DP = 122), and CSty-*alt*-CPMI (DP = 22).

Activities against IIIb and BaL were repeated to validate the initial results. All polymers showed excellent activity, expressed as μg/mL and nM, against both IIIb and BaL (Tables 4.5.1 and 4.5.2). Further, the polyanions showed excellent activity (Table 4.5.3) against infection in human peripheral blood mononuclear cells (PBMCs) by two clinical isolates from different clades, both tier 2: JR-CSF (clade B)[39] and 92UG037 (clade A).[40,41] In general, the activity against IIIb was greater than that against BaL, JR-CSF, and 92UG037; the latter three use the β-chemokine receptor, CCR5. No cytotoxicity was detected up to 100 μg/mL.

4.5.2Antiviral Activity Against the IIIb Strain

In the initial assay, all polyanions showed excellent activity against infection by the IIIb strain. Those excellent activities were validated in the repeat assays, although they were not measured below 0.32 μg/mL. In the DCSti-*alt*-MA series, the effect of DP on the

antiviral activity was explored in the initial assays; the two polyanions with lower DP had lower values of $IC_{50,}$ when expressed as μg/mL (Table 4.5.1). However, when expressed as nM, the copolymer with the lowest DP had the highest IC_{50}.

4.5.3Antiviral Activity Against the BaL Strain

In general, these polyanions had less activity against the BaL strain than that against the IIIb strain. All activities in both assays were ≤ 1.8 μg/mL. In the DCSti-*alt*-MA series, the effect of DP on the antiviral activity was explored in the initial assays (Table 4.5.1); the two polyanions with lower DP had lower values of $IC_{50,}$ when expressed as μg/mL. One copolymer, DCSti-*alt*-MA (DP = 10), had activities < 0.32 μg/mL in both assays (Tables 4.5.1 and 4.5.2). Although DCSti-*alt*-MA (DP = 42) was the most active in the initial assay (Table 4.5.1), the activity in the repeat assay (Table 4.5.2) was five-fold higher. The activities for CSty-*alt*-MA (DP = 136) were similar in both assays. The activity of CSty-*alt*-CPMI (DP = 22) in the repeat assay was better than CSty-*alt*-CPMI (DP = 197) when comparing IC_{50} in μg/mL but not when comparing IC_{50} in nM.

4.5.4 Antiviral Activity Against the JR-CSF Strain

In general, these polyanions had similar activities against the JR-CSF strain in PBMCs (Table 4.5.3) to those against the BaL strain in HeLa cells (Table 4.5.2). All copolymers had similar activities. Copolymer DCSti-*alt*-MA (DP = 42) was the most active in terms of IC_{50} in μg/mL; copolymer DCSti-*alt*-CPMI (DP = 122), in terms of nM.

4.5.5 Antiviral Activity Against the 92UG037 Strain

In general, these polyanions had similar activities against the 92UG037 strain in PBMCs (Table 4.5.3) to those against the BaL strain in HeLa cells (Table 4.5.2) and JR-CSF strain in PBMCs (Table 4.5.3). All copolymers had similar activities except for DCSti-*alt*-MA (DP = 10). Copolymer DCSti-*alt*-MA (DP = 42) was the most active in terms of IC_{50} in μg/mL; copolymer DCSti-*alt*-CPMI (DP = 122), in terms of nM.

4.6 *Discussion*

Organic-soluble precursor copolymers (Table 4.5.1, Figure 4.5.1) enable full polymer characterization (molar mass determination and DP) and circumvent characterization difficulties of water-soluble polymers. Converting precursor copolymers into water-soluble polyanions by TFA deprotection and alkaline neutralization (or hydrolysis of anhydride) renders carboxylated polyanions after dialysis, which removes excess small molecules (e.g., NaOH, NaO_2CCF_3). Confirmed by FTIR, complete hydrolytic ring opening of the anhydride occurs to give the final polyanions.[35] Having these precisely defined copolymers enables one to study structure–activity relationships with respect to anti-HIV activity.

4.6.1 Efficacy Against HIV Strains

In general, these copolymers (Tables 4.5.1–4.5.3) are more active against IIIb, which uses CXCR4, than the three strains that use CCR5. While all HIV viruses can be transmitted to the host cell, the R5 (BaL, JR-CSF, and 92UG037) viruses show higher replication and predominate over the X4 (IIIb) viruses after mucosal primary infections.[37] Consequently,

microbicides must have potent anti-HIV activity against R5 strains. From previous work,[29] Sty-*alt*-MA, PSS, and DS also show increased activity against the IIIb over the BaL strain; the authors attribute[29] this phenomenon to fewer basic residues in the V3 loop of the R5 strains.[7,41]

In examining Tables 4.5.2–4.5.3 for activity against three R5 strains, all copolymers have IC_{50}s in the range of 0.23–2.2 μg/mL. These excellent activities, especially against the two clinical isolates, make these copolymers promising anti-HIV agents. All four copolymers have lower IC_{50}s against BaL than those reported[29] for Sty-*alt*-MA, PSS, and DS. While one can consider antiviral activity in terms of both μg/mL and nM when comparing activities to other compounds, the selectivity index dictates the viability of a potential microbicide.

Given the similarly excellent anti-HIV results for all four copolymers, drawing any definitive conclusions about the overall pK_a, number of carboxyls per RU, chemical structure, DP, and physical properties within this set of copolymers remains speculation. In the paragraphs below, we suggest reasons for these excellent anti-HIV activity of this series.

4.6.2 Chemical Structure

The copolymers in Tables 4.5.1–4.5.3 are polycarboxylates and polycarboxylic acids. At neutral pH, the CSty and DCSti moieties are mono- and dicarboxylates, respectively. The CPMI moieties are carboxylates; the MA moieties, carboxylates and carboxylic acids.

The vicinal diacids formed on ring opening of MAn are not completely ionized at physiological pH. Titrations of Sty-*alt*-MA,[42-44] CSty-*alt*-MA,[45] and DCSti-*alt*-MA[45] reveal that at neutral pH the MA moiety has different microspecies: fully deprotonated, fully protonated, and a mixed degree of protonation. Caused by close proximity, the two vicinal carboxyl groups produce two different pK_a values (4.4 and 10.3 in deionized water)[42] that depend on the salt concentration and cause incomplete ionization between pH 3 and pH 12.5.[43,45] The small differences in activity among the four copolymers preclude drawing any conclusions based on number of carboxylates and carboxylic acids,

In contrast, sulfonated polymers and copolymers only contain charged moieties. Further, sulfonate ions are less basic than carboxylate ions. Consequently, carboxylates make stronger hydrogen bonds with ammonium ions than do sulfonates.[46] In addition, having a hydrogen bond donor (carboxylic acid) suggests that hydrogen bond acceptors on proteins can interact with MA-containing copolymers. The improved efficacy of MA-containing polyanions versus sulfonated-only polyanions may result from these hydrogen-bond-donor interactions in binding to gp41 on the HIV surface.[47]

CSty-*alt*-MA appears to be more active than Sty-*alt*-MA.[29,30] As stated above, Sty-*alt*-MA (DP = 1300) polyanion exhibits excellent antiviral activity with IC_{50} values of 5.0 μg/mL (14 nM) and 9 μg/mL (26 nM) for IIIb and BaL, respectively.[29] CSty-*alt*-MA has IC_{50} values of 0.47 μg/mL (15 nM) and 0.8 μg/mL (26 nM) for IIIb and BaL, respectively. Activity against the BaL strain has improved by replacing the phenyl (Sty)

with a 4-carboxyphenyl (CSty). Further, sulfonated Sty-*stat*-MA (3/1) has excellent activity (IC_{90} = 0.07 μg/mL, 11.5 nM) against infection by HIV-1 (unidentified, but likely the IIIb strain).[25] The increase in activity for copolymers containing a carboxylated or a sulfonated phenyl suggests that inhibition improves by decreasing the hydrophobicity of the phenyl.

A possible explanation for the decreased activity of Sty-*alt*-MA resides in the hydrophobic phenyl groups, which tend to promote aggregation,[44] which reduces the concentration available for inhibition. For CSty-*alt*-MA, the 4-carboxyphenyl ring diminishes the likelihood of aggregation. A side-by-side assay of CSty-*alt*-MA and Sty-*alt*-MA with similar DPs is needed to quantify the relationship between hydrophobicity and activity.

On the other hand, studies[31,47] on hydrophobized DIVEMA suggest a need for hydrophobicity in binding to gp41. DIVEMA, which has low cytotoxicity, has been extensively studied as an anti-tumor agent and an interferon inducer.[48] DIVEMA functionalized with bulky hydrophobic amines, which give maleamic acids, has excellent anti-HIV activity.[31,47] Tsetkov and Serbin[47] have identified by molecular modeling a hydrophobic pocket near the site where DIVEMA binds to gp41.

4.6.3 Degree of Polymerization

The data appear to support increased activity with lower DP for DCSti-*alt*-MA; the two copolymers (DP = 10 and 42) are more active against IIIb and BaL (Table 4.5.1) than two others (DP = 84 and 230). The better activity at lower DP for DCSti-*alt*-MA coincides with a similar study[25] of PSS, which displays optimal activity at a DP = 22.

4.6.4 Polymer Rigidity

Polymer rigidity, usually measured as persistence length or statistical segment length, depends on conformational constraints to chain flexibility. Systematically varying this property by changing comonomers can be compared to varying the amount of conformational constraints in a small molecule drug.[49] Moreover, the rigidity of the copolymer depends on composition and not DP. The rigidity of the polymer backbone could affect the antiviral activity of the copolymers.

By design, these sterically crowded copolymers have conformationally constrained backbones.[35] Measured by using SEC and small-angle X-ray scattering, the persistence lengths of the four uncharged copolymers (Figure 4.5.1) classify them as semi-rigid.[33] Persistence lengths (nm) from SEC of stilbene copolymers—DTBCSti-*alt*-MAn (3.0) and DTBCSti-*alt*-TBCPMI (6.1)—are longer than the comparable styrene copolymers—TBCSty-*alt*-MAn (2.6) and TBCsty-*alt*-TBCPMI (4.3).[33] Increasing rigidity follows the order: TBCSty-*alt*-MAn < DTBCSti-*alt*-MAn < TBCSty-*alt*-TBCPMI < DTBCSti-*alt*-TBCPMI. MAn-containing copolymers are less rigid than TBCPMI-containing copolymers with both stilbene and styrene.[33] As a reference, atactic polystyrene, a

flexible polymer, has a persistence length of 0.96 nm (measured by small angle neutron scattering);[50] carboxymethyl cellulose, a rigid cellulose derivative similar to cellulose sulfate (Ushercell), has a persistence length > 10 nm (measured by SEC).[51]

For charged polymers (Figure 4.4.1) in aqueous NaCl, the rigidity of the CSty-*alt*-MA, and DCSti-*alt*-MA polyanions can be calculated by using steady-state, solution rheology to measure the statistical segment length.[45] The intrinsic viscosity parallels the stiffness of the precursor copolymers, TBCSty-*alt*-MAn and DTBCSti-*alt*-MAn, where the latter is the stiffer polymer.[45] At 0.5% NaCl, statistical segment lengths of CSty-*alt*-MA and DCSti-*alt*-MA are 5.9 and 6.7 nm, ~2-fold longer than the persistence length of the uncharged precursor. As the concentration of salts in vaginal fluid[52] is 0.4–0.5 %, these polymers will remain semi-rigid. For comparison, PSS has a statistical segment length of 2.4–4.0 nm.[53,54] Aggregation prevents similar measurements being made for Sty-*alt*-MA,[44] whose rigidity is presumably less than or equal to that of CSty-*alt*-MA. By definition, the statistical segment lengths of CSty-*alt*-CPMI and DCSti-*alt*-CPMI are circa twice the persistence length. The statistical segment length follows the same order as increasing rigidity (viz., CSty-*alt*-MA < DCSti-*alt*-MA < CSty-*alt*-CPMI < DCSti-*alt*-CPMI). Consequently, these copolymers have longer statistical segment lengths than those of PSS, carrageenan, and PRO 2000 and shorter statistical segment lengths than those of cellulosic derivatives.

Is the statistical segment length (parentheses) relevant to anti-HIV activity? Perhaps! The consistently higher values for IC_{50} mentioned above for DCSti-*alt*-CPMI (12 nm) and the

consistently lower values for DCSti-*alt*-MA (6 nm) may be related to their statistical segment lengths. If one considers the dimensions of the gp120 and gp41 complexes as nano-targets on the surface of the virus, these copolymers can viewed as nano-agents. Having a nano-agent with the ideal size as defined by the statistical segment length might optimize anti-HIV activity.

4.6.5 Possible Modes of Inhibition

To speculate on the increased efficacy of these copolymers, we consider previous hypotheses for the mechanism of action of polyanions in preventing infection by HIV.[8,55] For infection to occur, HIV initially binds a V3 loop of gp120 to the host cell, $CD4^+$. Then, gp120 interacts with a co-receptor, CXCR4 or CCR5, inducing a six-helix bundle conversion of gp41, enabling membrane fusion.[44] In principle, interaction of a polyanion with gp120 or gp41 could inhibit any one (or more) of these three steps—binding, bundle conversion, and fusion. Polymers that contain carboxylates (e.g. cellulose acetate phthalate[4] and aurintricarboxylic acid[56]) are proposed to bind to the V3 loop of the gp120 complex. Copolymer DIVEMA is proposed to bind to the sub-trimolecular protein-like complex of the gp41 bundle.[47] An effective polyanion microbicide can be an entry inhibitor (neutralization of the V3 loops of the gp120 complexes)[57] and a fusion inhibitor (interaction with the gp41 complex to block bundle formation or fusion with host cell).[55]

These envelope proteins, gp120 and gp41, which are encoded by the env gene, form spikes on the surface of a virion (Figure 4.6.5.1). Each Env spike comprises a complex of three gp120 monomers atop a complex of three gp41 monomers in a mushroom-like

nano-structure. Each gp41 complex comprises three gp41 monomers in a tripod-like fashion and affixes the gp120 complex to the viral lipid membrane.[58] With 60–100 Env spikes on the surface of a virion,[58-61] it is estimated to take at least four to seven Env spikes binding to their respective co-receptors to infect the host cell.[60,62] By comparing the dimensions of the virion (nano-target) and the polyanion (nano-agent), one can speculate about the mechanism for interaction.[57-59,61,63] The sites where polyanions interact on both the gp120 complexes (V3 loop, ~2.5 × ~3.0 nm)[64] and the gp41 complexes (5.1 × 2.5 nm)[47] suggest that semi-rigid polymers are ideal nano-agents. The modeling study[47] on DIVEMA raises a critical question: do MA-containing polyanions bind to gp120 or gp41 or both?[8,55]

The topography of the viral surface (Figure 4.6.5.1) suggests different possible modes of inhibition by semi-rigid polyanions on the gp120 complex and on the gp41 complex. The increased rigidity of these copolymers compared to more flexible polyanions should increase interactions to the virion at gp120 or gp41 because of entropic gain.[65] We speculate that more rigid polymers with statistical segments lengths greater than 10 nm may only interact with gp120 because of the limited space to interact with gp41. Polymers with statistical segment lengths of < 7 nm have the potential to interact with both gp120 and gp41. As a result, they might inhibit viral entry more effectively than polymers with longer statistical segment lengths.

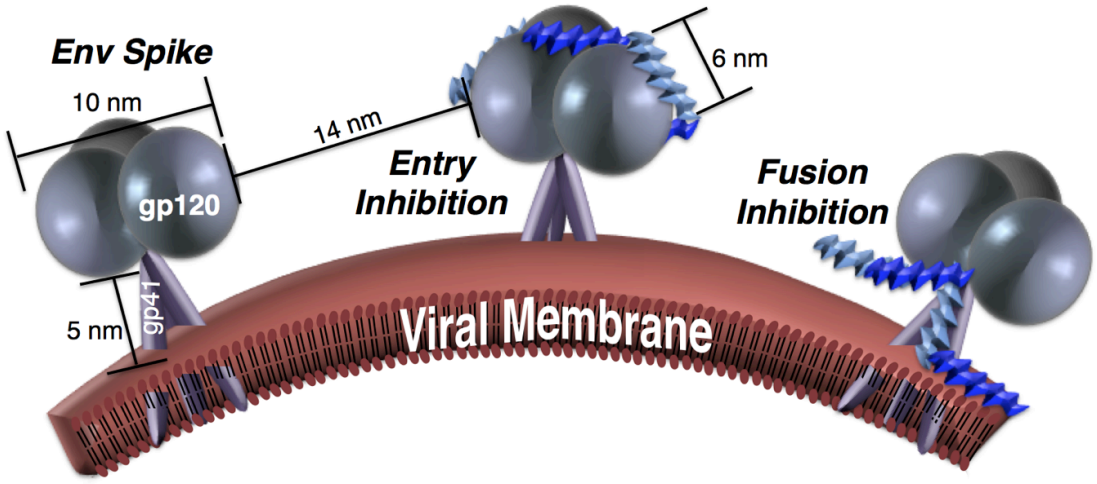

Figure 4.6.5.1 Speculative depiction of complexation of a semi-rigid polyanion to the Env spike, with distances from Zanetti et al.[59] Right: a bare Env spike with three gp120 monomers (grey spheres) atop three gp41 monomers (purple rods) assembled as a tripod following Sougrat et al.,[60] Liu et al.,[61] and Zhu et al.[58] Center and left: A semi-rigid polyanion indicated in blue and light blue to demarcate adjacent statistical segment lengths of DCSti-*alt*-MA. For entry inhibition, the polyanion is bridging two gp120 monomers. For fusion (or bundle formation) inhibition, a parallel axial alignment of the semi-rigid polyanion with gp41 stem, proposed by Tsvetkov and Serbin.[47]

4.7 *Conclusion*

With excellent anti-HIV activity, especially against infection by clinical isolates in PBMCs, and high selectivity indices, these carboxylated copolymers have potential as broad-spectrum polymer microbicides with reduced risks. They deserve further study as potential individual microbicides or as components of a combination of HIV inhibitors.

Importantly, unlike the very specific antiretroviral drugs currently in clinical testing, these polyanions have the potential to inhibit growth and replication of other sexually transmitted pathogens (e.g., HSV, HPV, *Neisseria gonorrhoeae*, and *Chlamydia trachomatis*); such studies are planned. Other beneficial properties are the high barrier to development of resistant virus and their lack of cross-resistance with drugs being utilized in HIV/AIDS therapy. With selectivity indices >100 against clinical isolates, these copolymers are among the most active broad-spectrum anti-HIV agents. The aqueous solubility of these polyanions ensures ease in microbicide formulation.

Systematic exploration of any polyanion must also include studies on the dependence of chemical structure, DP, and polymer rigidity in aqueous salt solutions. The results fuel our speculation that a nano target (Env spike) requires a nano drug (polyanion) because the statistical segment lengths of these polyanions match the dimensions of the proposed interaction sites on the Env spike. Finally, by combining high-tech, structural-biology methods with modern polymer science, one can design a polyanion as an optimal broad-spectrum microbicide.

4.8 *Experimental Section*

4.8.1 Materials

Di-*tert*-butyl (*E*)-4,4′-stilbenedicarboxylate (DTBCSti), *tert*-butyl 4-vinylbenzoate (TBCSty), *tert*-butyl 4-maleimidobenzoate (TBCPMI) monomers were synthesized as reported.[35] Maleic anhydride (MAn, Aldrich, ≥99.0%), 2,2′-azobisisobutyronitrile

(AIBN, Aldrich, 98%), dicumyl peroxide (DCP, Aldrich, 98%), benzoyl peroxide (BPO, Aldrich, ≥97.0%), 2-cyano-2-propyl dodecyl trithiocarbonate (CPDTC, Aldrich, 97%), TFA (Aldrich, 99%), sodium hydroxide (NaOH, Sigma-Aldrich, ≥98.0%), THF (Sigma-Aldrich, anhydrous, ≥99.9%), PhCl (Sigma-Aldrich, anhydrous, 99.8%), xylenes (Aldrich, ≥98.5%), hexanes (Fisher, HPLC grade), and CH_2Cl_2 (Fisher, HPLC grade) were used as received. Water was deionized before use.

4.8.2 Methods

tert-Butyl-protected copolymer precursors showed two peaks associated with the anhydride groups (1847 and 1777 cm^{-1}) in FTIR spectra. The 1:1 structures of the copolymers were confirmed by thermogravimetric analysis by comparing a mass loss of isobutylene caused by thermal cleavage of *tert*-butyl groups to the theoretical mass loss assuming the strictly alternating structure. Molar masses of the *tert*-butyl-protected copolymer precursors were measured by using SEC with a viscosity detector and a laser refractometer detector in $CHCl_3$ at 30 °C. Data were analyzed with a universal calibration made with polystyrene standards to obtain absolute molar mass. Polyanions were confirmed with FTIR by the absence of C=O absorptions for anhydride (1847 and 1777 cm^{-1}) and *tert*-butyl ester (1716 cm^{-1}). A Virtis lyophilizer (Gardiner, NY) equipped with a drum manifold and a condenser was used at a pressure of <30 mTorr.

4.8.3 Synthesis of Poly((di-*tert*-butyl 4,4′-stilbenedicarboxylate)-*alt*-maleic anhydride), (DTBCSti-*alt*-MAn), Initiated by DCP

DTBCSti (2.09 g, 5.5 mmol), MAn (0.54 g, 5.5 mmol), PhCl (8.4 mL, 20 wt%), DCP (0.0013 g, 0.05 wt%) were added to a 50-mL septum-sealed serum bottle with a stirbar.

The flask was purged with argon for 20 min, and then stirred at 110 °C for 24 h. A white solid was recovered by precipitating with hexanes (500 mL); then, redissolved in a minimal amount of THF and precipitated with hexanes (500 mL). A white solid was collected by vacuum filtration and dried under vacuum at 60 °C overnight (2.10 g, 80%). Molar mass was adjusted by varying the concentration of DCP initiator (0.05 and 1.0 wt%).

4.8.4 Synthesis of Poly((di-*tert*-butyl 4,4′-stilbenedicarboxylate)-*alt*-maleic anhydride), (DTBCSti-*alt*-MAn), Initiated by BPO

DTBCSti (0.96 g, 2.5 mmol), MAn (0.25 g, 2.5 mmol), PhCl (4.4 mL, 20 wt%), BPO (0.012 g, 1.0 wt%) were added to a 50-mL septum-sealed serum bottle with a stirbar. The flask was purged with argon for 20 min; then, stirred at 80 °C for 24 h. A white solid was recovered by precipitating with hexanes (500 mL); then, redissolved in a minimal amount of THF and precipitated with hexanes (500 mL). A white solid was collected by vacuum filtration and dried under vacuum at 60 °C overnight (0.75 g, 61%).

4.8.5 Synthesis of Poly((di-*tert*-butyl 4,4′-stilbenedicarboxylate)-*alt*-maleic anhydride), (DTBCSti-*alt*-MAn) by Using RAFT Polymerization

DTBCSti (1.5 g, 4 mmol), MAn (0.39 g, 4 mmol), CPDTC (0.079 g, 0.17 mmol), xylene (8.8 mL, 20 wt%), BPO (0.040 g, 2.0 wt%) were added to a 50-mL septum-sealed serum bottle with stirbar. The flask was purged with argon for 20 min, and then stirred for 24 h at 80 °C. A white solid was recovered by precipitating with hexanes (500 mL); then, redissolved in a minimal amount of THF and precipitated with hexanes (500 mL). A

white solid was collected by vacuum filtration and dried under vacuum at 60 °C overnight (1.08 g, 57%).

4.8.6 Synthesis of Poly((*tert*-butyl 4-vinylbenzoate)-*alt*-maleic anhydride), (TBCSty-*alt*-MAn), Initiated by AIBN

TBCSty (1.63 g, 8 mmol), MAn (0.78 g, 16 mmol), THF (10.9 mL, 20 wt%), AIBN (0.0242 g, 1.0 wt%) were added to a 50-mL septum-sealed serum bottle with stirbar. The flask was purged with argon for 20 min, and then stirred for 24 h at 60 °C. A white solid was recovered by precipitating with hexanes (500 mL); then, redissolved in a minimal amount of THF and precipitated with hexanes (500 mL). A white solid was collected by vacuum filtration and dried under vacuum at 60 °C overnight (1.31 g, 65%).

4.8.7 Synthesis of Poly((di-*tert*-butyl 4,4′-stilbenedicarboxylate)-*alt*-(*tert*-butyl 4-maleimidobenzoate)), (DTBCSti-*alt*-TBCPMI), Initiated by DCP

DTBCSti (1.02 g, 3 mmol), TBCPMI (0.73 g, 3 mmol), PhCl (6.3 mL, 20 wt%), DCP (0.003 g, 0.2 wt%) were added to a 50-mL septum-sealed serum bottle with stirbar. The flask was purged with argon for 20 min, and then stirred for 24 h at 110 °C. A white solid was recovered by precipitating with hexanes (500 mL); then, redissolved in a minimal amount of THF and precipitated with hexanes (500 mL). A white solid was collected by vacuum filtration and dried under vacuum at 60 °C overnight (1.29 g, 76%).

4.8.8 Synthesis of Poly((*tert*-butyl 4-vinylbenzoate)-*alt*-(*tert*-butyl 4-maleimidobenzoate)), (TBCSty-*alt*-TBCPMI), Initiated by AIBN

TBCSty (0.38 g, 2.0 mmol), TBCPMI (0.61 g, 2.4 mmol), THF (2.6 mL, 30 wt%), AIBN (0.001 g, 0.1 wt%) were added to a 50-mL septum-sealed serum bottle with stirbar. The flask was purged with argon for 20 min, and then stirred for 24 h at 60 °C. A white solid was recovered by precipitating with hexanes (500 mL); then, redissolved in a minimal amount of THF and precipitated with hexanes (500 mL). A white solid was collected by vacuum filtration and dried under vacuum at 60 °C overnight (0.40 g, 40%).

4.8.9 Synthesis of Poly((*tert*-butyl 4-vinylbenzoate)-*alt*-(*tert*-butyl 4-maleimidobenzoate)), (TBCSty-*alt*-TBCPMI) by Using RAFT Polymerization

TBCSty (0.57 g, 3 mmol), TBCPMI (0.76 g, 3 mmol), CPDTC (0.0091 g, 0.2 mmol), THF (6 mL, 20 wt%), AIBN (0.005 g, 0.03 mmol) were added to a 50-mL septum-sealed serum bottle with stirbar. The flask was purged with argon for 20 min, and then stirred for 24 h at 60 °C. A white solid was recovered by precipitating with hexanes (500 mL); then, redissolved in a minimal amount of THF and precipitated with hexanes (500 mL). A white solid was collected by vacuum filtration and dried under vacuum at 60 °C overnight (0.53 g, 40%).

4.8.10 Deprotection of MAn-containing Copolymers and Synthesis of Polyanions

. The typical procedure for deprotection and polyanion synthesis was as follows. DTBCSti-*alt*-MAn copolymer (0.70 g, 3 mmol of *tert*-butyl carboxylate group), TFA (0.75 g, 6.6 mmol) and CH_2Cl_2 (0.40 mL, 6.6 mmol) were added to a 10-mL round bottom flask and stirred for 12 h at room temperature. The excess of TFA and CH_2Cl_2

was evaporated by argon and the polymer was dried in vacuum oven for 24 h at 60 °C. The resulting white solid (0.54 g) was then dissolved in a stoichiometric amount of aq NaOH (H_2O, 12.8 mL and NaOH, 0.11 g). The solution was heated at 50 °C for 24 h. The solutions were placed in cellulose/ester membranes (MWCO 1000 g/mol), which were placed in a beaker with water (2 L); the water was stirred for 48 h after which time dialysis was presumed to be completed. The aqueous contents of the membranes were then frozen in liquid nitrogen and lyophilized for 24 h to yield a white fluffy solid, DCSti-*alt*-MA. Complete conversion into the polyanion was confirmed by FTIR.[35]

4.8.11 Deprotection of TBCPMI-containing Copolymers and Synthesis of Polyanions

For copolymers containing TBCPMI, deprotection with TFA gave a white solid, which was treated with NaOH, dialyzed and lyophilized in the same manner as the MAn-containing copolymers. Complete conversion into the polyanion was confirmed by FTIR.[35]

4.8.12 Anti-HIV and Cytotoxicity Assays [66]

Compound anti-HIV activity was evaluated in single-round (MAGI) infection assays by using X4 (IIIB) and R5 (BaL) HIV-1 and P4R5 cells expressing CD4 and co-receptors. In summary, P4R5 MAGI cells were cultured at a density of 1.2×10^4 cells/well in a 96-well plate approximately 18 h prior to infection. Cells were incubated for 2 h at 37 °C with purified, cell-free HIV-1 laboratory strains IIIb or BaL (Advanced Biotechnologies, Inc., Columbia, MD) in the absence or presence of each agent. After 2 h, cells were washed, cultured for an additional 46 h, and subsequently assayed for HIV-1 infection

using the Galacto-Star β-Galactosidase Reporter Gene Assay System for Mammalian Cells (Applied Biosystems, Bedford, MA). Reductions in infection were calculated as a percentage relative to the level of infection in the absence of agents, and 50% inhibitory concentrations (IC_{50}) were derived from regression analysis. Each compound concentration was tested in triplicate wells. Cell toxicity was evaluated by using the same experimental design but without the addition of virus. The impact of compounds on cell viability was assessed by using an MTT (reduction of tetrazolium salts) assay (Invitrogen, Carlsbad, CA).

4.8.13 Evaluation of Anti-HIV Activity in Single-Round Infection Assay

The single round infection assay was performed as previously described,[67] with slight modifications. MAGI-CCR5 cells derived from HeLa-CD4-LTR-β-gal cells (obtained from the NIH AIDS Research and Reference Reagent Program) were passaged in T-75 flasks prior to use in the antiviral assay. On the day preceding the assay, the cells were plated at 1.0×10^4 cells per well and incubated at 37 °C overnight in the presence or absence of virus. CXCR4-tropic virus strain HIV-1_{IIIB} or the CCR5-tropic virus strain HIV-1_{BaL} (obtained from the NIH AIDS Research and Reference Reagent Program) were diluted into tissue culture medium such that the amount of virus added to each well in a volume of 50 μL was approximately ten $TCID_{50}$/well. Compounds were evaluated at six concentrations (triplicate wells/concentration). Cell control wells (cells only) and virus control wells (cells plus virus) were included on each assay plate. Identical uninfected assay plates (virus replaced with media) were prepared for parallel cytotoxicity testing. The cultures were incubated for 48 h, after which antiviral efficacy was measured as the

inhibition of β-galactosidase reporter expression. Gal-screen™ reagent (Tropix, Bedford, MA) was added for chemiluminescent detection of β-galactosidase activity; the resulting chemiluminescence was measured with a Microbeta Trilux luminescence reader (PerkinElmer/Wallac). At assay termination, the cytotoxicity assay plates were stained with the soluble tetrazolium-based dye MTS (CellTiter Reagent, Promega) to determine cell viability and quantify compound toxicity.

4.8.14 Evaluation of Anti-HIV Activity in Human Peripheral Blood Mononuclear Cells (PBMCs)

As previously described for the standard PBMC assay,[68] phytohemagglutinin (PHA)-stimulated cells from at least two normal donors were pooled, diluted in fresh medium to a final concentration of 1×10^6 cells/mL, and plated in the interior wells of a 96 well round bottom microplate at 50 μL/well (5×10^4 cells/well). Each plate contained virus/cell control wells (cells plus virus), experimental wells (drug plus cells plus virus) and compound control wells (drug plus media without cells, necessary for MTS monitoring of cytotoxicity). Test drug dilutions were prepared at a 2× concentration in microtiter tubes; each concentration (100 μL, nine total concentrations) were placed in appropriate wells in the standard format. A predetermined dilution of virus stock (50 μL of HIV-1 JR-CSF or 92UG037) was placed in each test well (final MOI ≅ 0.1). The PBMC cultures were maintained for 7 d following infection at 37 °C and 5% CO_2. After this period, cell-free supernatant samples were collected for analysis of reverse transcriptase activity and/or p24 antigen content. Following removal of supernatant samples, compound cytotoxicity was measured by addition of the soluble tetrazolium-

based dye MTS (CellTiter 96 Reagent, Promega) to determine cell viability and quantify compound toxicity. IC_{50} (50% inhibition of virus replication), CC_{50} (50% cytotoxicity), and selectivity index values (CC/IC) were generated by using an in-house computer program.

4.9 *Author Information*

Corresponding Author

*540-231-3731, gandour@vt.edu (RDG)

Present Addresses

YL: Celanese Corporation

LEM: Case Western Reserve University, Cleveland, Ohio

Author Contributions

The manuscript was written through contributions of all authors. All authors have given approval to the final version of the manuscript.

4.10 *Abbreviations*

DTBCSti, di-*tert*-butyl (*E*)-4,4′-stilbenedicarboxylate; TBCSty, *tert*-butyl 4-vinylbenzoate; TBCPMI, *tert*-butyl 4-maleimidobenzoate; MAn, maleic anhydride; MA, maleic acid; AIBN, 2,2′-azobisisobutyronitrile; DCP, dicumyl peroxide; BPO, benzoyl peroxide; CPDTC, 2-cyano-2-propyl dodecyl trithiocarbonate; Sty-*alt*-MA, poly(styrene-*alt*-(maleic acid)); DCSti-*alt*-MA, poly((4,4′-stilbenedicarboxylate)-*alt*-(maleic acid));

CSty-*alt*-MA, poly((4-vinylbenzoate)-*alt*-(maleic acid)); DCSti-*alt*-CPMI, poly((4,4′-stilbenedicarboxylate)-*alt*-(4-maleimidobenzoate)); CSty-*alt*-CPMI, poly((4-vinylbenzoate)-*alt*-(4-maleimidobenzoate)); Env spike, envelope glycoprotein complex; gp120, glycoprotein 120; gp41, glycoprotein 41; PSS; poly(sodium 4-styrenesulfonate); DIVEMA, divinyl ether/maleic anhydride; DP, degree of polymerization; RU, repeat unit; Sty-*stat*-MA, poly (styrene-*stat*-maleic acid); IIIb, X4 variant of HIV-1; BaL, R5 variant of HIV-1; DS, dextran sulfate; M_n, number average molecular weight; CXCR4, α-chemokine receptor; CCR5, β-chemokine receptor; RAFT, reversible addition/fragmentation chain transfer; SEC, size exclusion chromatography; PDI, polydispersity index.

4.11 *References*

(1) WHO/UNAIDS. Joint United Nations Programme on HIV/AIDS/World Health Organization AIDS epidemic update http://www.who.int/hiv/en/ (accessed March 11, 2014).

(2) Mitsuya, H.; Looney, D. J.; Kuno, S.; Ueno, R.; Wong-Staal, F.; Broder, S. Dextran sulfate suppression of viruses in the HIV family: inhibition of virion binding to CD4+ cells. *Science* **1988**, *240*, 646–649.

(3) Ito, M.; Baba, M.; Sato, A.; Pauwels, R.; De Clercq, E.; Shigeta, S. Inhibitory effect of dextran sulfate and heparin on the replication of human immunodeficiency virus (HIV) in vitro. *Antiviral Res.* **1987**, *7*, 361–367.

(4) Neurath, A. R.; Strick, N.; Li, Y.-Y.; Debnath, A. K. Cellulose acetate phthalate, a common pharmaceutical excipient, inactivates HIV-1 and blocks the coreceptor binding site on the virus envelope glycoprotein gp120. *BMC Infect. Dis.* **2001**, *1*, 17.

(5) Baba, M.; Pauwels, R.; Balzarini, J.; Arnout, J.; Desmyter, J.; De Clercq, E. Mechanism of inhibitory effect of dextran sulfate and heparin on replication of human immunodeficiency virus in vitro. *Proc. Natl. Acad. Sci. USA* **1988**, *85*, 6132–6136.

(6) Callahan, L. N.; Phelan, M.; Mallinson, M.; Norcross, M. A. Dextran sulfate blocks antibody binding to the principal neutralizing domain of human immunodeficiency virus type 1 without interfering with gp120-CD4 interactions. *J. Virol.* **1991**, *65*, 1543–1550.

(7) Moulard, M.; Lortat-Jacob, H.; Mondor, I.; Roca, G.; Wyatt, R.; Sodroski, J.; Zhao, L.; Olson, W.; Kwong, P. D.; Sattentau, Q. J. Selective interactions of polyanions with basic surfaces on human immunodeficiency virus type 1 gp120. *J. Virol.* **2000**, *74*, 1948–1960.

(8) Pirrone, V.; Wigdahl, B.; Krebs, F. C. The rise and fall of polyanionic inhibitors of the human immunodeficiency virus type 1. *Antivir. Res.* **2011**, *90*, 168–182.

(9) McCarthy, T. D.; Karellas, P.; Henderson, S. A.; Giannis, M.; O'Keefe, D. F.; Heery, G.; Paull, J. R. A.; Matthews, B. R.; Holan, G. Dendrimers as drugs: discovery and preclinical and clinical development of dendrimer-based microbicides for HIV and STI prevention. *Mol. Pharm.* **2005**, *2*, 312–318.

(10) Van Damme, L.; Govinden, R.; Mirembe, F. M.; Guedou, F.; Solomon, S.; Becker, M. L.; Pradeep, B. S.; Krishnan, A. K.; Alary, M.; Pande, B.; Ramjee, G.; Deese, J.; Crucitti, T.; Taylor, D.; Murphy, S.; Wahala, L.; Callahan, M.; Gabelnick, H.; Acevedo, N.; Johnson, L.; Dube, K.; Chalkley, L.; Carayon-Lefebvre d'Hellencourt, F.; Combes, S.; Commins, M.; Tolley, E.; Corneli, A.; Law, M.; Rountree, W.; Saylor, L.; Fransen, K.; Beelaert, G.; Abdellati, S.; Mangelschots, M.; Buvé, A.; Moses, S.; Blanchard, J.; Washington, R. G.; Satyanarayana, R.; Mendonca, K.; Minani, I.; Massinga Loembé, M.; Anagonou, S.; Geraldo, N.; Ganesh, A. K.; Johnson, S.; Vasudevan, C. K.; Murugavel, K. G.; Edward, V.; Raju, E.; Singh, R.; Vasant, U.; Khoza, N.; Ganesh, S.; Nakabiito, C.; Nakintu, N.; Tenywa, T.; Musuuza, C.; Nagganda, J.; Nakimuli, M.; Gati, B.; Kagoda, J.; Kaddu, R.; Kintu, G.; Luzze, M.; Saunders, C. Lack of effectiveness of cellulose sulfate gel for the prevention of vaginal HIV transmission. *New. Engl. J. Med.* **2008**, *359*, 463–472.

(11) Cohen, J. Microbicide fails to protect against HIV. *Science* **2008**, *319*, 1026–1027.

(12) Halpern, V.; Ogunsola, F.; Obunge, O.; Wang, C.-H.; Onyejepu, N.; Oduyebo, O.; Taylor, D.; McNeil, L.; Mehta, N.; Umo-Otong, J.; Otusanya, S.; Crucitti, T.; Abdellati, S. Effectiveness of cellulose sulfate vaginal gel for the prevention of HIV infection: results of a Phase III trial in Nigeria. *PLoS ONE* **2008**, *3*, e3784.

(13) Warren, M.; Marshall, K. AVAC says MDP 301 microbicide trial results disappointing, but researchers and 9,400 trial volunteers deserve praise for successful trial. AVAC Global Advocacy for HIV Prevention

http://www.avac.org/press-release/avac-says-mdp-301-microbicide-trial-results-disappointing-researchers-and-9400-trial (accessed March 12, 2014).

(14) Romano, J. W.; Robbiani, M.; Doncel, G. F.; Moench, T. Non-specific microbicide product development: then and now. *Curr. HIV Res.* **2012**, *10*, 9–18.

(15) Witvrouw, M.; De Clercq, E. Sulfated polysaccharides extracted from sea algae as potential antiviral drugs. *Gen. Pharmacol.* **1997**, *29*, 497–511.

(16) Leydet, A.; Moullet, C.; Roque, J. P.; Witvrouw, M.; Pannecouque, C.; Andrei, G.; Snoeck, R.; Neyts, J.; Schols, D.; De Clercq, E. Polyanion inhibitors of HIV and other viruses. 7. Polyanionic compounds and polyzwitterionic compounds derived from cyclodextrins as inhibitors of HIV transmission. *J. Med. Chem.* **1998**, *41*, 4927–4932.

(17) Buck, C. B.; Thompson, C. D.; Roberts, J. N.; Müller, M.; Lowy, D. R.; Schiller, J. T. Carrageenan is a potent inhibitor of papillomavirus infection. *PLoS PATHOG* **2006**, *2*, e69.

(18) Anderson, R. A.; Feathergill, K., A.; Diao, X.-H.; Cooper, M.; Kirkpatrick, R.; Spear, P.; Waller, D. P.; Chany, C.; Doncel, G. F.; Herold, B.; Zaneveld, L. J. D. Evaluation of poly(styrene-4-sulfonate) as a preventive agent for conception and sexually transmitted diseases. *J. Androl.* **2000**, *21*, 862–875.

(19) De Clercq, E. Suramin in the treatment of AIDS: mechanism of action. *Antiviral Res.* **1987**, *7*, 1–10.

(20) Pauwels, R.; De Clercq, E. Development of vaginal microbicides for the prevention of heterosexual transmission of HIV. *J. Acquired Immune Defic. Syndr. Hum. Retrovirol.* **1996**, *11*, 211–221.

(21) Holt Young, B.; Kilbourne-Brook, M.; Stone, A.; Harrison, P.; Shields, W. C. Multipurpose prevention technologies for sexual and reproductive health: gaining momentum and promise. *Contraception* **2010**, *81*, 177–180.

(22) Herold, B. C.; Bourne, N.; Marcellino, D.; Kirkpatrick, R.; Strauss, D. M.; Zaneveld, L. J. D.; Waller, D. P.; Anderson, R. A.; Chany, C. J.; Barham, B. J.; Stanberry, L. R.; Cooper, M. D. Poly(sodium 4-styrene sulfonate): an effective candidate topical antimicrobial for the prevention of sexually transmitted diseases. *J. Infect. Dis.* **2000**, *181*, 770–773.

(23) Zaneveld, L. J. D.; Waller, D. P.; Anderson, R. A.; Chany, C., II; Rencher, W. F.; Feathergill, K.; Diao, X.-H.; Doncel, G. F.; Herold, B.; Cooper, M. Efficacy and safety of a new vaginal contraceptive antimicrobial formulation containing high molecular weight poly(sodium 4-styrenesulfonate). *Biol. Reprod.* **2002**, *66*, 886–894.

(24) Mauck, C. K.; Weiner, D. H.; Ballagh, S. A.; Creinin, M. D.; Archer, D. F.; Schwartz, J. L.; Pymar, H. C.; Lai, J.-J.; Rencher, W. F.; Callahan, M. M. Single and multiple exposure tolerance study of polystyrene sulfonate gel: a phase I safety and colposcopy study. *Contraception* **2004**, *70*, 77–83.

(25) Bellettini, A. G.; Bellettini, R. J. Method for the treatment of HIV infected cells; U.S. Patent 6,210,653 B, April 3, 2001.

(26) Harel, Z.; Harel, S.; Shah, P. S.; Wald, R.; Perl, J.; Bell, C. M. Gastrointestinal adverse events with sodium polystyrene sulfonate (Kayexalate) use: a systematic review. *Am. J. Med.* **2013**, *126*, 264.e269–264.e224.

(27) Pirrone, V.; Passic, S.; Wigdahl, B.; Krebs, F. C. Application and removal of polyanionic microbicide compounds enhances subsequent infection by HIV-1. *Virol. J.* **2012**, *9*, 1–13.

(28) Ding, J. L.; Ottenbrite, R. M. Optimization of poly(maleic acid-*alt*-2-cyclohexyl-1,3-dioxepin-5-ene) for anti-human immunodeficiency virus activity In *Polymeric Drugs and Drug Administration*; Ottenbrite, R. M., Ed.; ACS Symposium Series 545, American Chemical Society: Washington, DC, 1994, pp 135–147.

(29) Pirrone, V.; Passic, S.; Wigdahl, B.; Rando, R. F.; Labib, M.; Krebs, F. C. A styrene-*alt*-maleic acid copolymer is an effective inhibitor of R5 and X4 human immunodeficiency virus type 1 infection. *J. Biomed. Biotechnol.* **2010**, *2010*, 1–11.

(30) Fang, W.; Cai, Y.; Chen, X.; Su, R.; Chen, T.; Xia, N.; Li, L.; Yang, Q.; Han, J.; Han, S. Poly(styrene-*alt*-maleic anhydride) derivatives as potent anti-HIV microbicide candidates. *Bioorg. Med. Chem. Lett.* **2009**, *19*, 1903–1907.

(31) Serbin, A.; Karaseva, E.; Tsvetkov, V.; Alikhanova, O.; Rodionov, I. Hybrid polymeric systems for nano-selective counter intervention in virus life cycle. *Macromol. Symp.* **2010**, *296*, 466–477.

(32) Lewis, F. M.; Mayo, F. R. Copolymerization. IX. Comparison of some cis and trans isomers. *J. Am. Chem. Soc.* **1948**, *70*, 1533–1536.

(33) Li, Y.; Zhang, M.; Mao, M.; Turner, S. R.; Moore, R. B.; Mourey, T. H.; Slater, L. A.; Hauenstein, J. R. Chain stiffness of stilbene containing alternating copolymers by SAXS and SEC. *Macromolecules* **2012**, *45*, 1595–1601.

(34) Li, Y.; Turner, S. R. Free radical copolymerization of methyl substituted stilbenes with maleic anhydride. *Eur. Polym. J.* **2010**, *46*, 821–828.

(35) Li, Y.; Mao, M.; Matolyak, L. E.; Turner, S. R. Sterically crowded anionic polyelectrolytes with tunable charge densities based on stilbene-containing copolymers. *ACS Macro Lett.* **2012**, *1*, 257–260.

(36) Rando, R. F.; Obara, S.; Osterling, M. C.; Mankowski, M.; Miller, S. R.; Ferguson, M. L.; Krebs, F. C.; Wigdahl, B.; Labib, M.; Kokubo, H. Critical design features of phenyl carboxylate-containing polymer microbicides. *Antimicrob. Agents Chemother.* **2006**, *50*, 3081–3089.

(37) Locher, C. P.; Witt, S. A.; Kassel, R.; Dowell, N. L.; Fujimura, S.; Levy, J. A. Differential effects of R5 and X4 human immunodeficiency virus type 1 infection on $CD4^+$ cell proliferation and activation. *J. Gen. Virol.* **2005**, *86*, 1171–1179.

(38) Berger, E. A.; Doms, R. W.; Fenyö, E.-M.; Korber, B. T. M.; Littman, D. R.; Moore, J. P.; Sattentau, Q. J.; Schuitemaker, H.; Sodroski, J.; Weiss, R. A. A new classification for HIV-1. *Nature* **1998**, *391*, 240.

(39) Koyanagi, Y.; Miles, S.; Mitsuyasu, R. T.; Merrill, J. E.; Vinters, H. V.; Chen, I. S. Y. Dual infection of the central-nervous-system by AIDS viruses with distinct cellular tropisms. *Science* **1987**, *236*, 819–822.

(40) Gao, F.; Morrison, S. G.; Robertson, D. L.; Thornton, C. L.; Craig, S.; Karlsson, G.; Sodroski, J.; Morgado, M.; Galvao-Castro, B.; von Briesen, H.; Beddows, S.; Weber, J.; Sharp, P. M.; Shaw, G. M.; Hahn, B. H.; Osmanov, S.; Heyward, W. L.; Esparza, J.; van de Perre, P.; Karita, E.; Sempala, S.; Tugume, B.; Biryahwaho, B.; Wasi, C.; Rübsamen-Waigmann, H.; Holmes, H.; Newberry, A.;

Ranjbar, S.; Tomlinson, P.; Bradac, J.; Mullins, J. I.; Delwart, E. L.; Cheingsong-Popov, R.; Kaleebu, P.; Myers, G.; Korber, B. T. M.; Chiphangwi, J.; Taha, T.; Desormeaux, J.; Eiumtrakul, S.; Natpratan, C.; Khamboonruang, C.; Miotti, P.; Halsey, N. A.; Vlahov, D.; Nelson, K. E.; Phair, J.; Cao, Y.; Moore, J. P.; Ho, D. D.; Matocha, M.; Fowler, A.; Dilworth, S.; Sharma, O.; Brown, R.; Dusing, S.; Whitman, J.; Hoekzema, D.; Vogel, F. Molecular cloning and analysis of functional envelope genes from human immunodeficiency virus type 1 sequence subtypes A through G. *J. Virol.* **1996**, *70*, 1651–1667.

(41) Krachmarov, C.; Pinter, A.; Honnen, W. J.; Gorny, M. K.; Nyambi, P. N.; Zolla-Pazner, S.; Kayman, S. C. Antibodies that are cross-reactive for human immunodeficiency virus type 1 clade A and clade B V3 domains are common in patient sera from Cameroon, but their neutralization activity is usually restricted by epitope masking. *J. Virol.* **2005**, *79*, 780–790.

(42) Lazzara, T. D.; Whitehead, M. A.; van de Ven, T. G. M. Linear nano-templates of styrene and maleic anhydride alternating copolymers. *Eur. Polym. J.* **2009**, *45*, 1883–1890.

(43) Garrett, E. R.; Guile, R. L. Potentiometric titrations of a polydicarboxylic acid: maleic acid–styrene copolymer. *J. Am. Chem. Soc.* **1951**, *73*, 4533–4535.

(44) Garnier, G.; Duskova-Smrckova, M.; Vyhnalkova, R.; van de Ven, T. G. M.; Revol, J.-F. Association in solution and adsorption at an air–water interface of alternating copolymers of maleic anhydride and styrene. *Langmuir* **2000**, *16*, 3757–3763.

(45) Li, Y.; Savage, A. M.; Zhou, X.; Turner, S. R.; Davis, R. M. Solution properties of stilbene-containing sterically crowded alternating polyanions *J. Polym. Sci. Pol. Phys.* **2013**, *51*, 1565–1570.

(46) Gilli, P.; Pretto, L.; Bertolasi, V.; Gilli, G. Predicting hydrogen-bond strengths from acid-base molecular properties. The pK_a slide rule: toward the solution of a long-lasting problem. *Acc. Chem. Res.* **2009**, *42*, 33–44.

(47) Tsvetkov, V. B.; Serbin, A. V. A novel view of modelling interactions between synthetic and biological polymers via docking. *J. Comput. Aid. Mol. Des.* **2012**, *26*, 1369–1388.

(48) Butler, G. B. In *Cyclopolymerization and Cyclocopolymerization*; Marcel Dekker, Inc.: New York, New York, **1992**; Vol. 1, pp 472–474.

(49) Udugamasooriya, D. G.; Spaller, M. R. Conformational constraint in protein ligand design and the inconsistency of binding entropy. *Biopolymers* **2008**, *89*, 653–667.

(50) Fetters, L.; Lohse, D.; Colby, R. Chain dimensions and entanglement spacings In *Physical Properties of Polymers Handbook*; Mark, J. E., Ed.; Springer: New York, 2006, pp 445–452.

(51) Hoogendam, C. W.; de Keizer, A.; Cohen Stuart, M. A.; Bijsterbosch, B. H.; Smit, J. A. M.; van Dijk, J. A. P. P.; van der Horst, P. M.; Batelaan, J. G. Persistence length of carboxymethyl cellulose as evaluated from size exclusion chromatography and potentiometric titrations. *Macromolecules* **1998**, *31*, 6297–6309.

(52) Owen, D. H.; Katz, D. F. A vaginal fluid simulant. *Contraception* **1999**, *59*, 91–95.

(53) Oostwal, M.; Odijk, T. Novel dynamic scaling hypothesis for semidilute and concentrated solutions of polymers and polyelectrolytes. *Macromolecules* **1993**, *26*, 6489–6497.

(54) Pavlov, G. M.; Zaitseva, I. I.; Gubarev, A. S.; Gavrilova, I. I.; Panarin, E. F. Diffusion-viscometric analysis and conformational characteristics of sodium polystyrenesulfonate molecules. *Russ. J. Appl. Chem.* **2006**, *79*, 1490–1493.

(55) Cai, L.; Jiang, S. Development of peptide and small-molecule HIV-1 fusion inhibitors that target gp41. *ChemMedChem* **2010**, *5*, 1813–1824.

(56) Schols, D.; Pauwels, R.; Desmyter, J.; De Clercq, E. Dextran sulfate and other polyanionic anti-HIV compounds specifically interact with the viral gp120 glycoprotein expressed by T-cells persistently infected with HIV-1. *Virology* **1990**, *175*, 556–561.

(57) Magnus, C.; Regoes, R. R. Analysis of the subunit stoichiometries in viral entry. *PLoS ONE* **2012**, *7*, e33441.

(58) Zhu, P.; Winkler, H.; Chertova, E.; Taylor, K. A.; Roux, K. H. Cryoelectron tomography of HIV-1 envelope spikes: further evidence for tripod-like legs. *PLoS PATHOG* **2008**, *4*, e1000203.

(59) Zanetti, G.; Briggs, J. A. G.; Grünewald, K.; Sattentau, Q. J.; Fuller, S. D. Cryo-electron tomographic structure of an immunodeficiency virus envelope complex in situ. *PLoS PATHOG* **2006**, *2*, e83.

(60) Sougrat, R.; Bartesaghi, A.; Lifson, J. D.; Bennett, A. E.; Bess, J. W.; Zabransky, D. J.; Subramaniam, S. Electron tomography of the contact between T cells and SIV/HIV-1: implications for viral entry. *PLoS PATHOG* **2007**, *3*, e63.

(61) Liu, J.; Bartesaghi, A.; Borgnia, M. J.; Sapiro, G.; Subramaniam, S. Molecular architecture of native HIV-1 gp120 trimers. *Nature* **2008**, *455*, 109–114.

(62) Mulampaka, S. N.; Dixit, N. M. Estimating the threshold surface density of gp120-CCR5 complexes necessary for HIV-1 envelope-mediated cell-cell fusion. *PLoS ONE* **2011**, *6*, e19941.

(63) Roux, K. H.; Taylor, K. A. AIDS virus envelope spike structure. *Curr. Opin Struct. Biol.* **2007**, *17*, 244–252.

(64) Sander, O.; Sing, T.; Sommer, I.; Low, A. J.; Cheung, P. K.; Harrigan, P. R.; Lengauer, T.; Domingues, F. S. Structural descriptors of gp120 V3 loop for the prediction of HIV-1 coreceptor usage. *PLoS Comput. Biol.* **2007**, *3*, e58.

(65) Smyda, M. R.; Harvey, S. C. The entropic cost of polymer confinement. *J. Phys. Chem. B* **2012**, *116*, 10928–10934.

(66) Agarwal, H. K.; Doncel, G. F.; Parang, K. Synthesis and anti-HIV activities of suramin conjugates of 3'-fluoro-2',3'-dideoxythymidine and 3'-azido-2',3'-dideoxythymidine. *Med. Chem.* **2012**, *8*, 193–197.

(67) McMahon, J. B.; Currens, M. J.; Gulakowski, R. J.; Buckheit, R. W., Jr.; Lackman-Smith, C.; Hallock, Y. F.; Boyd, M. R. Michellamine B, a novel plant alkaloid, inhibits human immunodeficiency virus-induced cell killing by at least 2 distinct mechanisms. *Antimicrob. Agents Chemother.* **1995**, *39*, 484–488.

(68) Lackman-Smith, C.; Osterling, C.; Luckenbaugh, K.; Mankowski, M.; Snyder, B.; Lewis, G.; Paull, J.; Profy, A.; Ptak, R. G.; Buckheit, R. W., Jr.; Watson, K. M.; Cummins, J. E., Jr.; Sanders-Beer, B. E. Development of a comprehensive human immunodeficiency virus type 1 screening algorithm for discovery and preclinical testing of topical microbicides. *Antimicrob. Agents Chemother.* **2008**, *52*, 1768–1781.

4.12 *Supporting Information*

4.12.1 TOC Graphic

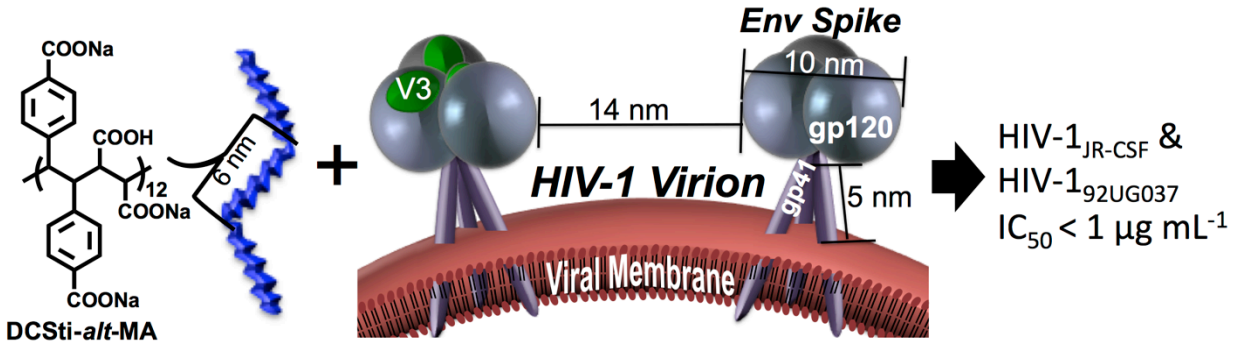

4.12.2 Experimental Error Analysis

Table 4.12.2.2 Standard Deviation of original Assays and repeat assays of antiviral activity of carboxylated polyanions in single-round infection against HIV-1_{BaL} and HIV-1_{IIIB}

Copolymer	carboxyl/RU[a]	DP	IC_{50} (µg/mL) IIIb		Std. dev.	IC_{50} (µg/mL) BaL		Std. dev.
			Trial 1	Trial 2	IIIb (µg/mL)	Trial 1	Trial 2	BaL (µg/mL)
DCSti-*alt*-MA	4	10	0.099	0.32	0.16	0.3	0.32	0.01
	4	42	0.095	0.32	0.16	0.23	1.22	0.70
CSty-*alt*-MA	3	136	0.66	0.32	0.24	0.45	0.56	0.08
DCSti-*alt*-CPMI	3	122	0.76	0.32	0.31	1.2	1.81	0.43

[a]repeat unit.

Chapter 5: **Synthesis, Diffusion-Ordered-NMR Characterization, and Anti-HIV Activity of Alternating, Sulfonated, Semi-rigid Polyanions**

5.1 *Abstract*

As a method to combat HIV-1 infection, a family of sulfonated, semi-rigid polyelectrolytes were synthesized and exhibited potent anti-HIV microbicidal behavior. Sodium *p*-styrenesulfonate and sodium *N*-(4-sulfophenyl)maleimide were copolymerized via reversible addition fragmentation chain transfer polymerization techniques by using a trithiocarbonate and a PEGylated-trithiocarbonate chain transfer agents. In what appears to be the first time, a diffusion-ordered NMR spectroscopy (DOSY-NMR) technique was used to calculate the molar mass of the respective polyanions because of severe difficulties encountered in our attempted aqueous SEC analysis of these charged polymers. Both the semi-rigid copolymers and diblock copolymers exhibited excellent activity against both the IIIb and BaL HIV-1 strains with the lowest IC_{50} of the series (0.316 and 1.46 μg/mL, respectively) obtained from poly(sodium *p*-styrenesulfonate-*alt*-sodium *N*-(4-sulfophenyl)maleimide)) with a degree of polymerization of 162. The effects of copolymer or block copolymer composition and polymer rigidity on antiviral activity were assessed. These semi-rigid, sulfonated polyanions appeared to improve activity compared to that reported for the more flexible polystyrene sulfonate (PSS).

5.2 *Introduction*

Anti-HIV microbicides have been developed in recent decades[1] to control the spread of HIV-1 and reduce the number of newly infected people (nearly 2.3 million people infected per year).[2] Polyanions (anionic polyelectrolytes) were demonstrated to display potential as anti-HIV microbicides for preventing infection by HIV-1. Presumably, polyanions block entry through electrostatic interactions with the glycoprotein (gp) complexes of gp120 or gp41 on the surface of the virion while still maintaining relatively low cytotoxicity.[1,3] Various polyanions have been assayed against HIV-1 and some have advanced to clinical trials: PRO2000 (naphthalene sulfonate),[4] cellulose sulfate,[5,6] and λ-carrageenan.[7] Even with good in-vitro efficacy, the Phase III clinical trials failed due to low in-vivo efficacy and, possibly, enhanced HIV infection.[1] Even with this checkered past, new polyanionic microbicides have potential to provide inexpensive protection against HIV infection to women across the world.[8] More recently, our study of carboxylated, semi-rigid, polyanions indicated that statistical segment lengths of 5–12 nm enhanced anti-HIV activity.[9]

From a biological perspective, PEG-containing polyanionic nanodrugs may increase efficacy in cervical mucosal tissue.[10] Polymeric nanoparticles coated with PEG, especially of low molar mass, show increased flow rates in cervical mucus.[11] Random PEGylation of cyanovirin decreases anti-HIV efficacy, perhaps due to a reduction in binding sites available for electrostatic intramolecular inhibition interactions.[12] However, a single-site, PEG-modified cyanovirin increases activity while reducing the production of cytokines.[12] These prior studies suggest that a single PEG block attached to an active, anionic polymer, would not decrease the efficacy *in vitro* by maintaining equal number of

anionic charges available for attachment. Yet, PEG-containing polyanions could be potentially safer and more active *in vivo*.

Synthetic polyanions or polyelectrolytes (water-soluble polymers with a high degree of ionizable groups of anionic, cationic, or ampholytic nature) have seemingly countless structural varieties and potential applications, e.g., anti-HIV microbicides,[1] water treatment,[13] oil recovery,[14] viscosity enhancers for drilling muds,[15,16] drug[17] and nonviral gene[18] delivery vehicles, and cosmetics.[19] Over the past decades, interest in synthesizing sequence-controlled polyelectrolytes increased due to a need for defect-free, precisely defined, sequenced polymers for biological applications.[20,21] With a lack of hierarchal structure control caused by limited control of microstructure and monomer sequences, synthetic polyelectrolytes have been plagued with a reduced efficacy or performance compared to the naturally occurring analogs.[20]

Researchers use reactivity ratios between monomers to predict monomer sequences from random, gradient, and to alternating.[22] These fundamental copolymerization parameters are important for controlling the sequence distribution of comonomers in the backbone which can affect the resulting polymer structure and ultimately the efficacy of the nanodrug. For example, copolymerizations of electron-rich styrenic monomers and electron-poor maleimide monomers with reactivity ratios equal to zero result in predominately alternating monomer sequences (styrene-maleimide dyads).[23] The alternating sequences and enchained maleimide rings give rise to sterically congested polymer backbones with more extended or semi-rigid polymer chains.[24] These strategies

(utilizing monomers with reactivity ratios equal to zero) provide a method to synthesize polyelectrolytes with predicted monomer sequences, which is imperative for use in drug design. For instance, the semi-rigid character of a family of carboxylated polyanions[25] appeared to increase the efficacy against HIV-1 infection compared to the flexible poly(sodium styrenesulfonate) (PSS) polyanion (864 kg/mol M_w, 30 μg/mL IC_{50} HIV-$1_{IIIb,}$ and 7 μg/mL IC_{50} HIV-1_{BaL})[26].

Characterizing these polymers presents another substantial challenge, since traditional aqueous size exclusion chromatography (SEC) can require specific optimal solvents and columns per polymer. As a result of failed SEC trials, diffusion-ordered (DOSY) NMR was employed to measure the molar masses of a family of sulfonated, semi-rigid polyanions. This appears to be the first reported study to apply this NMR technique to measure the molar mass of charged polymers.

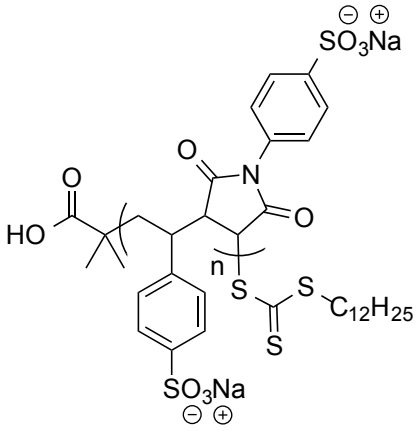

SSty-*alt*-SPMI

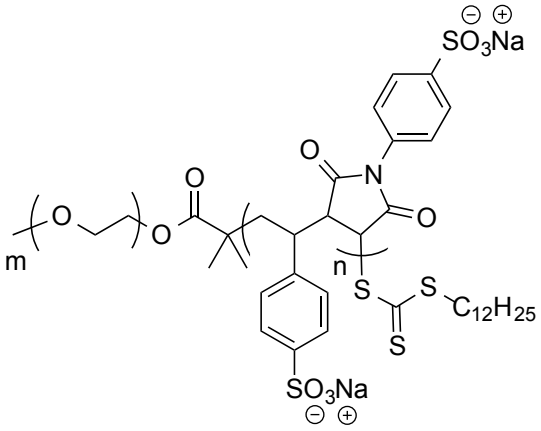

(SSty-*alt*-SPMI)-*b*-PEG

Figure 5.4.1 The structures of the alternating copolymers and block copolymers SSty-*alt*-SPMI, and (SSty-*alt*-SPMI)-*b*-PEG**.**

In this paper, we report the synthesis of a family of sulfonated alternating polyanions and block polyanions (Figure 5.4.1) and the determination of their molar mass by DOSY-NMR. Because these copolymers are examples of semi-rigid, polyanions, we have investigated their anti-HIV microbicidal properties.[25] Aqueous reversible addition fragmentation chain transfer (RAFT) polymerization techniques were used to polymerize sulfonated vinyl monomers (SSty and SPMI) as alternating polyanions (SSty-*alt*-SPMI and block polyanions, (SSty-*alt*-SPMI)-*b*-PEG (Figure 5.4.1). These polyanions (both copolymers and block copolymers) exhibited excellent antiviral activities when assayed against both the IIIb (X4) and the BaL (R5) variants of HIV-1. Both the IIIb and BaL strains are two of the most commonly assayed lab-adapted viral strains and were available to the researchers. These sulfonated copolymers provide a useful comparison with similar carboxylated copolymers as to how anionic structure affects anti-HIV activity.

5.3 *Results*

SPMI was synthesized[16,27,28] and copolymerized with SSty by using RAFT controlled radical polymerization techniques resulting in a family of alternating sulfonated copolymers and block copolymers (Figures 5.5.1). The mole percent of CTA was varied in order to achieve different molar mass. All copolymerizations proceeded to high monomer conversions (>90%). Dialysis was used to purify the resulting aqueous soluble copolymers.

The sulfonate polyanions were readily water-soluble; however, aqueous SEC analysis

was found to be problematic and no reliable results were obtained using different column packings with various aqueous solvents and additives. Because of this problem, we investigated the use of DOSY-NMR to determine molar mass for these polyanions. DOSY-NMR has been reported for the molar mass measurement of non-ionic organic-soluble polymers,[29-33] but we believe this is the first successful application of this technique to polyelectrolytes. The MWDs of the polyanions were not calculated due to the limited signal to noise ratio of the polyanion samples, although this is possible for many samples and will form the basis of future work in our laboratory.

Table 5.5.1. Antiviral Activity of Sulfonated Polyanions

Copolymer	M_w (kg/mol)	DP	IC_{50} (μg/mL)		IC_{50} (nM)[b]		Selectivity Index[a]	
			IIIb	BaL	IIIb	BaL	IIIb	BaL
SSty-*alt*-SPMI	73	152	0.44	1.8	6.0	25	>230	>56
	78	162	0.32	1.5	4.0	19	>320	>69
	82	170	0.38	2.4	4.6	30	>260	>43
	125	260	0.43	2.2	3.4	17	>230	>46
(SSty-*alt*-SPMI)-*b*-PEG	51	101	0.35	1.6	6.9	31	>290	>65
	123	250	0.32	2.0	2.6	15	>320	>51
	154	315	0.40	2.3	2.6	15	>250	>44
PSS[b26]	864	4190	30	7	35	8.1	–	–
CSty-*alt*-CPMI[b,c25]	94(M_n)	197	0.23	1.0	2.9	12	>440	>100

[a] CC_{50}(cytotoxicity)/IC_{50}, where CC_{50}(cytotoxicity) >100 μg/mL for all polyanions. [b] Results from previously reported assays.[25,26] [c] carboxystyrene-*alt*-carboxy-*N*-phenylmaleimide

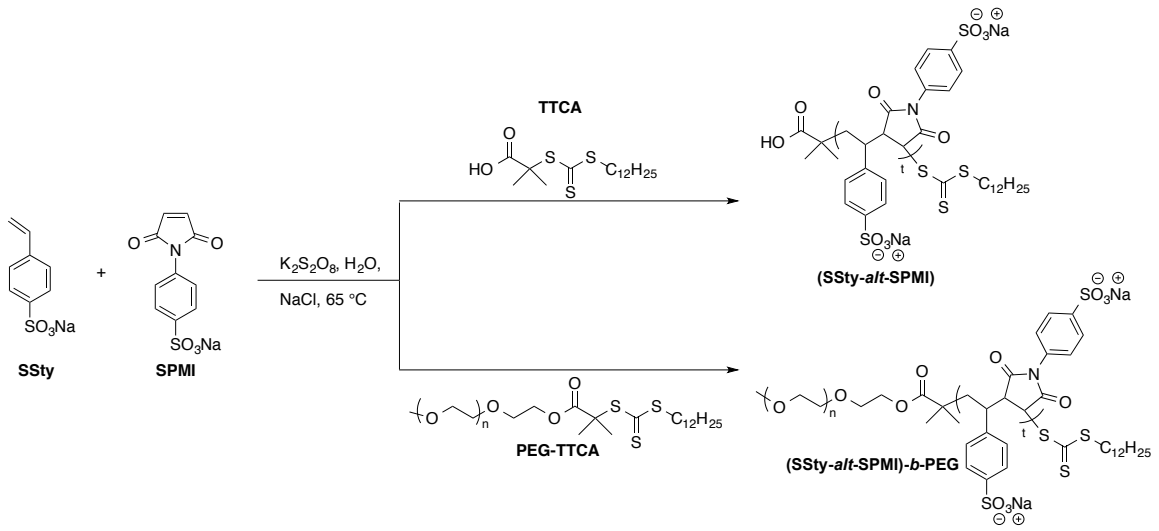

Figure 5.5.1 The RAFT polymerization of (SSty-*alt*-SPMI) copolymers and (SSty-*alt*-SPMI)-*b*-PEG block copolymers with TTCA and PEG-TTCA macroRAFT agents in water.

5.3.1 Molar Mass Measurements with DOSY-NMR

The correlation between polymer molar mass and self-diffusion coefficients was originally proposed Callaghan et al.[29] and was used to measure the size and shape of amylopectin. This method has been frequently used to measure the molar masses of uncharged polymers.[30-33] Here we implement DOSY-NMR to solve the long-standing problem in polymer science–that of measuring molar masses of ionic polymers. The dependence of molar mass M on self-diffusion coefficient D for a monodisperse polymer system[30] is described in equation 5.5.1.1, which can be linearized as equation 5.5.1.2. Parameters A and α vary for different polymer systems.

$$D = AM^{\alpha} \qquad \text{(eq, 5.5.1.1)}$$

$$logD = \alpha logM + logA \qquad \text{(eq, 5.5.1.1)}$$

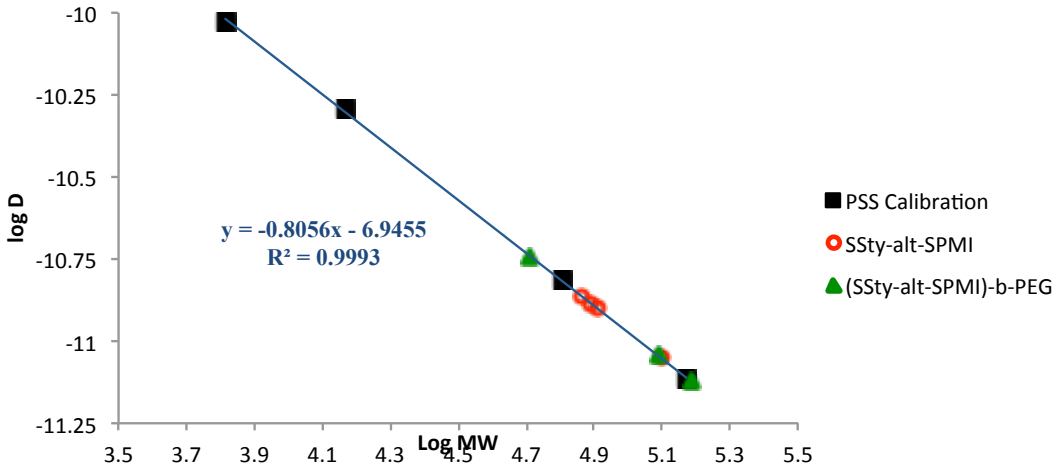

Figure 5.5.1.1 Calibration plot of the diffusion coefficients of four PSS standards measured by DOSY-NMR. For reference, the SSty-*alt*-SPMI and (SSty-*alt*-SPMI)-*b*-PEG polyanions were added.

All diffusion measurements were performed at 25 °C in dilute aqueous solutions of polymers with a concentration of 1 mg/mL. Polystyrene sulfonate (PSS) sodium salt standards were used to construct the linear calibration curve between the log D and M_w (Figure 5.5.1.1). Substituting measured D's for these copolymers into the resulting equation from the linear regression analysis of the calibration curve with α = -0.81and A = $10^{6.95}$ gave values of M_w (Table 5.5.1). Diffusion of water molecules was measured in each sample, and the consistency of water diffusion coefficients were used to correct for the effect of viscosity variation in all polymer solutions.

5.3.2 Biological Activity

Knowing the molar masses of SSty-*alt*-SPMI and (SSty-*alt*-SPMI)-*b*-PEG (Table 5.5.1) enabled evaluations of polymer properties and anti-HIV efficacy against the IIIb and BaL strains of the HIV-1 with respect to molar mass. Polyanions were assayed against infection in HeLa cells by two viral strains: IIIb (X4), which uses the α-chemokine receptor, CXCR4, and BaL (R5), which uses the β-chemokine receptor, CCR5.[34,35] All polymers showed excellent activity, expressed as μg/mL and nM, against both variants of HIV-1 (Table 5.5.1). In general, the activity against IIIb was greater than that against BaL. No cytotoxicity was detected up to 100 μg/mL. For the IIIb strain, both SSty-*alt*-SPMI and (SSty-*alt*-SPMI)-*b*-PEG exhibited no trends in IC_{50} versus M_w. For the BaL strain, SSty-*alt*-SPMI exhibited no trend in IC_{50} versus M_w. However, assays of (SSty-*alt*-SPMI)-*b*-PEG displayed a slight decrease in IC_{50} (μg/mL) with increasing M_w.

5.4 *Discussion*

Directly polymerizing water-soluble, sulfonate salt monomers with RAFT controlled radical techniques produces high yields of sulfonated polyanions. Unfortunately, neither SEC nor ^{1}H NMR spectroscopy can be used to measure the molar masses of these polyanions due to polymer-column interactions, slow molecular tumbling, short T_2 relaxation times, and broad peaks in ^{1}H NMR. However, DOSY-NMR provides an alternative solution for measuring the molar masses. To the best of our knowledge, our studies are the first example of using DOSY-NMR for this purpose with charged polymers; further investigations with this method are currently under study in our

laboratory.

Calibrating molar masses of PSS standards with measured diffusion coefficients by DOSY-NMR enables measuring molar masses of these polyanions from their measured diffusion coefficients. Notably, the measured molar masses are M_ws (weight-average molar masses); unfortunately, PDIs were not measured in this case due to low signal-to-noise ratio. Typical controlled radical polymerizations can produce polymers with PDI's <1.2, and conventional radical polymerizations typically produce polymers with PDI ~ 2. Unfortunately, for comparison with our previous study,[25] the number average molar masses (M_ns) cannot be estimated; they would be predicted to be approximately ≤ ½ of the M_w.

Comparing polymers produced by the two CTAs reveals similarities and differences in M_ws (Table 5.5.1). The polymers are listed by ascending M_w, which was controlled by concentrations of TTCA (4.6, 0.92, 0.46, and 0.23 mol%) and PEG-TTCA (0.92, 0.46, and 0.23 mol%). For SSty-*alt*-SPMI, three molar masses are very similar to each other even with different starting concentrations of TTCA. This could be due to the long reaction time (19 h), which results in higher monomer conversions. With controlled radical polymerization techniques like RAFT, monomer conversion should increase linearly as time increases. At high monomer conversions, typically the polydispersity increases due to unwanted polymer chain-end couplings or other termination reactions and could result in higher than expected molar masses. Therefore, more variation in molar mass is possible if shorter reaction times were used. For (SSty-*alt*-SPMI)-*b*-PEG,

the increasing molar masses correspond, within experimental error, with decreasing PEG-TTCA concentration. Perhaps the much larger size of PEG-TTCA prevents aggregation, which may have occurred with TTCA, a potential micelle former.

In conventional radical and controlled radical polymerizations, reactivity ratios of comonomers dictate monomer sequences in the resulting polymers.[22] With reactivity ratios of styrenic and maleimide monomers close to zero,[23] both (SSty-*alt*-SPMI) and (SSty-*alt*-SPMI)-*b*-PEG polyanions contain predominately alternating monomer sequences of SSty-SPMI dyads.

5.4.1 Anti-viral Activities of Sulfonated Polyanions and Block Polyanions

In general, (SSty-*alt*-SPMI) and (SSty-*alt*-SPMI)-*b*-PEG both show an increased activity against the IIIb virus (X4) over the BaL virus (R5). Other potential microbicides (e.g., poly(styrene-*alt*-maleic acid), dextran sulfate, and PSS) show this trend, where the increased activity could be due to the fewer positive charges on the BaL strain.[36] Both HIV viruses can be transmitted to the host cell; however, BaL viruses have higher replication after mucosal primary infections.[34] Therefore, microbicides must have high activity against R5 HIV viruses and still maintain high activity against X4 viruses.

For SSty-*alt*-SPMI, the small molar mass differences among polyanions result in only minor differences in efficacies against infection by either viral strain. For (SSty-*alt*-SPMI)-*b*-PEG, the anti-HIV activities for the BaL strain improve slightly with lower molar mass of SSty-*alt*-SPMI block; however, they remain similar for the IIIb strain.

Synthesizing copolymers with lower molar mass (< 40 kg/mol) may result in lower IC_{50}s for both SSty-*alt*-SPMI and (SSty-*alt*-SPMI)-*b*-PEG as seen for other polyanions.[37]

When comparing efficacies of SSty-*alt*-SPMI to (SSty-*alt*-SPMI)-*b*-PEG based on chemical structure, one must consider the architecture and functional groups of the copolymers. SSty-*alt*-SPMI copolymers are linear with alternating, sulfonated monomer sequences. While (SSty-*alt*-SPMI)-*b*-PEG copolymers contain linear polymer blocks of alternating, sulfonated monomer sequences attached to an additional linear PEG block. This diblock copolymer should enable the anionic (SSty-*alt*-SPMI) block to interact with binding sites on a virion similarly to the non-block copolymer. Indeed, the activities are quite similar among the seven copolymers.

The hypothesized retention of activity by adding a PEG block occurs as seen in the very minimal differences in activities between (SSty-*alt*-SPMI) and (SSty-*alt*-SPMI)-*b*-PEG for both IIIb and BaL strains. As expected, without a decrease or increase in functional groups that interact with the HIV virion, the anti-HIV activity would remain the same *in vitro*. Future *in-vivo* studies will compare the efficacies of (SSty-*alt*-SPMI) and (SSty-*alt*-SPMI)-*b*-PEG.

5.4.2 Copolymer Rigidity

Our recently published work[25] shows that polymer rigidity can significantly affect polyanion microbicide efficacy. Through electrostatic interactions, polyanions are

proposed to inhibit HIV-1 infection by blocking the attachment of the HIV virion to the host cell[1] or by interrupting fusion of the virion with host cell membranes.[32] Semi-rigid carboxylated polyanions[27] demonstrate an increased efficacy against HIV-1 infection due to their more extended polymer chains[25] that match the dimensions of the gp120 and gp41 complex.

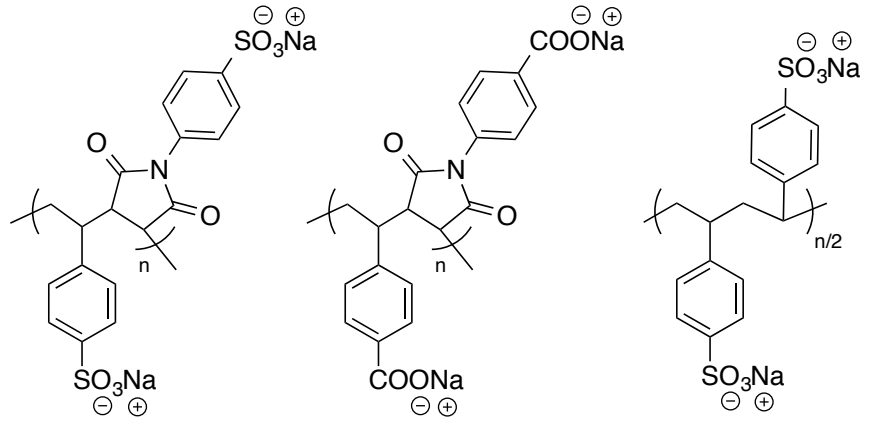

(SSty-*alt*-SPMI) **(CSty-*alt*-CPMI)** **PSS**

Figure 5.6.2.1 Formula comparison of anti-HIV polyanions: SSty-*alt*-SPMI, CSty-*alt*-CPMI, and PSS.

The polyanions synthesized herein contain very similar copolymer structures to those in our previous work.[25] As mentioned above, SSty-*alt*-SPMI and (SSty-*alt*-SPMI)-*b*-PEG copolymers contain predominately alternating monomer sequences with SSty-SPMI dyads and two sulfonate, anionic groups per repeat unit. These copolymers have the same polymer backbone (styrene–maleimide alternating monomer sequences) as poly(4-vinylbenzoate-*alt*-4-maleimidobenzoate) (CSty-*alt*-CPMI), which contains carboxylates in lieu of sulfonates. The intrinsic persistence length of the CSty-*alt*-CPMI copolymer is

4.3 nm (~8.6 nm statistical segment length).[24] The rigidities of both copolymers SSty-*alt*-SPMI and CSty-*alt*-CPMI are presumed to be the same.

Two semi-rigid copolymers, CSty-*alt*-CPMI and SSty-*alt*-SPMI (Figure 5.6.2.1), show an increased efficacy against IIIb and BaL compared to a flexible polyanion like PSS, which only contains SSty-SSty dyads. PSS has a statistical segment length of 2.4–4.0 nm[38,39] and exhibits an IC_{50} for the IIIb strain of 30 μg/mL and 7 μg/mL for the BaL strain.[26] CSty-*alt*-CPMI (94,000 g/mol M_n) exhibits an IC_{50} concentration of 0.23 μg/mL and 1.0 μg/mL for the IIIb and BaL HIV-1 strains, respectively.[25] CSty-*alt*-CPMI and SSty-*alt*-SPMI (82 kg/mol M_w, 0.38 μg/mL IC_{50} HIV-1_{IIIb} and 2.4 μg/mL IC_{50} HIV-1_{BaL}) have very similar activities but exhibit over a 10-fold increase in anti-HIV activity compared to PSS. With very similar anionic functional groups (sulfonatophenyl), the increased efficacy of SSty-*alt*-SPMI compared to PSS is likely due to the increased rigidity of the polymer backbone.

5.5 *Conclusions*

The copolymerization of SSty and SPMI accomplished with aqueous soluble RAFT agents results in new sulfonated polyanions and diblock polyanions. DOSY-NMR was employed for the first time on charged polyelectrolytes to measure the molar mass of the sulfonated polyanions, which show excellent potential as anti-HIV microbicidal candidates. Even though previous sulfonated polyanions have failed clinical trials,[1] SSty-*alt*-SPMI and (SSty-*alt*-SPMI)-*b*-PEG could potentially surpass their predecessors as an

effective anti-HIV microbicide with a one hundred-fold lower dosage (IC_{50}). These polyanions could also serve as more broad-spectrum microbicides to potentially inhibit other sexually transmitted pathogens like HSV, HPV, *Neisseria gonorrhoeae*, and *Chlamydia trachomatis*. Further biological testing is planned and needed to more accurately determine the efficacy of these polyanions *in vivo* and the effects of polymer rigidity on infection inhibition.

5.6 *Experimental*

5.6.1 Materials

2-(((Dodecylthio)carbonothioyl)thio)-2-methylpropanoic acid (TTCA) RAFT agent was synthesized as reported.[40] Maleic anhydride (MAn, Aldrich, ≥99.0%), sulfanilic acid (Aldrich, 98%), methanol (MeOH, Aldrich, 98%), ethanol (EtOH, Aldrich, ≥97.0%), potassium persulfate ($K_2S_2O_8$, Aldrich, 97%), sodium chloride (NaCl, Sigma-Aldrich, ≥98.0%), tetrahydrofuran (THF, Aldrich, anhydrous, ≥99.9%), sodium acetate (NaOAc, Sigma-Aldrich, ≥98.0%), acetic anhydride (Ac_2O, Sigma-Aldrich, ≥98.0%), *N*,*N*′-dicyclohexylcarbodiimide (DCC, Alrdrich, ≥98.0%), and 4-dimethyl-aminopyridine (DMAP, Aldrich, ≥98.0%) were used as received. Water was deionized before use. Sodium *p*-styrenesulfonate (SSty, Aldrich ≥98.0%) was recrystallized from 24:1 MeOH/H_2O.[41] Poly(ethylene glycol) monomethyl ether (2.5 kg/mol, PDI = 1.1, PEG, Aldrich, ≥98.0%) was dried in a vacuum oven at 40 °C for 24 h.

5.6.2 Methods

Unless stated otherwise, all reagents and solvents were used as received. Solutions were concentrated by rotary evaporation unless noted otherwise. Water was de-gassed under high vacuum for 20 min. A Virtis lyophilizer (Gardiner, NY) equipped with a drum manifold and a condenser was used at a pressure of <30 mTorr.

DOSY experiments were performed on a Bruker Avance III WB 400 MHz (9.4 *T*) NMR equipped with a single-axis diffusion probe (Diff60) having a maximum gradient of 2982 G/cm 50 A current. Pulsed-gradient stimulated echo (PGSTE) experiments[42,43] were used with gradient pulse durations δ of 1 ms and diffusion times Δ of 20 ms for all samples. Number of gradient steps was set from 10 to 16 with selection of maximum gradient strength from 500 to 1500 G/cm resulting in 10 to 30% of NMR signal attenuation. Number of scans varied from 4096 to 16384 in order to achieve sufficient signal-to-noise ratio due to differences in signal intensity among samples. Polystyrene sulfonate sodium salt SEC standards were purchased from Polymer Standards Service-USA with M_w 6520, 15800, 65400, and 14800, g mol^{-1} and MWDs <1.20. M_ws were measured in dihydrogen phosphate buffer at pH 11.

5.6.3 Synthesis of Sodium *N*-(4-sulfophenyl)maleimide (SPMI)

In a one-neck 1000-mL RBF equipped with a stir bar and septum, sulfanilic acid (20.0 g, 86.5 mmol) was dissolved in MeOH (400 mL) to produce a slightly purple solution. MAn (9.8 g, 100 mmol) was dissolved in MeOH (30 mL) in a separate 100-mL RBF. Under constant stirring, the MAn solution was added slowly with a syringe over 10 min to the

sulfanilic-acid solution to give a pale yellow solution. Ten minutes later, a yellow precipitate formed. The mixture was stirred at room temperature for 1 h. The yellow solid was filtered under vacuum, washed with MeOH (~300 mL), and dried in a vacuum oven at 60 °C overnight to yield *N*-(4-sulfophenyl)maleamic acid as a white solid (21.46 g, 85%). ^{1}H NMR (500 MHz, DMSO-d_6, δ): 10.45 (s, 1H, -COOH), 7.57 (m, 4H, Ar H), 6.49 (d, *J* = 15 Hz, 1H, -C*H*=), 6.32 (d, J = 15 Hz, 1H, -C*H*=). lit.[28] (90 MHz, D_2O)

N-(4-Sulfophenyl)maleamic acid (27.6 g, 94 mmol), NaOAc (3.95 g, 47 mmol), and Ac_2O (125 mL) were added to a 500-mL RBF with stir bar and septum with a needle to the atmosphere. *N*-(4-Sulfophenyl)maleamic acid did not completely dissolve, appearing as a yellow solid. The reaction flask was placed in an oil bath (80 °C) and stirred for 24 h. Green solids formed. The solids were filtered hot under vacuum and washed with EtOH (500 mL). The solids were heated with hot 30:2 EtOH/H_2O (1200 mL). The hot suspension was filtered; the filtrate was place a refrigerator (4 °C) for 2 d. The yellow solid was collected by vacuum filtration and analyzed by ^{1}H NMR for the presence of the maleamic acid (δ 6.49 & 6.32). The yellow solid was redissolved in hot 15:1 EtOH/H_2O (1200 mL). The hot suspension was filtered; the filtrate was placed in a refrigerator (4 °C) for 2 d. The yellow solids were collected by vacuum filtration and reanalyzed by ^{1}H NMR for the presence of maleamic acid. Finding none, the yellow solid was dried in the vacuum oven at 60 °C overnight to give a white solid (9.66 g, 35%). ^{1}H NMR (500 MHz, DMSO-d_6, δ): 7.68 (d, *J* = 10 Hz, 2H, Ar H), 7.28 (d, *J* = 10 Hz, 2H, Ar H), 7.18 (s, 2H, -C*H*=) lit.[27] (100 MHz, D_2O); lit.[16] (60 MHz, D_2O) ; lit.[28] (90 MHz, D_2O).

5.6.4 Synthesis of Methyl(poly(ethylene glycol))yl 2-(((dodecylthio)carbonothioyl)thio)-2-methylpropionate (PEG-TTCA)

TTCA (1.82 g, 5.00 mmol), dry poly(ethylene glycol) monomethyl ether (2.5 kg/mol, M_w/M_n = 1.1, 5.00 g, 2.50 mmol), DCC (1.03 g, 5.00 mmol), and DMAP (0.0600 g, 0.500 mmol) were added to a 100-mL RBF with stir bar and septa and purged with argon for 30 min. THF (40 mL) was added via a degassed syringe to the 100-mL RBF and stirred for 12 d at room temperature. The reaction solution was poured into of diethyl ether (500 mL), which was chilled in a dry ice/acetone bath. The resulting precipitate was filtered under vacuum to isolate a yellow solid, which was dried in a vacuum oven overnight at room temperature (1.00 g, 18.0%) (M_n = 2800 g/mol, PDI = 1.1, $CHCl_3$ SEC). ^{1}H NMR (500 MHz, DMSO-d_6, δ) 3.64 (t, 2 H), 3.50 (s, 232 H), 3.22 (t, 2 H), 1.70 (s, 6 H), 1.57 (p, 2 H), 1.29 (m, 18 H), 0.85 (t, 3 H).

5.6.5 Synthesis of Poly((sodium *p*-styrenesulfonate)-*alt*-(*N*-4-sulfophenylmaleimide)) (SSty-*alt*-SPMI)

SPMI (1.000 g, 3.6 mmol), SSty (0.749 g, 3.6 mmol), TTCA, ((0.006–0.121) g, ((0.016–0.332) mmol), NaCl (0.420 g, 7 mmol) and $K_2S_2O_8$, ((0.002–0.045) g, ((0.008–0.167) mmol) were added to a 50-mL serum bottle equipped with a stir bar and a septum. The flask was purged with argon, followed by adding degassed H_2O (16 mL) via syringe. The solution was purged with argon for 30 min, and then stirred for 19 h at 65 °C. The solution was cooled to room temperature and poured into acetone (600 mL). The precipitated white solid was filtered under vacuum, redissolved in water, and

reprecipitated in acetone (600 mL). The white solid was filtered under vacuum and dried in the vacuum oven at 60 °C overnight ((0.91–1.55 g), (51–91%)).

5.6.6 Synthesis of Poly((sodium 4-styrenesulfonate-*alt*-*N*-4-sulfophenylmaleimide)-*b*-poly(ethylene glycol)) ((SSty-*alt*-SPMI)-*b*-PEG)

SPMI (1.000 g, 3.6 mmol), SSty (0.749 g, 3.6 mmol), PEG-TTCA ((0.094–0.19) g, (0.033–0.072) mmol), NaCl (0.420 g, 0.007 mol) and $K_2S_2O_8$, (0.005 g, 0.016 mmol) were added to a 50-mL serum bottle equipped with a stir bar and a septum. The flask was purged with argon, followed by adding degassed H_2O (16 mL) via syringe. The solution was purged with argon for 30 min and then stirred for 19 h at 65 °C. The solution was cooled to room temperature and poured into acetone (600 mL). The precipitated white solid was filtered under vacuum, redissolved in water, and reprecipitated in acetone (600 mL). The white solid was vacuum filtered and dried in the vacuum oven at 60 °C overnight ((1.77–1.39) g, (71–97)%).

5.6.7 Purification of Polyanions

Samples (0.50 g) of SSty-*alt*-SPMI copolymers and (SSty-*alt*-SPMI)-*b*-PEG block copolymers were dissolved separately in H_2O (20 mL). Each solution was then individually added to a Spectra/Por® Cellulose Dialysis Membrane (MWCO: 1,000 g/mol) and placed in H_2O (1.0 L) for 2 d. For the first 12 h, the solution was replaced every 2 h with H_2O (1 L). The polymer solutions were taken out of the membranes, transferred to 100-mL RBFs, and placed in the freezer until solidified. Each solution was then lyophilized for 2 d to produce a white, fluffy solid.

5.6.8 Anti-HIV and Cytotoxicity Assays[44]

Compound anti-HIV activity was evaluated in single-round (MAGI) infection assays by using X4 (IIIB) and R5 (BaL) HIV-1 and P4R5 cells expressing CD4 and co-receptors. In summary, P4R5 MAGI cells were cultured at a density of 1.2×10^4 cells/well in a 96-well plate approximately 18 h prior to infection. Cells were incubated for 2 h at 37 °C with purified, cell-free HIV-1 laboratory strains IIIb or BaL (Advanced Biotechnologies, Inc., Columbia, MD) in the absence or presence of each agent. After 2 h, cells were washed, cultured for an additional 46 h, and subsequently assayed for HIV-1 infection using the Galacto-Star β-Galactosidase Reporter Gene Assay System for Mammalian Cells (Applied Biosystems, Bedford, MA). Reductions in infection were calculated as a percentage relative to the level of infection in the absence of agents, and 50% inhibitory concentrations (IC_{50}) were derived from regression analysis. Each compound concentration was tested in triplicate wells. Cell toxicity was evaluated by using the same experimental design but without the addition of virus. The impact of compounds on cell viability was assessed by using an MTT (reduction of tetrazolium salts) assay (Invitrogen, Carlsbad, CA).

5.7 *References*

(1) Pirrone, V.; Wigdahl, B.; Krebs, F. C. The rise and fall of polyanionic inhibitors of the human immunodeficiency virus type 1, *Antivir. Res.* **2011**, *90*, 168–182.

(2) Joint United Nations Programme on HIV/AIDS/World Health Organization AIDS epidemic update; WHO/UNAIDS, http://www.who.int/hiv/en/ (accessed June 12, 2014).

(3) Pirrone, V.; Passic, S.; Wigdahl, B.; Krebs, F. C. Application and removal of polyanionic microbicide compounds enhances subsequent infection by HIV-1, *Virol. J.* **2012**, *9*, 1–13.

(4) AVAC says MDP 301 microbicide trial results disappointing, but researchers and 9,400 trial volunteers deserve praise for successful trial.; Warren, M., Marshall, K., AVAC Global Advocacy for HIV Prevention: AVAC Global Advocacy for HIV Prevention, http://www.avac.org/ht/display/ReleaseDetails/i/4251/pid/212 (accessed March 12, 2014).

(5) Van Damme, L.; Wright, A.; Depraetere, K.; Rosenstein, I.; Vandersmissen, V.; Poulter, L.; McKinlay, M.; Van Dyck, E.; Weber, J.; Profy, A.; Laga, M.; Kitchen, V. A phase I study of a novel potential intravaginal microbicide, PRO 2000, in healthy sexually inactive women, *Sex Transm Infect* **2000**, *76*, 126-130.

(6) Halpern, V.; Ogunsola, F.; Obunge, O.; Wang, C. H.; Onyejepu, N.; Oduyebo, O.; Taylor, D.; McNeil, L.; Mehta, N.; Umo-Otong, J.; Otusanya, S.; Crucitti, T.; Abdellati, S. Effectiveness of cellulose sulfate vaginal gel for the prevention of HIV infection: results of a Phase III trial in Nigeria., *PLoS ONE* **2008**, *3*, e3784.

(7) Cohen, J. Microbicide fails to protect against HIV, *Science* **2008**, *319*, 1026–1027.

(8) Romano, J. W.; Robbiani, M.; Doncel, G. F.; Moench, T. Non-specific microbicide product development: then and now, *Curr. HIV Res.* **2012**, *10*, 9–18.

(9) Savage, A. M.; Li, Y.; Matolyak, L.; Doncel Gustavo, F.; Turner, S. R.; Gandour, R. D. Anti-HIV activities of precisely defined, semi-rigid, carboxylated alternating copolymers, *J. Med. Chem.* **2014**.

(10) Ensign, L. M.; Tang, B. C.; Wang, Y.-y.; Tse, T. A.; Hoen, T.; Cone, R.; Hanes, J. Mucus-penetrating nanoparticles for vaginal drug delivery protect against herpes simplex virus, *Sci. Transl. Med.* **2012**, *4*, 138ra179.

(11) Wang, Y.-Y.; Lai, S. K.; Suk, J. S.; Race, A.; Cone, R.; Hanes, J. Addressing the PEG mucoadhesivity paradox to engineer nanoparticles that "slip" through the human mucus barrier, *Angew. Chem., Int. Ed.* **2008**, *47*, 9726-9729.

(12) Zappe, H.; Snell, M. E.; Bossard, M. J. PEGylation of cyanovirin–N, an entry inhibitor of HIV, *Advanced Drug Delivery Reviews* **2008**, *60*, 79-87.

(13) Goldblatt, M. Wastewater treatment, *Chem. Eng. Prog.* **2008**, *104*, 35-36.

(14) Liao, W. P.; Chen, F.; Vasconcellos, S. R. Water soluble block copolymers and methods of use therof; United States Patent 5,234,604, August 10, 1993.

(15) Thaler, W. A.; Turner, S. R.; Walker, T. O. Sodium styrene sulfonate-co-sodium-*N*-(4-sulfophenyl)-maleimide- and improved viscosity control additive, United States Patent 4,425,461 A, Jan. 10, 1984.

(16) Turner, S. R.; Wardle, R.; Thaler, W. A. Poly(sodium styrene sulfonate-*alt*-sodium-*N*(4-sulfophenyl) maleimide): A new water-soluble alternating copolymer, *J. Polym. Sci. Pol. Chem. Ed.* **1984**, *22*, 2281–2285.

(17) Hu, S.-H.; Tsai, C.-H.; Liao, C.-F.; Liu, D.-M.; Chen, S.-Y. Controlled rupture of magnetic polyelectrolyte microcapsules for drug delivery, *Langmuir* **2008**, *24*, 11811–11818.

(18) Hemp, S. T.; Allen, M. H.; Green, M. D.; Long, T. E. Phosphonium-containing polyelectrolytes for nonviral gene delivery, *Biomacromolecules* **2011**, *13*, 231–238.

(19) Deckner, G. E.; Lombardo, B. S.; Containing a crosslinked polyacrylamide-type polymer and an active compound, optionally a humectant and an emollient, United States patent 5,707,635 A, Jan 13, 1998.

(20) Palermo, E. F.; Vemparala, S.; Kuroda, K. Antimicrobial polymers: Molecular design as synthetic mimics of host-defense peptides, *Tailored Polymer Architectures for Pharmaceutical and Biomedical Applications* **2013**, *1135*, 319–330.

(21) Lutz, J. F.; Ouchi, M.; Liu, D. R.; Sawamoto, M. Sequence-controlled polymers, *Science* **2013**, *341*, 628–635.

(22) Lewis, F. M.; Mayo, F. R. Copolymerization. IX. Comparison of some cis and trans isomers, *J. Am. Chem. Soc.* **1948**, *70*, 1533–1536.

(23) Hulubei, C.; Morariu, S. Functional copolymers of *N*-(4-formyl-phenoxy-4'-carbonylphenyl) maleimide with styrene, *High Perform. Polym.* **2000**, *12*, 367–375.

(24) Li, Y.; Zhang, M.; Mao, M.; Turner, S. R.; Moore, R. B.; Mourey, T. H.; Slater, L. A.; Hauenstein, J. R. Chain stiffness of stilbene containing alternating copolymers by SAXS and SEC, *Macromolecules* **2012**, *45*, 1595–1601.

(25) Savage, A. M.; Li, Y.; Matolyak, L.; Doncel, G. F.; Turner, S. R.; Gandour, R. D. Anti-HIV activities of precisely defined, semi-rigid, carboxylated alternating copolymers, *J. Med. Chem.* **2014**.

(26) Cheshenko, N.; Keller, M. J.; MasCasullo, V.; Jarvis, G. A.; Cheng, H.; John, M.; Li, J. H.; Hogarty, K.; Anderson, R. A.; Waller, D. P.; Zaneveld, L. J. D.; Profy, A. T.; Klotman, M. E.; Herold, B. C. Candidate topical microbicides bind herpes simplex virus glycoprotein B and prevent viral entry and cell-to-cell spread, *Antimicrob. Agents Chemother.* **2004**, *48*, 2025–2036.

(27) Keana, J. F. W.; Guzikowski, A. P.; Morat, C.; Volwerk, J. J. Detergents containing a If-diene group in the hydrophobic segment. Facile chemical modification by a Diels-Alder reaction with hydrophilic dienophiles in aqueous solution, *J. Org. Chem.* **1983**, *48*, 2661–2666.

(28) Hocking, M. B.; Syme, D. T.; Axelson, D. E.; Michaelian, K. H. Water- soluble imide- amide copolymers. I. Preparation and characterization of poly[acrylamide-*co*-sodium N-(4-sulfophenyl) maleimide], *J. Polym. Sci. Pol Chem.* **1990**, *28*, 2949–2968.

(29) Callaghan, P. T.; Lelievre, J. The size and shape of amylopectin: A study using pulsed-field gradient nuclear magnetic resonance, *Biopolymers* **1985**, *24*, 441–460.

(30) Chen, A.; Wu, D.; Johnson, C. S. Determination of molecular weight distributions for polymers by diffusion-ordered NMR, *J. Am. Chem. Soc.* **1995**, *117*, 7965–7970.

(31) Augé, S.; Schmit, P.-O.; Crutchfield, C. A.; Islam, M. T.; Harris, D. J.; Durand, E.; Clemancey, M.; Quoineaud, A.-A.; Lancelin, J.-M.; Prigent, Y.; Taulelle, F.; Delsuc, M.-A. NMR measure of translational diffusion and fractal dimension. application to molecular mass measurement, *J. Phys. Chem. B* **2009**, *113*, 1914–1918.

(32) Floquet, S.; Brun, S.; Lemonnier, J.-F.; Henry, M.; Delsuc, M.-A.; Prigent, Y.; Cadot, E.; Taulelle, F. Molecular weights of cyclic and hollow clusters measured by DOSY NMR spectroscopy, *J. Am. Chem. Soc.* **2009**, *131*, 17254–17259.

(33) Li, W.; Chung, H.; Daeffler, C.; Johnson, J. A.; Grubbs, R. H. Application of ^{1}H DOSY for facile measurement of polymer molecular weights, *Macromolecules* **2012**, *45*, 9595–9603.

(34) Locher, C. P.; Witt, S. A.; Kassel, R.; Dowell, N. L.; Fujimura, S.; Levy, J. A. Differential effects of R5 and X4 human immunodeficiency virus type 1 infection on CD4+ cell proliferation and activation, *J. Gen. Virol.* **2005**, *86*, 1171–1179.

(35) Berger, E. A.; Doms, R. W.; Fenyo, E.-M.; Korber, B. T. M.; Littman, D. R.; Moore, J. P.; Sattentau, Q. J.; Schuitemaker, H.; Sodroski, J.; Weiss, R. A. HIV-1 phenotypes classified by co-receptor usage, *Nature* **1997**, *391*, 240.

(36) Pirrone, V.; Passic, S.; Wigdahl, B.; Rando, R. F.; Labib, M.; Krebs, F. C. A styrene-alt-maleic acid copolymer is an effective inhibitor of R5 and X4 human immunodeficiency virus type 1 infection, *J. Biomed. Biotechnol.* **2010**, *2010*, 1–11.

(37) Bellettini, A. G., Bellettini, Richard J., Method for the treatment of HIV infected cells; USA Patent US 6,210,653 B, April 3, 2001.

(38) Oostwal, M.; Odijk, T. Novel dynamic scaling hypothesis for semidilute and concentrated solutions of polymers and polyelectrolytes, *Macromolecules* **1993**, *26*, 6489–6497.

(39) Pavlov, G. M.; Zaitseva, I. I.; Gibarev, A. S.; Gavrilova, I. I.; Panarin, E. F. Diffusion-viscometric analysis and conformational characteristics of sodium polystyrenesulfonate molecules, *Russ. J. Appl. Chem.* **2006**, *79*, 1506–1509.

(40) Skey, J.; O'reilly, R. K. Facile one pot synthesis of a range of reversible addition-fragmentation chain transfer (RAFT) agents, *Chem. Comm.* **2008**, 4183–4185.

(41) Nowakowska, M.; Kepczyński, M.; Szczubialka, K. Polymeric photosensitizers, Synthesis and photochemical properties of poly(sodium p-styrenesulfonate)-co-(4-vinylbenzylc hloride) containing rose bengal chromophores, *Macromol. Chem. Phys.* **1995**, *196*, 2073–2080.

(42) Tanner, J. E. Use of the Stimulated Echo in NMR Diffusion Studies, *J. Chem. Phys.* **1970**, *52*, 2523–2526.

(43) Cotts, R. M.; Hoch, M. J. R.; Sun, T.; Markert, J. T. Pulsed field gradient stimulated echo methods for improved NMR diffusion measurements in heterogeneous systems, *J. Magn. Reson.* **1989**, *83*, 252–266.

(44) Agarwal, H. K.; Doncel, G. F.; Parang, K. Synthesis and anti-HIV activities of suramin conjugates of 3'-fluoro-2',3'-dideoxythymidine and 3'-azido-2',3'-dideoxythymidine, *Med. Chem.* **2012**, *8*, 193–197.

5.8 *Future Work*

Using the method outlined in Chapter 3, the statistical segment lengths of SSty-*alt*-SPMI with a DP of 152 (L_{RU} = 0.508 nm, M_{RU} = 480.4 g/mol, L_{ko} = 8.6 nm[24]) in different salt and polymer concentrations. Table 5.10.1 summarizes the findings. The polyelectrolytes should exhibit chain expansion at low salt and polymer concentration based on these calculations. More information is needed to confirm this polyelectrolyte effect such as measuring the intrinsic viscosity of these polymers in water at 1 mg/mL.

Table 5.10.1 Statistical Segment Length Calculations for SSty-*alt*-SPMI

DP	Cp (g/dL)	I_s (mg/mL)	I x 10^{-3} (mol/L)	κ^{-1} (nm)	L_{Ke}	L_K (nm)	N_K
152	0.16	0	1.2	8.8	55	64	1.2
152	1.0	0	7.5	3.5	8.8	17	4.4
152	0.16	0.1	2.9	5.7	23	31	2.5
152	1.0	0.1	9.2	3.2	7.6	16	4.9
152	0.16	5.0	87	1.04	0.76	9.4	8.3
152	1.0	5.0	93	1.00	0.70	9.3	8.3

Chapter 6:**Synthesis and Characterization of Double Hydrophilic Block Copolymers Containing Semi-rigid and Flexible Segments**

6.1 *Authors*

Alice M. Savage, Elizabeth Ullrich, Stacey M. Chin, Zachary Kiernan, Caitlyn Kost, S. Richard Turner

Department of Chemistry (MC0212) and Macromolecules and Interfaces Institute (MC0344), Virginia Tech, Blacksburg, Virginia 24061, United States

6.2 *Abstract*

3-Methyl-(*E*)-stilbene (3MSti) and 4-(diethylamino)-(*E*)-stilbene (DEASti) monomers are synthesized and polymerized separately with maleic anhydride (MAn) in a strictly alternating fashion using reversible addition-fragmentation chain transfer (RAFT) polymerization techniques. The optimal RAFT chain transfer agents (CTA) for each copolymerization affect the reaction kinetics and CTA compatibilities. Psuedo-first order polymerization kinetics are demonstrated for the synthesis of poly((3-methyl-(*E*)-stilbene)-*alt*-maleic anhydride) (3MSti-*alt*-MAn) with a thiocarbonylthio CTA (methyl 2-

(dodecylthiocarbonothioylthio)-2-methylpropionate, TTCMe). Contrarily, a dithioester CTA (cumyl dithiobenzoate, CDB) controlls the synthesis of poly((4-(diethylamino)-(*E*)-stilbene)-*alt*-maleic anhydride) (DEASti-*alt*-MAn) with pseudo-first order polymerization kinetics. DEASti-*alt*-MAn is chain extended with 4-acryloylmorpholine (ACMO) to synthesize diblock copolymers and subsequently converted to a double hydrophilic polyampholyte block copolymers (poly((4-(diethylamino)-(*E*)-stilbene)-*alt*-maleic acid))-*b*-acryloylmorpholine) (DEASti-*alt*-MA)-*b*-ACMO) via acid hydrolysis. The isoelectric point (IEP) and dissociation behavior of these maleic acid-containing copolymers are determined using ζ-potential and acid-base titrations, respectively.

6.3 *Keywords*

stilbene, double hydrophilic block copolymers, RAFT, alternating copolymers

6.4 *Introduction*

The precise control over monomer sequence in synthetic copolymers attracted researchers' interest over the past few decades.[1,2] Random-sequenced copolymers are often used as replacements for defined biological polymers. Unfortunately, due to the random monomer sequences, synthetic copolymers typically lack the hierarchal structure proven critical for biological activity, recognition, self-replication, and self-assembly.[1,3] Synthetically, it remains challenging to control the precise sequence of monomers with conventional radical polymerization techniques. Typically, reactivity ratios between vinyl monomers are used to predict monomer sequence.[4] However, unavoidable defects in monomer sequence result in unwanted or uncontrollable conformational and

morphological changes. Nevertheless, examples of radical copolymerizations with controlled monomer sequences[4-6] exist like poly(stilbene-*alt*-maleic anhydride) (Sti-*alt*-MAn). Neither comonomer self-propagates under radical polymerization conditions and they display reactivity ratios close to zero,[4,7] resulting in strictly alternating monomer sequences. The syntheses of substituted Sti-*alt*-MAn copolymer derivatives afford a variety of copolymers and polyelectrolytes with precise control over the alternating monomer sequence.

Due to a decreased solubility, Sti-*alt*-MAn originally appeared to be a cross-linked copolymer[8] but upon dissolution in sodium hydroxide solution, the linear topology of these copolymers was confirmed.[9] Recently, copolymers synthesized from functionalized stilbene monomers resulted in linear, organic-soluble copolymers with sterically congested polymer backbones.[7,10-12] Investigation into the copolymer rigidity revealed that these copolymers are classified as semi-rigid (or semi-flexible),[13] stemming from the sterically crowded, 1,2-diphenylethylene structures of stilbene monomers and the ring structures of maleic anhydride/maleimide comonomers. The sterically congested backbone gives brittle films with very high T_gs (glass transition temperature) with no visible T_g below 250 °C.[12]

Protected, stilbene-containing, organic-soluble copolymer precursors easily convert to semi-rigid, aqueous-soluble, polyelectrolytes via acid or alkaline hydrolysis.[10,14,15] This deprotection strategy allows for molar mass determination of the precursors using organic solvents and circumvents the typical difficulties in the molar mass determination of

polyelectrolytes.[16] This strategy also allows for other traditional polymer characterization: ^{1}H NMR, TGA, DSC, DLS (dynamic light scattering), and solution SAXS (small angle x-ray scattering).[13] These precisely defined, semi-rigid polyelectrolytes afford pH and salt-responsive copolymers,[14,15] likely due to the semi-rigid polymer backbone. Incorporating the stilbene-containing copolymers into more sophisticated polymer architectures, such as block copolymers, enables investigation into the effects of the semi-rigid polymer segments on the polyelectrolyte solution properties.

Our group previously reported the synthesis of polyampholyte diblock copolymers containing alternating *N,N*-dialkylamino-substituted stilbene-maleic anhydride segments by using RAFT polymerization techniques.[14] The asymmetric stilbene monomer synthesis by the Wittig-Horner reaction resulted predominately in the trans isomer.[17] This asymmetry promoted the solubility of both copolymers with 3MSti or DEASti comonomers in organic solvents.[11] Also, the basic functional group (diethylamino) of the DEASti monomer promoted copolymer solubility in aqueous solutions.[12,14] Further investigation into polymerizing stilbene comonomers via RAFT polymerization techniques proved difficult due to the steric congestion of the 1,2-diphenylethylene structure[18,19] and the electron-donating capabilities of functional groups that significantly affect the copolymerizability with certain RAFT agents, Table 6.5.1.

Since 1998,[18,20,21] the number of investigations into RAFT polymerization techniques skyrocketed with advances in new RAFT CTAs, different monomer compatibilities, and combining RAFT with other CRP techniques (ATRP and NMP).[22] With reaction

conditions similar to conventional radical polymerization techniques, RAFT provides a means to polymerize functionalized vinyl monomers with a choice of solvent, monomer concentration, and radical initiator. With control over the polymer chain-end structure, chain extension of polymers synthesized by RAFT techniques produces well-defined block copolymers.

To synthesize double hydrophilic block copolymers with semi-rigid and flexible blocks, RAFT controlled radical polymerization (CRP) techniques were employed. RAFT was chosen as the optimal CRP technique for these copolymers due to the mild reaction conditions and functional group compatibilities of the RAFT polymerization mechanism.[23] ATRP (atom transfer radical polymerization) and NMP (nitroxide mediated polymerizations) were not compatible CRP techniques due to acidic monomer (MAn) incompatibilities with the ATRP copper-catalyst[19,24] and high reaction temperatures of the NMP techniques.[25]

Two types of RAFT agents (thiocarbonylthio and dithiobenzoate) where chosen as possible CTAs. The choice of RAFT agent for these copolymerizations was found to be critical for controlling molar mass and molecular weight distributions (PDI). The effects of RAFT agent on the time dependence of monomer conversion and dependence of molar mass on monomer conversion were investigated for both copolymers: 3MSti-*alt*-MAn (poly((3-methyl-(*E*)-stilbene)-*alt*-maleic anhydride)) and DEASti-*alt*-MAn (poly((4-(diethylamino)-(*E*)-stilbene)-*alt*-maleic anhydride) (Figure 6.4.1). Chain extension of DEA-*alt*-MAn copolymers with a non-stimuli responsive, amphiphilic, acrylamide (4-

acryloylmorpholine (ACMO))[26-28] resulted in linear, organic-soluble block copolymer precursors and revealed end group control. Using acid hydrolysis, the block copolymers were easily converted to their respective polyampholyte structures and used to measure the IEP and dissociation behavior of the semi-rigid, stilbene-containing segments within the double hydrophilic block copolymers.

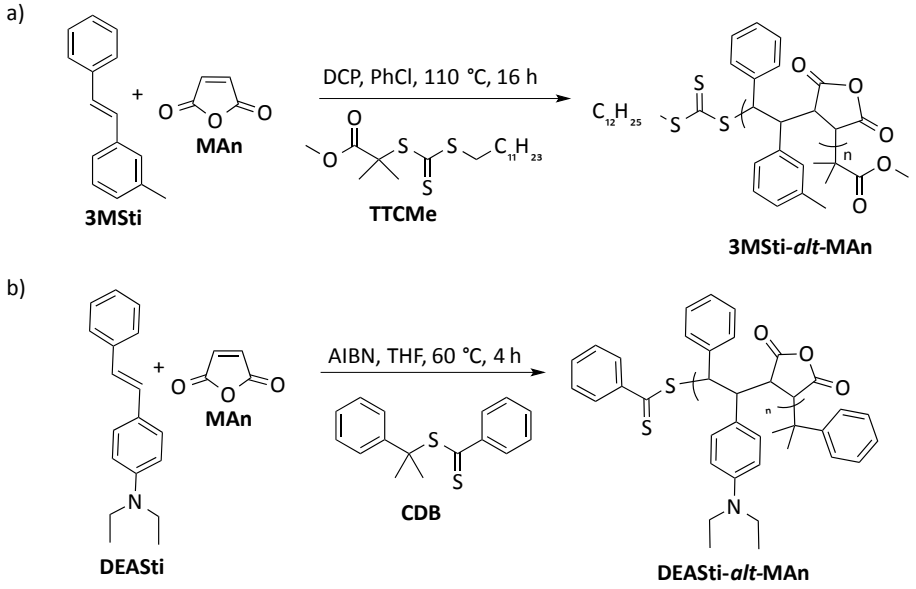

Figure 6.4.1 Synthesis of stilbene-containing alternating copolymers. a) Synthesis of 3MSti-*alt*-MAn copolymers with TTCMe CTA. b) Synthesis of DEASti-*alt*-MAn copolymers with CDB CTA.

6.5 *Experimental*

6.5.1 Chemicals

Diethyl benzylphosphonate was synthesized as reported.[11] Maleic anhydride (MAn, Aldrich, ≥99.0%), methyl 2-(dodecylthiocarbonothioylthio)-2-methylpropionate (TTCMe, Aldrich, 97%), hexanes (spectrum, ACS), *m*-tolualdehyde (Aldrich), tetrahydrofuran

(THF, Aldrich, anhydrous, ≥99.9%), potassium *tert*-butoxide (1.0 M THF solution, Aldrich), 4-(diethylamino)benzaldehyde (Aldrich, 99%), dicumyl peroxide (DCP, Aldrich, 98%), and 2,2′-azobis(2-methylpropionitrile) (AIBN, Aldrich, 98%), chlorobenzene (PhCl, Aldrich, anhydrous 98.8%), and calcium chloride ($CaCl_2$, Aldrich, anhydrous, ≥93.0%) were used as received. 4-Acryloylmorpholine (ACMO, Aldrich, 97%) was distilled before use at 60 °C and 1 mmHg of pressure.

6.5.2 Instruments

Size exclusion chromatography (SEC) determined the molar mass of the polymers at 35 °C in THF at 1 $mL \cdot min^{-1}$ flow rate. The THF SEC system was equipped with a Waters 717plus autosampler, a Waters 515 HPLC pump, three Polymer Laboratories PLGel 5 μm Mixed-C columns, multiangle laser light scattering (MALLS) detector and a Waters 2414 differential refractive index detector. Absolute molecular masses were obtained from the MALLS detector after determining the dn/dc offline using a Wyatt Optilab T- rEX differential refractometer at 658 nm and 35 °C.

pH titrations were carried out with a pH glass electrode in conjunction with a pH meter at room temperature. The polyampholyte concentration used for the titrations was 1.0 mg mL^{-1} in 0.02 M $CaCl_2$ solution,[29] starting with 25 mg of polyampholyte sample. The pH of the starting solution was adjusted to pH 11 using 1.0 M NaOH stock solution. The aqueous HCl titrant (0.0075 M) was delivered into the stirred polymer solution from a 50-mL burette and pH readings were stable and accurate to 0.01 pH unit. Dissociation

behavior of the polyampholyte was studied by using backward titration procedures (basic conditions titrated with HCl).[15]

^{1}H NMR spectra were obtained on a Varian Unity 400 MHz spectrometer in $CDCl_3$.

Zeta potential measurements were performed using a MALVERN Zatasizer (Nano ZS, ZEN3600) with a He-Ne laser (λ= 632.8 nm) and a folded disposable capillary cell (DTS1060). pH of the solutions was adjusted and measured before each zeta potential measurement in 1 mg mL^{-1} polymer solutions.

Table 6.5.1 THF SEC Results for the Synthesis of 3MSti-*alt*-MAn and DEASti-*alt*-MAn using RAFT CRP Techniques.

Copolymer	RAFT Agent	Initiator	T	[CTA]:[I]	Target M_n (g mol^{-1})	M_n (g mol^{-1})	PDI	Modality
3MSti-*alt*-MAn	TTCMe	AIBN	60 °C	2:1	15000	—	—	—
	TTCMe	DCP	110 °C	2:1	15000	15000	1.11	Unimodal
	CDB	AIBN	60 °C	2:1	20000	—	—	—
	CDB	DCP	110 °C	2:1	15000	—	—	—
DEASti-*alt*-MAn	TTCMe	AIBN	60 °C	8:1	20000	—	—	—
	TTCMe	DCP	110 °C	8:1	25000	2000	1.31	Bimodal
	CDB	AIBN	60 °C	2:1	20000	17000	1.13	Unimodal
	CDB	DCP	110 °C	2:1	20000	10000	2.56	Bimodal

6.5.3 Synthesis

6.5.3.1 Synthesis of 3-methyl-(E)-stilbene (3MSti)

Diethyl benzylphosphonate (11.3 g, 0.050 mol), *m*-tolualdehyde (5.95 g, 0.050 mol), and dry THF (200 mL) were added to a 500-mL round bottom flask with stir bar, septum, and needle under argon. The reaction flask was chilled in an ice bath for 30 min. A 1.0 M solution of potassium *tert*-butoxide in THF (55 mL, 0.055 mmol) was added slowly by using a syringe over 30 min to the reaction flask. After the addition of potassium *tert*-butoxide solution was completed, green solids began to crash out of solution. The reaction was allowed to warm to room temperature and stirred for a total of 24 h. The green liquid was poured into 600 mL of saturated ammonium chloride solution. After 1 day, a brownish/red solid appeared and was filtered by using vacuum filtration. The product was purified by using column chromatography (hexanes) to yield a white solid (7.90 g, 82%). mp 59.3–59.4 °C; Lit. mp 48 °C;[30] ^{1}H NMR (500 MHz, $CDCl_3$, δ): 7.51 (m, 2H, Ar H), 7.34 (m, 4H, Ar H), 7.26 (m, 2H, Ar H), 7.08 (m, 3H, Ar H), 2.38 (s, 3H, -*CH*$_3$). HRMS (ESI, *m/z*): $[M + H]^+$ calcd for $C_{15}H_{14}$, 195.1222; found, 195.1229.

6.5.3.2 Synthesis of 4-Diethylamino- (E)-stilbene (DEASti)

Diethyl benzylphosphonate (15.0 g, 0.07 mol), 4-(diethylamino)benzaldehyde (11.69 g, 0.070 mol), and dry THF (200 mL) were added to a 500-mL round bottom flask with stir bar, septum, and needle under argon. The reaction flask was chilled in an ice bath for 30

min. A 1.0 M solution of potassium *tert*-butoxide (72 mL, 0.072 mol) was added slowly by using a syringe over 30 min to the reaction flask. After the addition of potassium *tert*-butoxide solution was completed, red solids began to crash out of solution. The reaction was allowed to warm to room temperature and stirred for a total of 24 h. The orange liquid was poured into 600 mL of saturated ammonium chloride solution. After 1 hr, a yellow/green solid appeared and was filtered by using vacuum filtration. The pail yellow solid product was purified by recrystallization in hot hexanes. (15.70 g, 95%). mp 85.4–86.0 °C; Lit. mp 96 °C;[31] ^{1}H NMR (500 MHz, $CDCl_3$, δ): 7.37 (m, 6H, Ar H), 7.18 (t, J = 10 Hz, 1H, Ar H), 7.03 (d, J = 20 Hz, 1H, –CH=CH–), 6.88 (d, J = 20 Hz, 1H, –CH=CH–), 6.65 (d, J = 10 Hz, 2H, Ar H), 3.37 (q, 4H, J = 10 Hz, –N-CH_2-CH_3), 6.65 (d, J = 10 Hz, 2H, Ar H). HRMS (ESI, *m/z*): $[M + H]^+$ calcd for $C_{18}H_{22}N$, 252.1745; found, 252.1747.

6.5.3.3 Typical RAFT Copolymerization of DEASti and MAn (21,000 g mol^{-1} Target M_n).

DEASti (1.000 g, 4.0 mmol), MAn (0.3905 g, 4.0 mmol), CDB, (0.018 g, 0.066 mmol), and AIBN (0.005 g, 0.033 mmol) were added to a 50 mL reaction flask with stir bar and septum. The flask was purged with argon and 16 mL of anhydrous THF were added to the flask with a syringe. The solution was purged with argon for 30 min, and then stirred for 3.5 h at 60 °C. The reaction was cooled to room temperature and the polymer solution was precipitated into 400 mL of hexanes. The orange solid was collected by using vacuum filtration. The solid was then redissolved in THF and precipitated into hexanes

(400 mL). The white solid was collected by using vacuum filtration and dried in the vacuum oven at 60 °C overnight (0.45 g, 30%) (M_n = 12000 g mol^{-1}, and PDI= 1.13).

6.5.3.4 Typical RAFT Copolymerization of 3MSti and MAn (51,000 g mol^{-1} Target M_n).

3MSti (1.000 g, 5.1 mmol), MAn (0.505 g, 5.1 mmol), TTCMe, (0.010 g, 0.029 mmol), and DCP (0.004 g, 0.014 mmol) were added to a 50 mL reaction flask with stir bar and septum. The flask was purged with argon and 16 mL of anhydrous chlorobenzene were added to the flask with a syringe. The solution was purged with argon for 30 min, and then stirred for 24 h at 110 °C. The reaction was cooled to room temperature and the polymer solution was precipitated into 400 mL of hexanes. The white solid was collected by using vacuum filtration. The solid was then redissolved in THF and precipitated into hexanes (400 mL). The white solid was collected by using vacuum filtration and dried in the vacuum oven at 60 °C overnight (1.28 g, 85%) (M_n = 15000 g mol^{-1}, and PDI = 1.11).

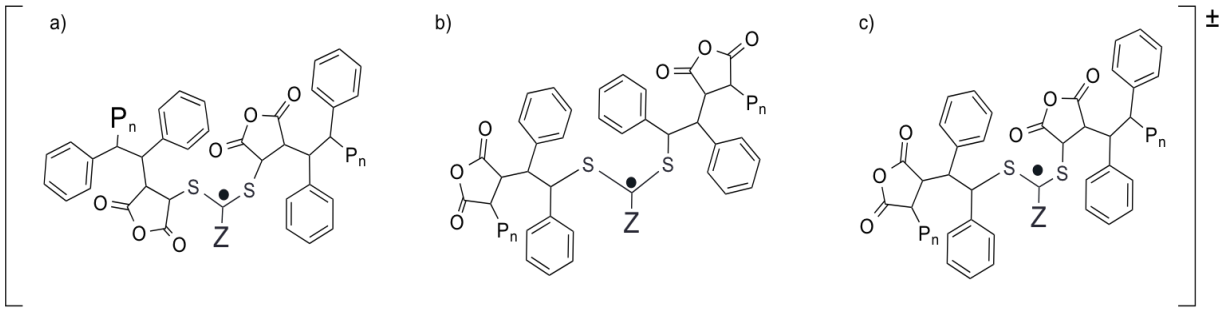

Figure 6.5.3.1 Possible structures for the RAFT main chain equilibrium structures of stilbene-maleic anhydride RAFT copolymerizations.

6.5.3.5 Synthesis of (DEASti-*alt*-MAn)-b-ACMO Block Copolymers with RAFT Polymerization (90,000 g mol^{-1} Target M_n).

DEASti-*alt*-MAn (macroRAFT agent) (0.39 g, 0.03 mmol, M_n=12,000 g mol^{-1}, PDI = 1.13), ACMO (3.00 g, 11 mmol), and AIBN (0.003 g, 0.02 mmol, [CTA]:[I]=2:1) were added to a 50 mL reaction flask with stir bar and septum. The flask was purged with argon and 40 mL of anhydrous THF were added to the flask with a syringe. The solution was purged with argon for 30 min, and then stirred 4 h at 60 °C. The reaction was cooled to room temperature and the polymer solution was precipitated into 400 mL of hexanes. The white solid was collected by using vacuum filtration. The solid was then redissolved in THF and precipitated into hexanes (400 mL). The white solid was collected by using vacuum filtration and dried in the vacuum oven at RT overnight (1.37 g, 40%) (M_n = 45000 g mol^{-1}, and PDI= 1.25)

6.5.3.6 Deprotection of (DEASti-*alt*-MAn)-*b*-ACMO and Synthesis of Polyampholyte (DEASti-*alt*-MA)-*b*-ACMO.

The typical procedure for deprotection and polyampholyte synthesis was as follows. (DEASti-*alt*-MAn)-*b*-ACMO (0.50 g, 0.01 mmol), HCl (3 mL, 0.04 mol) and deionized water (15 mL) were added to a 50-mL round bottom flask and stirred for 2 h at 50 °C. The solutions were placed in cellulose/ester membranes (MWCO 1000 g mol^{-1}), which were placed in a beaker with water (2 L); the water was stirred for 48 h after which time dialysis was presumed to be completed. The aqueous contents of the membranes were

then frozen in liquid nitrogen and lyophilized for 24 h to yield a white fluffy solid. Complete conversion into the polyanion was confirmed by FTIR.[10,14]

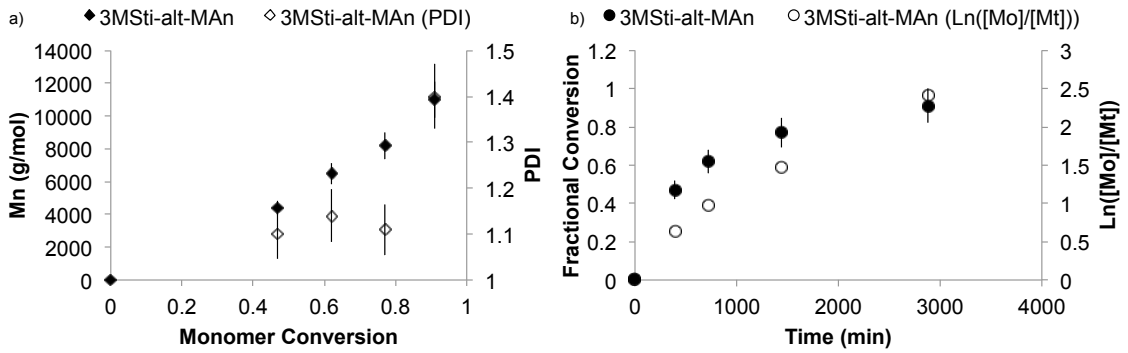

Figure 6.5.3.2 Reaction kinetics data of 3MSti-*alt*-MAn copolymers with AIBN and TTCMe CTA at 110 °C in PhCl (Target M_n = 15000 g mol^{-1}, [Monomer] = 0.5 M).

6.6 *Results and Discussion*

The stilbene monomers 3MSti and DEASti were successfully synthesized and polymerization by using controlled radial polymerization techniques. As summarized in Table 6.5.1, TTCMe RAFT agent was used to control the polymerization 3MSti with MAn at 110 °C with DCP initiator and resulted in unimodal SEC chromatograms with linear pseudo-first order reaction kinetics. Whereas CDB prevented the polymerization of

3MSti with MAn at 60 °C or 110 °C. Conversely, the CDB RAFT agent sufficiently controlled the polymerization of DEASti with MAn at 60 °C with AIBN and exhibited pseudo-first order reaction kinetics and TTCMe did not control this polymerization at either 60 °C nor 110 °C.

DEASti-*alt*-MAn copolymers were then chain extended with ACMO to synthesis linear block copolymers. These organic-soluble copolymers were then converted to polyampholytes via acid hydrolysis. By measuring the zeta-potential of 1 mg ml^{-1} polymer solutions at different pH, the IEP of these polyampholytes was observed at 4.32 pH. Acid-base titration curves reveal multi-step dissociation behavior of double hydrophilic block copolymers.

6.6.1 Monomer and CTA Ratio Calculations

For each reaction kinetic study, the CTA, initiator, and monomer concentration ratios followed the initial conditions set forth by Davies et al.[19] It is also important to note that the monomer conversions were based on the isolated yield of each polymerization. Due to the semi-rigid polymer backbone,[13] very broad aromatic and polymer backbone peaks appear in every ^{1}H NMR spectrum of these copolymers (even at low conversion). Also, vinyl peaks from both comonomers overlap with the polymer backbone peaks; thus, making it impossible to calculate monomer conversion with ^{1}H NMR.

6.6.2 Polymerization of 3MSti and MAn

Cumyl dithiobenzoate (CDB) (R-group = cumyl, Z-group = dithiobenzoate) did not copolymerize 3MSti and maleic anhydride at either low or high temperatures. However, styrene-*alt*-MAn (poly(styrene-*alt*-maleic anhydride)) copolymers have been synthesized by RAFT CRP techniques by using benzyl dithiobenzoate (R-group = benzyl, Z-group = dithiobenzoate).[19,32] The dithiobenzoate CTA exhibited effective molar mass control, and pseudo-first order reaction kinetics.[19] Since there are minimal electronic differences between the vinyl moieties of styrene and 3MSti,[33] the steric congestion of 3MSti likely prevented or drastically slowed monomer conversion with CDB. In the RAFT polymerization mechanism, there are three possible main chain equilibrium structures with stilbene and maleic anhydride comonomers (Figure 6.5.3.1). If a stilbene radical is the propagating radical and reacts with a dormant RAFT adduct chain, then the steric hindrance remains large and could potentially decrease polymerization rates. This decreased polymerization rate also occurred with another sterically hindered monomer, α-methylstyrene, polymerized with maleic anhydride copolymers compared to styrene-*alt*-MAn using RAFT polymerization techniques.[19]

TTCMe (R-group = $–C(CH_3)_2(COOMe)$, Z-group = thiocarbonylthio) polymerized 3MSti and maleic anhydride but only at high temperatures (110 °C) (Table 6.5.1). 3MSti-maleic anhydride did not polymerize at 60 °C with TTCMe and AIBN. Polymerizations with TTCMe and DCP at 110 °C demonstrated linear pseudo-first order polymerization kinetics with a linear time dependence of monomer conversion and linear dependence of molar mass on monomer conversion (Figure 6.5.3.2). At reaction times less than 6.5 h, copolymers could not be isolated by precipitation and filtration; thus, monomer

conversion could not be calculated. However, copolymer molar mass could be directly measured using SEC from reaction aliquots at shorter reaction times; therefore, this is likely not a retardation period. PDIs remained constant as monomer conversion increased.

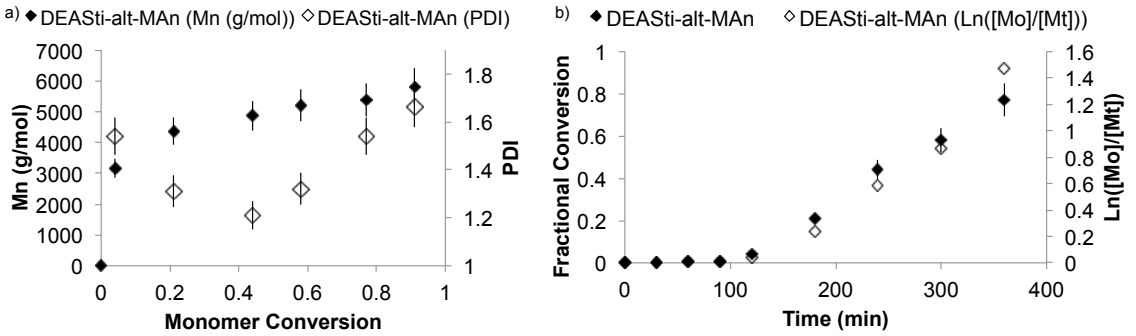

Figure 6.6.2.1 Reaction kinetics data of DEASti-*alt*-MAn copolymers with AIBN and CDB CTA at 60 °C in THF (Target M_n = 10000 g mol^{-1}, [Monomer] = 0.5 M).

6.6.3 Polymerization of DEASti and MAn

A different trend occurred with DEASti and maleic anhydride comonomer polymerization. In the synthesis of DEASti-*alt*-MAn, only CDB controlled molar mass and the reaction demonstrated linear pseudo-first order kinetics (Figure 6.6.2.1), while TTCMe polymerizations exhibited bimodal THF SEC-MALLS chromatograms and a lack of molar mass control.

Again for TTCMe mediated copolymerizations, the polymerization only proceeded at 110 °C with DCP initiator, Table 6.5.1. However, probable side reactions between DCP and the diethylamino functional group[34] were the likely cause of the uncontrolled molar

mass and the bimodal peaks seen in the THF SEC-MALLS chromatogram. Higher temperature azo-initiators like 1,1′-azobis(cyclohexanecarbonitrile) which exhibits a ten hour half life at 88 °C,[35] were also unsuccessful when employed with this comonomer pair.

In the polymerization of DEASti and MAn with CDB, molar mass control was achieved along with a linear dependence of molar mass on monomer conversion (Table 6.5.1, Figure 6.6.2.1). Possibly, the more electron-rich vinyl moiety of DEASti (compared to 3MSti) increased the reactivity of the stilbene monomer[36] and the copolymerization rate (cross-propagation); thus, increasing the copolymerization rate with CDB. The increase in polymerization rate of alternating copolymers where the electron-rich monomer (donor monomer) is rendered more electron-rich and/or the electron-poor monomer (acceptor monomer) is made more electron-poor is well documented in the literature.[37,38] For example, the copolymerization of p-methoxystyrene with maleic anhydride has a faster polymerization rate than the copolymerization of styrene and maleic anhydride.[19]

Like styrene homopolymerizations with dithiobenzoate CTAs, a retardation period (2 h) appeared due to the over stabilization of the RAFT adduct arising from the dithiobenzoate Z- group of CDB.[18] Pseudo-first order polymerization kinetics resumed after this period of polymerization retardation. An increase in the PDI occurred with monomer conversions above 0.5 due to possible termination through chain-end combination. In addition, bimodal peaks appear in the THF SEC-MALLS chromatogram

at higher monomer conversions from these possible termination processes, which indicates a lack of chain-end control at higher monomer conversions.

To compare R group effects and to reduce the polymerization retardation effect with CDB, a thiocarbonylthio CTA with a benzylic R-group (S-1-dodecyl-S′-(1-phenyl ethyl) trithiocarbonate (DPET)) (Figure 6.6.3.1) was used to polymerize DEASti with maleic anhydride.[39] The retardation period disappeared. However, the polymerization was uncontrolled and again, bimodal peaks appeared in the THF SEC-MALLS chromatogram like copolymerizations with TTCMe.

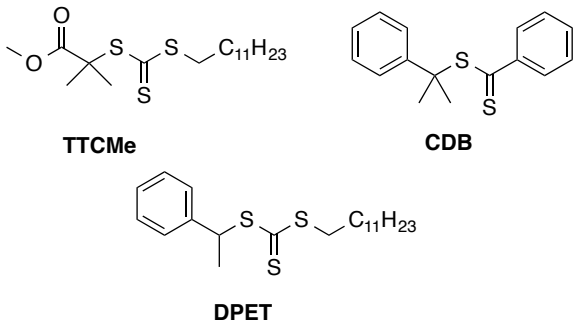

Figure 6.6.3.1 RAFT CTA agents used to synthesize both 3MSti-*alt*-MAn and DEASti-*alt*-MAn.

6.6.4 (DEASti-*alt*-MA)-*b*-ACMO Polyampholyte Double Hydrophilic Block Copolymers

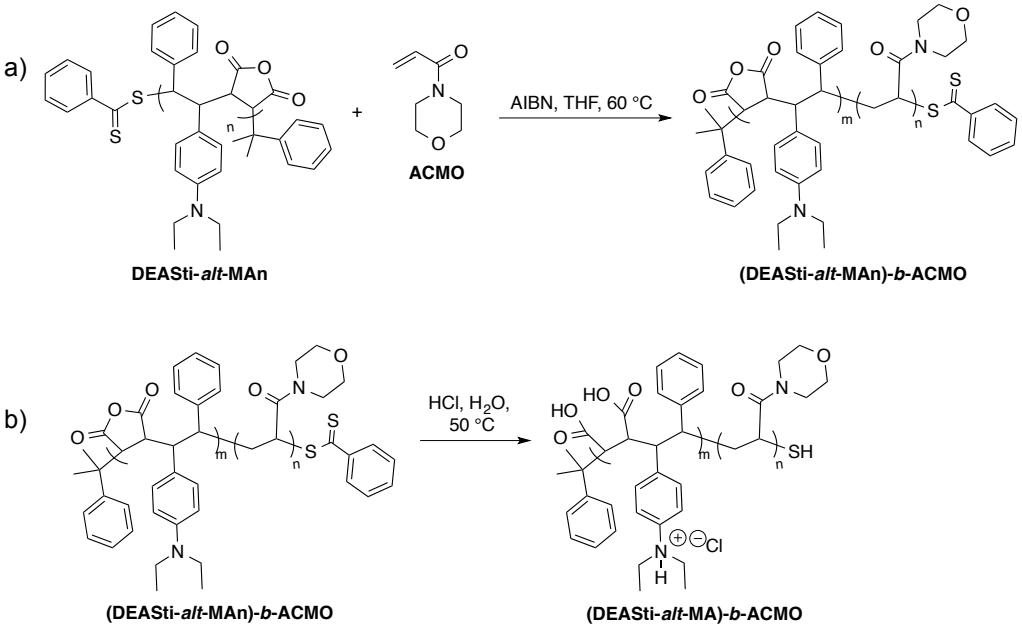

Figure 6.6.4.1 Synthesis of (DEASti-*alt*-MA)-*b*-ACMO polyampholyte block copolymers. a) Chain extension of DEASti-*alt*-MAn macroRAFT agent with ACMO in THF at 60 °C. b) Acid hydrolysis of (DEASti-*alt*-MAn)-*b*-ACMO to synthesize final polyampholyte block copolymer.

TABLE 6.6.4.1 THF SEC Results for the Chain Extension of DEASti-*alt*-MAn with ACMO

DEASti-*alt*-MAn M_n (g mol^{-1})	PDI	Block Copolymer M_n (g mol^{-1})	PDI
12000	1.13	44500	1.25
14500	1.25	21500	1.24
17000	1.26	33000	1.33

Poly(ACMO) is an acrylamide homopolymer with gaining interest due to its amphiphilic nature, and low cytotoxicity.[26-28] Particularly, poly(ACMO) was chosen for these block copolymers due to its non-stimuli responsive nature with respect to pH, temperature, or salt. Conditions for the block copolymerization of ACMO onto the DEASti-*alt*-MAn macroCTA were implemented according to similar procedures previously described (Figure 6.6.4.1).[28] THF SEC-MALLS chromatogram confirmed an increase in molar mass of the block copolymer with a shift to shorter elution times (Figure 6.6.4.2). In addition, the unimodal and narrow PDIs of the THF SEC-MALLS chromatograms imply the absence of uncontrolled ACMO homopolymerization and of high molar mass termination reaction products (Table 6.6.4.1, Figure 6.6.4.2).

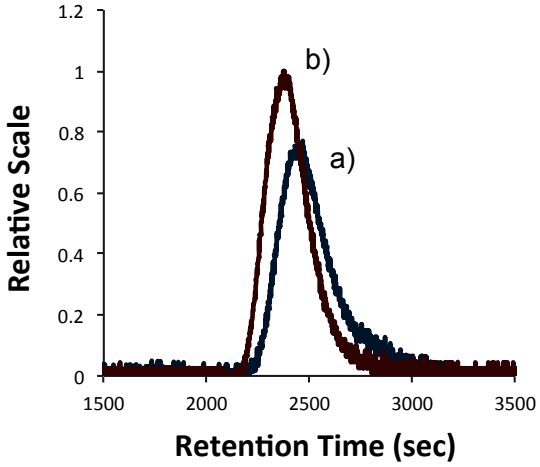

Figure 6.6.4.2 THF SEC-MALLS chromatograms of a) DEASti-*alt*-MAn macroRAFT CTA copolymer and b) block copolymer (DEASti-*alt*-MAn)-*b*-ACMO.

Acid hydrolysis converts the organic-soluble block copolymers to water-soluble polyampholytes with two acidic residues (carboxyl groups) and one basic residue (diethylamino group) per repeat unit (Figure 6.6.4.1 b). Acidic conditions were chosen during the synthesis of the polyampholyte (instead of alkaline conditions) to increase the solubility of the block copolymer precursor in water during this ring-opening reaction. The IEP of the copolymers was calculated using an acid-base equilibrium calculation[40,41] and measured by monitoring the ζ-potential of these copolymers at different pH (Figure 6.6.4.3). By using the pK_as calculated for the maleic acid residues on Sty-*alt*-MA (pK_a = 4 and 10),[42] an IEP of 4.30 pH was calculated which was in very good agreement with the experimental IEP of 4.32 pH. Ultimately, IEP determination serves as a reference point for further polymer solution characterization.

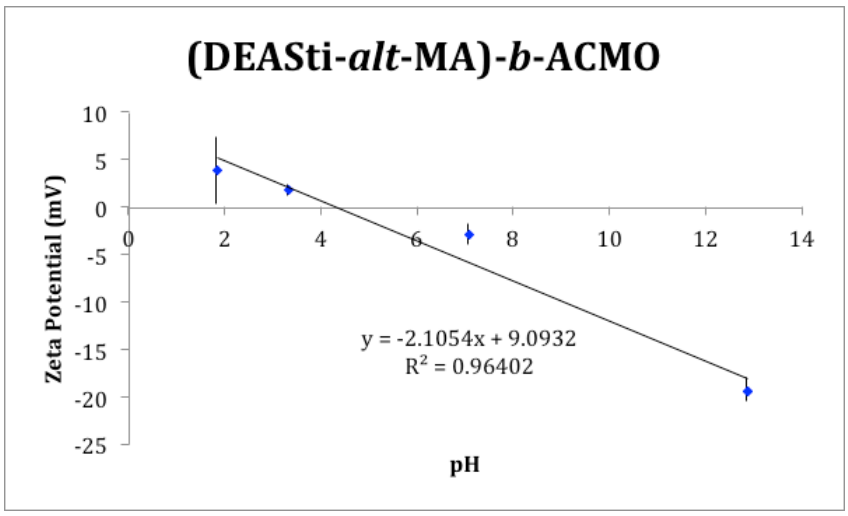

Figure 6.6.4.3 Zeta potential versus pH of block copolymer (DEASti-*alt*-MA)-*b*-ACMO at varying pH with 1 mg/mL polymer concentration. The block copolymer used has an overall M_n of 45,000 g mol^{-1} (PDI of 1.25) with a DEASti-*alt*-MA segment of 12,000 g mol^{-1}.

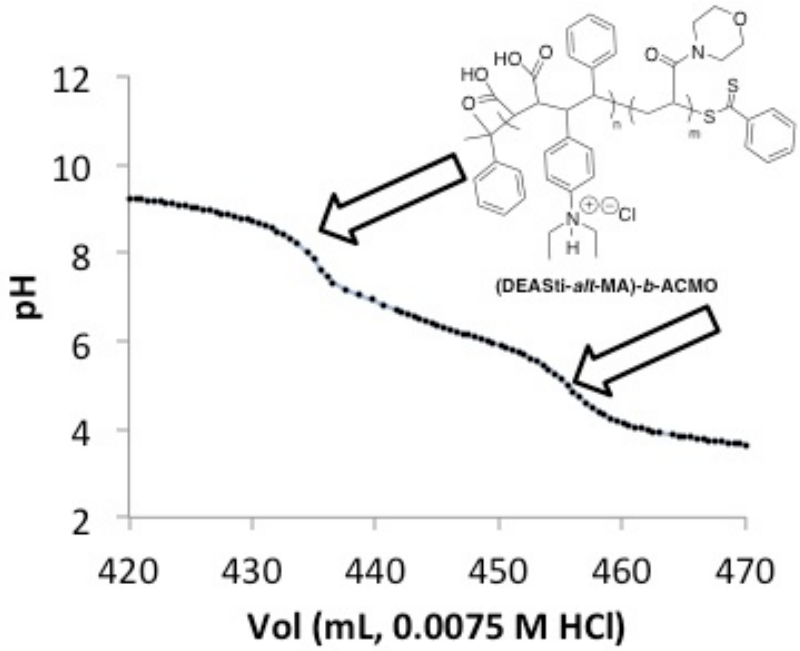

Figure 6.6.4.4 Titration curve of (DEASti-*alt*-MA)-*b*-ACMO (20 mg) in $CaCl_2$ solution (20 mL, 0.02 M) with excess NaOH (1.0 M, 0.6 mL). Solutions titrated with 0.0075 M HCl solution.

The dissociation behavior of the maleic acid-containing polyampholyte block copolymer was also evaluated using backward titration procedures.[15,29] A multi-step dissociation behavior was observed and consistent with previously reported copolymers containing maleic acid (Figure 6.6.4.4).[29,43] The vicinal diacids that originated from the enchained maleic anhydride comonomer exhibit two distinct pK_as[42] and are responsible for the multi-step dissociation behavior. The two pK_as arise from the sharing of only one sodium ion[44] per pair of carboxyl groups. This sharing/stabilization of the charged vicinal diacids is only possible due to the close proximity of the neighboring groups and is amplified with the addition of $CaCl_2$.[15,29] Based on the pK_as of the vicinal diacids (4 and 10)[42] and pK_bs of the diethylamino groups (dimethylaniline, 5.5 pK_b),[45] we hypothesize that the protonation of the diethylamino groups over laps with protonation of the second carboxyl group between pH 4–5. The dissociation behavior of these polyampholytes allows for more control over the degree of ionization by simply varying the pH of the polymer solution. This degree of ionization control becomes imperative for stimuli response polymer applications.[46 47]

6.7 *Conclusions*

In summary, two stilbene derivatives (3MSti and DEASti) were successfully copolymerized with maleic anhydride by RAFT CRP techniques. Electron-donating groups like tertiary amino groups on stilbene not only affect the increased polymerization rate but also CTA compatibilities. Psuedo-first order polymerization kinetics appeared for both 3MSti and DEASti alternating copolymers. These RAFT polymerization

techniques offer new pathways to synthesizing precisely defined alternating copolymers and block copolymers with semi-rigid segments. Further investigation into the solution properties and stimuli responsive nature of these copolymers is underway and will be reported in the future.

6.8 *References*

(1) Lutz, J. F.; Ouchi, M.; Liu, D. R.; Sawamoto, M. Sequence-controlled polymers, *Science* **2013**, *341*, 628–635.

(2) Zamfir, M.; Lutz, J. F. In *Controlling polymer primary structure using CRP: synthesis of sequence-controlled and sequence-defined polymers,* , **2012**; Vol. 1101, pp 112.

(3) Palermo, E. F.; Vemparala, S.; Kuroda, K. In *Tailored polymer architectures for pharmaceutical and biomedical applications*, **2013**; Vol. 1135, pp 319–330

(4) Lewis, F. M.; Mayo, F. R. Copolymerization. IX. Comparison of some cis and trans isomers, *J. Am. Chem. Soc.* **1948**, *70*, 1533–1536.

(5) Davis, R. M.; Russel, W. B. On the theory of dilute polyelectrolyte solutions: extensions, refinements, and experimental tests, *J. Polym. Sci. Pol. Phys.* **1986**, *24*, 511–533.

(6) Houlihan, F. M.; Wallow, T. I.; Nalamasu, O.; Reichmanis, E. Synthesis of cycloolefin−maleic anhydride alternating copolymers for 193 nm imaging, *Macromolecules* **1997**, *30*, 6517–6524.

(7) Ha, N. T. H. Determination of triad sequence distribution of copolymers of maleic anhydride and its derivatives with donor monomers by ^{13}C NMR spectroscopy, *Polymer* **1998**, *40*, 1081–1086.

(8) Wagner-Jauregg, T. Additive heteropolymerization, *Ber. Dtsch. Chem. Ges. B* **1930**, *63B*, 3213–3224.

(9) Tanaka, T.; Vogl, O. Preparation and characterization of head-to-head polymer. 1. Head-to-head poly(methyl cinnamate), *Polym. J.* **1974**, *6*, 522–531.

(10) Li, Y.; Mao, M.; Matolyak, L. E.; Turner, S. R. Sterically crowded anionic polyelectrolytes with tunable charge densities based on stilbene-containing copolymers, *ACS Macro Lett.* **2012**, *1*, 257–260.

(11) Li, Y.; Turner, S. R. Free radical copolymerization of methyl substituted stilbenes with maleic anhydride, *Eur. Polym. J.* **2010**, *46*, 821–828.

(12) Mao, M.; Turner, S. R. Synthesis and characterization of highly functionalized polymers based on N,N,N',N'-tetraalkyl-4,4'-diaminostilbene and maleic anhydride, *Polymer* **2006**, *47*, 8101–8105.

(13) Li, Y.; Zhang, M.; Mao, M.; Turner, S. R.; Moore, R. B.; Mourey, T. H.; Slater, L. A.; Hauenstein, J. R. Chain stiffness of stilbene containing alternating copolymers by SAXS and SEC, *Macromolecules* **2012**, *45*, 1595–1601.

(14) Mao, M.; Turner, S. R. Aggregation of rod-coil block copolymers containing rigid polyampholyte blocks in aqueous solution, *J. Am. Chem. Soc.* **2007**, *129*, 3832–3833.

(15) Li, Y.; Savage, A. M.; Zhou, X.; Richard Turner, S.; Davis, R. M. Solution properties of stilbene-containing sterically crowded alternating polyanions, *J. Polym. Sci. Pol. Phys.* **2013**, *51*, 1565–1570.

(16) Bruessau, R. J. Size exclusion chromatography of polyelectrolytes with aqueous elution solvents, *Makromol. Chem-M Symp.* **1992**, *61*, 199–218.

(17) Wadsworth, W. S., Jr.; Emmons, W. D. The utility of phosphonate carbanions in olefin synthesis, *J. Am. Chem. Soc.* **1961**, *83*, 1733–1738.

(18) Moad, G.; Chiefari, J.; Chong, Y. K.; Krstina, J.; Mayadunne, R. T. A.; Postma, A.; Rizzardo, E.; Thang, S. H. Living free radical polymerization with reversible addition-fragmentation chain transfer (the life of RAFT), *Polym. Int.* **2000**, *49*, 993–1001.

(19) Davies, M. C.; Dawkins, J. V.; Hourston, D. J. Radical copolymerization of maleic anhydride and substituted styrenes by reversible addition-fragmentation chain transfer (RAFT) polymerization, *Polymer* **2005**, *46*, 1739–1753.

(20) Moad, C. L.; Winzor, D. J. Quantitative characterization of radiation degradation in polymers by evaluation of scission and cross-linking yields, *Prog. Polym. Sci.* **1998**, *23*, 759–813.

(21) Chiefari, J.; Chong, Y. K.; Ercole, F.; Krstina, J.; Jeffery, J.; Le, T. P. T.; Mayadunne, R. T. A.; Meijs, G. F.; Moad, C. L.; Moad, G.; Rizzardo, E.; Thang, S. H. Living free-radical polymerization by reversible addition-fragmentation chain transfer: The RAFT process, *Macromolecules* **1998**, *31*, 5559–5562.

(22) Zehm, D.; Laschewsky, A.; Liang, H.; Rabe, J. P. Straightforward access to amphiphilic dual bottle brushes by combining RAFT, ATRP, and NMP polymerization in one sequence, *Macromolecules* **2011**, *44*, 9635–9641.

(23) Lowe, A. B.; McCormick, C. L. Reversible addition-fragmentation chain transfer (RAFT) radical polymerization and the synthesis of water-soluble (co)polymers under homogeneous conditions in organic and aqueous media, *Prog. Polym. Sci.* **2007**, *32*, 283–351.

(24) Qiu, J.; Charleux, B.; Matyjaszewski, K. Controlled/living radical polymerization in aqueous media: homogeneous and heterogeneous systems, *Prog. Polym. Sci.* **2001**, *26*, 2083–2134.

(25) Hawker, C. J.; Bosman, A. W.; Harth, E. New polymer synthesis by nitroxide mediated living radical polymerizations, *Chem. Rev.* **2001**, *101*, 3661–3688.

(26) Jo, Y. S.; van der Vlies, A. J.; Gantz, J.; Antonijevic, S.; Demurtas, D.; Velluto, D.; Hubbell, J. A. RAFT homo- and copolymerization of *N*-acryloyl-morpholine, piperidine, and azocane and their self-assembled structures, *Macromolecules* **2008**, *41*, 1140–1150.

(27) Torchilin, V. P.; Shtilman, M. I.; Trubetskoy, V. S.; Whiteman, K.; Milstein, A. M. Amphiphilic vinyl-polymers effectively prolong liposome circulation time in-vivo, *BBA-Biomembranes* **1994**, *1195*, 181–184.

(28) Li, W.; Nakayama, M.; Akimoto, J.; Okano, T. Effect of block compositions of amphiphilic block copolymers on the physicochemical properties of polymeric micelles, *Polymer* **2011**, *52*, 3783–3790.

(29) Sauvage, E.; Amos, D. A.; Antalek, B.; Schroeder, K. M.; Tan, J. S.; Plucktaveesak, N.; Colby, R. H. Amphiphilic maleic acid-containing alternating copolymers - 1. Dissociation behavior and compositions, *J. Polym. Sci. Pol. Phys.* **2004**, *42*, 3571–3583.

(30) Bergmann, F.; Schapiro, D. Application of the Meerwein reaction. IV. The synthesis of new mono- and disubstituted stilbenes, *J. Org. Chem.* **1947**, *12*, 57–66.

(31) Fu, Y.; Li, H.; Hu, W. Small molecular chromogenic sensors for Hg2+: a strong "push-pull" system exists after binding, *Eur. J. Org. Chem.* **2007**, 2459–2463.

(32) Zhu, M. Q.; Wei, L. H.; Li, M.; Jiang, L.; Du, F. S.; Li, Z. C.; Li, F. M. A unique synthesis of a well-defined block copolymer having alternating segments constituted by maleic anhydride and styrene and the self-assembly aggregating behavior thereof, *Chem. Commun.* **2001**, 365–366.

(33) Fischer, H.; Radom, L. Factors controlling the addition of carbon-centered radicals to alkenes-an experimental and theoretical perspective, *Angew. Chem. Int. Edit.* **2001**, *40*, 1340–1371.

(34) Grob, C. A.; Link, H.; Schiess, P. W. Cyclodecapolyenes. II. Valency isomerization of 1,5-cyclodecadiene, *Helv. Chim. Acta* **1963**, *46*, 483–492.

(35) Overberger, C. G.; Biletch, H.; Finestone, A. B.; Lilker, J.; Herbert, J. Azo-bis Nitriles.1 The decomposition of azo compounds derived from cycloalkanones. An accurate measure of differences in ring strain, *J. Am. Chem. Soc.* **1953**, *75*, 2078–2082.

(36) Walling, C.; Briggs, E. R.; Wolfstirn, K. B.; Mayo, F. R. Copolymerization. X. The effect of meta- and para-substitution on the reactivity of the styrene double bond, *J. Am. Chem. Soc.* **1948**, *70*, 1537–1542.

(37) Hall, H. K.; Padias, A. B. "Charge transfer" polymerization - and the absence thereof!, *J. Polym. Sci. Pol. Chem.* **2001**, *39*, 2069–2077.

(38) Hall, H. K.; Padias, A. B. Zwitterion and diradical tetramethylenes as initiators of charge-transfer polymerizations, *Accounts Chem. Res.* **1990**, *23*, 3–9.

(39) Ponnusamy, K.; Babu, R. P.; Dhamodharan, R. Synthesis of block and graft copolymers of styrene by raft polymerization, using dodecyl-based trithiocarbonates as initiators and chain transfer agents, *J. Polym. Sci. Pol. Chem.* **2013**, *51*, 1066–1078.

(40) Patrickios, C. S. Polypeptide amino acid composition and isoelectric point: 1. A closed-form approximation, *J. Colloid Interface Sci.* **1995**, *175*, 256–260.

(41) Lowe, A. B.; McCormick, C. L. Synthesis and solution properties of zwitterionic polymers, *Chem. Rev.* **2002**, *102*, 4177–4189.

(42) Garrett, E. R.; Guile, R. L. Potentiometric titrations of a polydicarboxylic acid: maleic acid-styrene copolymer, *J. Am. Chem. Soc.* **1951**, *73*, 4533–4535.

(43) Brissova, M.; Staudner, E. Behavior of MAn-based polyelectrolytes in water solutions: influence of pH and ionic strength, *Eur. Polym. J.* **1996**, *32*, 529–533.

(44) Garnier, G.; Duskova-Smrckova, M.; Vyhnalkova, R.; Van de Ven, T. G. M.; Revol, J.-F. Association in solution and adsorption at an air-water interface of alternating copolymers of maleic anhydride and styrene, *Langmuir* **2000**, *16*, 3757–3763.

(45) Kolling, O. W.; Garber, D. A. Potentiometric study of base strengths in the binary solvent, acetic acid-p-dioxane, *Anal. Chem.* **1967**, *39*, 1562–1567.

(46) Raposo, M.; Lourenço, J. M. C.; Botelho do Rego, A. M.; Ferraria, A. M.; Ribeiro, P. A. Counterions – A new approach to control the degree of ionization of polyelectrolytes in layer-by-layer films, *Colloid Surface A* **2012**, *412*, 1–10.

(47) Lankalapalli, S.; Kolapalli, V. R. M. Polyelectrolyte complexes: A review of their applicability in drug delivery technology, *Indian J. Pharm. Sci.* **2009**, *71*, 481–487.

6.9 *Supporting information*

* Figures were updated to reflect the standard experimental error.*

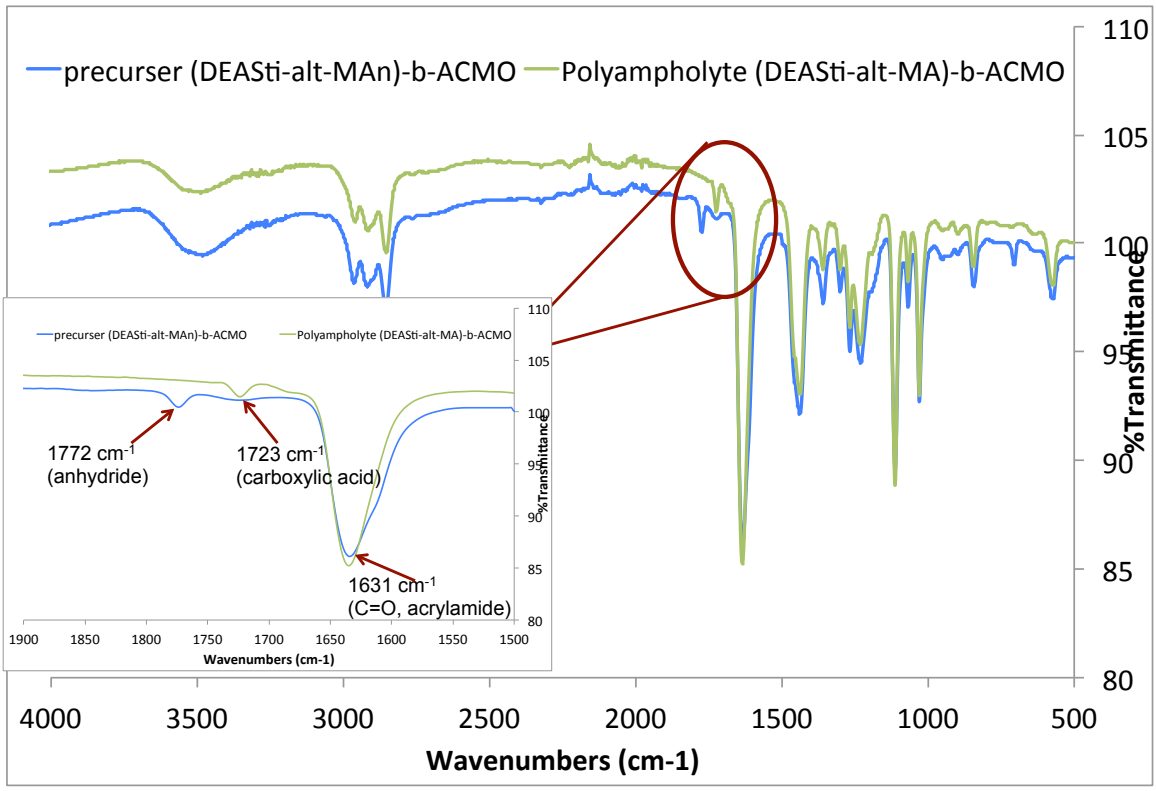

Figure 6.9.1 FTIR Spectra of the organic-soluble (DEASti-*alt*-MAn)-*b*-ACMO (blue line) and (DEASti-*alt*-MA)-*b*-ACMO (green line) deprotected polyampholyte. After the deprotection reaction, there is a disappearance of the signal at 1772 cm^{-1} corresponding to the anhydride unit and the increase in signal (1723 cm^{-1}) from the carboxylic acid groups of the polyampholyte. Typically, anhydride units appear as two peaks (1841 and 1772 cm^{-1}).[1] Based on the appearance of the –OH stretch at 3500 cm^{-1}, the precursor copolymers appear to contain some opened anhydride rings (maleic acid) from the

precipitation and workup. Therefore, the remaining anhydride concentration in the backbone is reduced.

1. Mao, M. and S.R. Turner, *J. Am. Chem. Soc.*, **2007**, *129***,** 3832–3833.

Potentiometric Titration Inflection Points

Table 6.9.1 Titration curve of (DEASti-*alt*-MA)-*b*-ACMO (20 mg) in $CaCl_2$ solution (20 mL, 0.02 M) with excess NaOH (1.0 M, 0.6 mL). Solutions titrated with 0.0075 M HCl solution		
	pH	**Std. Dev (pH)**
1st inflection pt	8.3	0.08
2nd inflection pt	5.3	0.10

6.9.1 Graphical Abstract

Two sterically crowded stilbene comonomers 3-methyl-(*E*)-stilbene (3MSti) and 4-(diethylamino)-(*E*)-stilbene (DEASti) are polymerized separately with maleic anhydride (MAn) using reversible addition-fragmentation chain transfer (RAFT) polymerization techniques. RAFT agent compatibilities and reaction kinetics for each comonomer system are compared. Double hydrophilic block copolymers are synthesized from these

copolymers and converted to polyelectrolytes. The isoelectric point (IEP) and dissociation behavior of the polyelectrolytes are determined using ζ-potential and acid-base titrations, respectively.

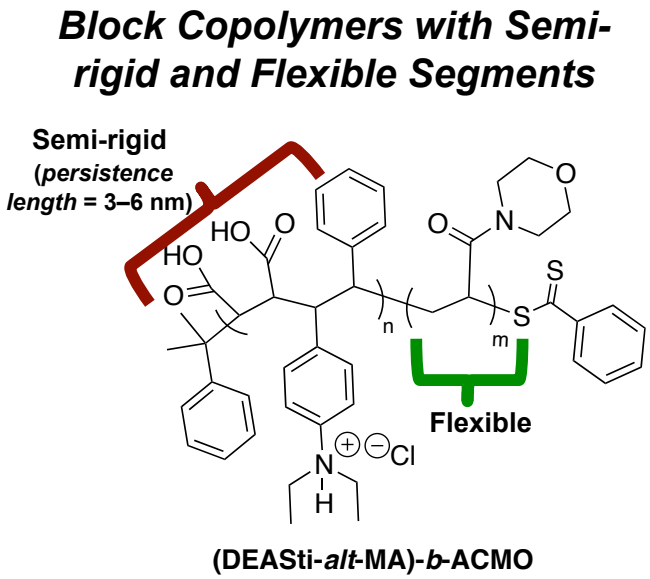

Figure 6.8.1 Graphical Abstract of Chapter 6

Chapter 7: **Salt and pH Responsive Double Hydrophilic Block Copolymers Containing Semi-rigid and Flexible Segments**

7.1 *Abstract*

Four double hydrophilic block copolymers (DHBCs) of differing molar mass containing semi-rigid and flexible segments were studied. Poly((4-(diethylamino)-(*E*)-stilbene)-*alt*-maleic acid)-*b*-acryloyl morpholine (DEASti-*alt*-MA)-*b*-ACMO) was synthesized from its organic-soluble, precursor, copolymers poly((4-(diethylamino)-(*E*)-stilbene)-*alt*-maleic anhydride))-*b*-acryloyl morpholine). These polyampholyte DHBCs formed polyion complexes (PICs) in aqueous solutions. Using dynamic light scattering (DLS), the pH and salt (NaCl) responsiveness of the DHBCs were evaluated. PIC complex formation was dependent on pH and the particle size increased as the pH approached the IEP (isoelectric point) of the DHBC. The salt responsiveness was also measured by using DLS to monitor PIC size for all four DHBCs. These PICs exhibited an antipolyelectrolyte effect with increasing hydrodynamic diameter as ionic strength (NaCl) increased from 0.01–2.0 M. PICs were more stable at higher ionic strengths with higher the ACMO molar mass. Responsiveness of the DHBCs with added calcium chloride and sodium tetrafluoroborate were also measured.

7.2 *Introduction*

In recent decades, the synthesis and investigation of smart polymers (stimuli responsive) rapidly increased due to a strong interest in dynamic, adaptable, and low cytotoxic polymer systems.[1,2] With three different types of external stimuli (physical, chemical, or biological),[3] these smart polymers have numerous applications like water treatment,[4] drug and gene delivery vehicles,[1] and stabilizers.[5] For salt (ionic strength) and pH responsive polymers, the typical physiochemical response to stimuli is a change of polymer solubility from hydrophilic to hydrophobic in addition to bond cleavage, degradation, or conformational changes. In biological systems, the wide range of pH and ionic strength can be utilized as different stimuli to promote the physiochemical change associated with each stimuli-responsive polymer.[3]

Double hydrophilic block copolymers (DHBCs) are a unique type of amphiphilic diblock copolymer where one or both blocks are stimuli responsive. Since the Antonietti group coined the name DHBC in 1998,[6] the number of DHBCs reported has grown exponentially due to their stimuli responsiveness in aqueous solutions, which is advantageous in biological applications[5] and other aqueous systems.[7] Our group recently reported the synthesis and solution characterization of two different polyampholyte DHBCs with semi-rigid and flexible segments.[8,9] The semi-rigid block segments (persistence lengths of 3–6 nm)[10] comprise stilbene-maleic acid, strictly alternating, monomer sequences.[10,11] The semi-rigid character of these copolymers arises from the steric congestion of the stilbene monomer derivatives and the ring-structures from the maleic anhydride monomers.[10]

Previously, we reported[9] the synthesis of poly((oligo-(ethylene glycol)methacrylate)-*b*-(N,N,N′,N′-tetraethyl-4,4′-diamino-(*E*)-stilbene-*alt*-maleic anhydride)) (OEGMA-*b*-(TEDASti-*alt*-MAn)) which consisted of a polymerized methoxy-capped (OEGMA) block chain extended with a semi-rigid block of TEDASti-*alt*-Man. The resulting block copolymers were then converted to polyampholyte DHBCs (poly((oligo-(ethylene glycol)methacrylate)-*b*-(N,N,N′,N′-tetraethyl-4,4′-diamino-(*E*)-stilbene-*alt*-maleic acid)) (OEGMA-*b*-(TEDASti-*alt*-MA)) via acid hydrolysis and contained two basic residues (diethylamino) and two acid residues (carboxylates) per repeat unit in the semi-rigid segments only. Polyion complexes (PICs) formed between 5.0–7.0 pH due to the electrostatic interactions of the polyampholyte segments. The polyampholyte DHBC displayed increasing particle (PIC) size as the salt concentration increased (0.0-0.5 M NaCl). It was proposed that this anti-polyelectrolyte effect[12-14] resulted from the "like-charge" intermolecular attraction of these semi-rigid polymer chains.[9] Based upon Manning's counterion condensation theory[15] and the counterion mediated attraction of like-charged rods,[16] condensed counterions along the polymer backbone induced dipoles and intermolecular interactions. Due to the more extended polymer chains of these semi-rigid copolymers, dipole-dipole intermolecular interactions increased as the polymer aggregate/particle size increased.

Our goal is to investigate if the "like-charge" attraction and antipolyelectrolyte effects can operate in other semi-rigid and flexible DHBCs or with salts of asymmetric valency and size. Therefore, we have prepared and synthesized new polyampholyte DHBCs with semi-rigid and flexible block segments[8] by using reversible addition fragmentation chain

transfer (RAFT) polymerization and investigated this antipolyelectrolyte effect with three salts (NaCl, $CaCl_2$, and $NaBF_4$), individually. Salts of higher and asymmetric valencies should exhibit significantly larger effects possibly due to stronger dipole-dipole interactions.

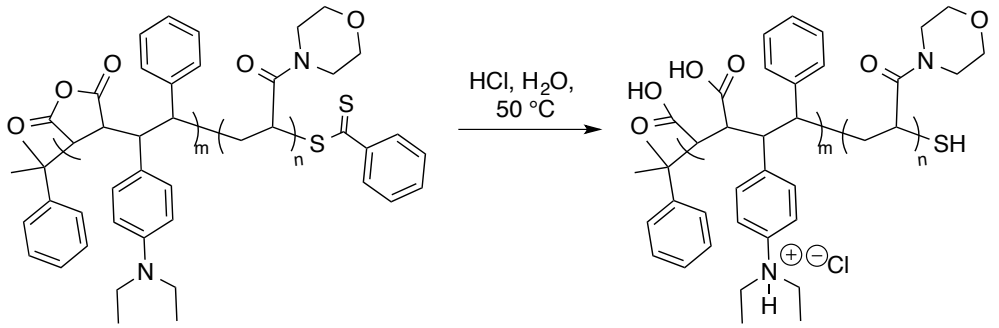

Figure 7.4.1 Deprotection and synthesis of (DEASti-*alt*-MA)-*b*-ACMO) by acid hydrolysis.[8]

These new DHBCs contained similar semi-rigid segments to OEGMA-*b*-(TEDASti-*alt*-MAn) but contained a different charge density (one basic residue (diethylamino) and two acid residues (carboxylates)) and a linear, amphiphilic, acrylamide, flexible polymer segment. This charge imbalance was promoted by asymmetrical stilbene monomers. By measuring ζ-potential as a function of pH, a 4.3 pH IEP (isoelectric point) was observed for poly((4-(diethylamino)-(*E*)-stilbene)-*alt*-maleic acid))-*b*-acryloylmorpholine) (DEASti-*alt*-MA)-*b*-ACMO) (Figure 7.4.1).[8] In addition, acid-base titrations revealed a two-step dissociation behavior, corresponding to the two distinct vicinal diacids pKas of the maleic acid repeat unit.[8,11,17,18] ACMO was chosen as the second block of this DHBC due to its amphiphilic nature and low cytotoxicity.[19-21] ACMO was also an attractive

candidate for this flexible block due to its non-stimuli responsive nature with respect to pH and temperature.

In this chapter, we investigated the pH and ionic strength responsiveness of the charge imbalanced polyampholyte DHBC (DEASti-*alt*-MA)-*b*-ACMO) by monitoring PIC size (hydrodynamic diameter) and solubility as a function of pH or ionic strength of three different salts by using dynamic light scattering (DLS). The effects of molar mass of the flexible acrylamide block were also investigated with respect to their salt responsiveness.

7.3 *Experimental*

7.3.1 Chemicals

Monomer, 4-diethylamino-(*E*)-stilbene (DEASti), and block copolymers were synthesized as reported.[8] Maleic anhydride (MAn, Aldrich, ≥99.0%), hexanes (Spectrum Chemical, ACS), tetrahydrofuran (THF, Aldrich, anhydrous, inhibitor free, ≥99.9%), 2,2′-azobis(2-methylpropionitrile) (AIBN, Aldrich, 98%), calcium chloride ($CaCl_2$, Aldrich, anhydrous, ≥93.0%), sodium chloride (NaCl, Spectrum Chemical), sodium tetrafluoroborate ($NaBF_4$, Aldrich, 98%), were used as received. 4-Acryloylmorpholine (ACMO, Aldrich, 97%) was distilled before use at 60 °C and 1 mmHg of pressure.

7.3.2 Instruments

The molar mass of the polymers was measured by size exclusion chromatography (SEC) at 35 °C in THF at 1 $mL \cdot min^{-1}$ flow rate. The THF SEC system was equipped with a Waters 717plus autosampler, a Waters 515 HPLC pump, three Polymer Laboratories

PLGel 5 μm Mixed-C columns, multiangle laser light scattering (MALLS) detector and a Waters 2414 differential refractive index detector. Absolute molecular masses were obtained from the MALLS detector after determining the dn/dc offline using a Wyatt Optilab T- rEX differential refractometer at 658 nm and 35 °C.

^{1}H NMR spectra were obtained on a Varian Unity 400 MHz spectrometer in $CDCl_3$.

pH and salt responsiveness/solubility measurements were assessed using dynamic light scattering (DLS) with a Malvern Zetasizer NanoZS particle analyzer equipped with a He-Ne linear polarized laser (λ= 632.8 nm) at a scattering angle of 173 and at 25 °C. All experiments were conducted in 12 mm square disposable polystyrene cuvettes. pH of the solutions was adjusted before each size measurement in 1 mg mL^{-1} polymer solutions. Polymer solutions were filtered through a 0.45 μm PTFE filter and allowed to sit for 15 min before measurement. Ionic strengths were adjusted by the addition of concentrated salt solutions (NaCl = 4 M, $CaCl_2$ = 3 M, and $NaBF_4$ = 5 M) directly to the cuvette containing 1 mL of a 1 mg/mL polymer solution in DI water filtered through a 0.45 μm PTFE filter (pH 6.6). Salt solutions were filtered before addition. After each addition, the polymer-salt solution was stirred and allowed to sit for 15 min before measurement. All hydrodynamic diameter measurements are intensity-average diameters unless otherwise specified.

7.3.3 Synthesis

7.3.3.1 Typical RAFT Copolymerization of DEASti and MAn (Copolymers 1–4)[8]

DEASti (1.000 g, 4.0 mmol), MAn (0.3905 g, 4.0 mmol), CDB, (0.040 g, 0.146 mmol), and AIBN (0.012 g, 0.072 mmol) were added to a 50 mL reaction flask with stir bar and septum. The flask was purged with argon and 16 mL of anhydrous THF were added to the flask with a syringe. The solution was purged with argon for 30 min, and then stirred for 3.5–4.0 h at 60 °C. The reaction was cooled to room temperature and the polymer solution was precipitated into 400 mL of hexanes. The orange solid was collected by using vacuum filtration. The solid was then redissolved in THF and precipitated into hexanes (400 mL). The white solid was collected by using vacuum filtration and dried in the vacuum oven at 60 °C overnight (0.45 g, 30%) (M_n = 17000 g mol^{-1}, and PDI= 1.13).

7.3.3.2 Synthesis of (DEASti-*alt*-MAn)-*b*-ACMO Block Copolymers with RAFT Polymerization (Block Copolymers 1–4)[8]

DEASti-*alt*-MAn (macroRAFT agent) (0.39 g, 0.02 mmol, M_n= (17,000) g mol^{-1}, PDI = 1.13), ACMO (3.00 g, 11 mmol), and AIBN (0.003 g, 0.01 mmol, [CTA]:[I]=2:1) were added to a 50 mL reaction flask with stir bar and septum. The flask was purged with argon and 40 mL of anhydrous THF were added to the flask with a syringe. The solution was purged with argon for 30 min, and then stirred 3–4 h at 60 °C. The reaction was cooled to room temperature and the polymer solution was precipitated into 400 mL of hexanes. The white solid was collected by using vacuum filtration. The solid was then redissolved in THF and precipitated into hexanes (400 mL). The white solid was

collected by using vacuum filtration and dried in the vacuum oven at RT overnight (1.37 g, 40%) (M_n = 45000 g mol^{-1}, and PDI= 1.24).

7.3.3.3 Deprotection of (DEASti-*alt*-MAn)-*b*-ACMO and Synthesis of Polyampholyte (DEASti-alt-MA)-b-ACMO (DHBCs 1–4)[8]

The typical procedure for deprotection and polyampholyte synthesis was as follows. (DEASti-*alt*-MAn)-*b*-ACMO (0.50 g, 0.01 mmol), HCl (3 mL, 0.04 mol) and deionized water (15 mL) were added to a 50-mL round bottom flask and stirred for 2 h at 50 °C. The solutions were placed in cellulose/ester membranes (MWCO 1000 g mol^{-1}), which were placed in a beaker with water (2 L); the water was stirred for 48 h after which time dialysis was presumed to be completed. The aqueous contents of the membranes were then frozen in liquid nitrogen and lyophilized for 24 h to yield a white fluffy solid. Conversion into the polyampholyte was monitored by FTIR by measuring the disappearance of the anhydride signal (1841 cm^{-1} and 1772 cm^{-1}) and the appearance of the carboxylic acid signal at 1723 cm^{-1}.[8,9,22]

7.3.3.4 Synthesis of poly(4-acryloyl morpholine) (ACMO) Homopolymer with Conventional Radical Polymerization

ACMO (2.00 g, 14 mmol), and AIBN (0.02 g, 1 wt%) were added to a 50 mL reaction flask with stir bar and septum. The flask was purged with argon and 10 mL of anhydrous THF were added to the flask with a syringe. The solution was purged with argon for 30 min, and then stirred 24 h at 60 °C. The reaction was cooled to room temperature and the polymer solution was precipitated into 400 mL of hexanes. The white solid was collected by using vacuum filtration. The solid was then redissolved in THF (10 mL) and

precipitated into hexanes (400 mL). The white solid was collected by using vacuum filtration and dried in the vacuum oven at RT overnight (1.70 g, 85%) (M_n = 15000 g mol^{-1}, and PDI= 2.5).

7.4 *Results*

RAFT controlled radical polymerization techniques were employed to synthesize DEASti-*alt*-MAn copolymers-(1–4) (Table 7.6.1). The chain extension of these alternating copolymers with ACMO resulted in organic-soluble, block copolymers-(1–4) (Table 7.6.1). After molar mass measurements with SEC in THF, block copolymer precursors were converted to their respective polyampholyte DHBCs-(1–4) via acid hydrolysis (Figure 7.4.1). The molar masses of the DHBCs were assumed to be equal to the block copolymer precursors since the hydrolysis conditions were unlikely to cause chain cleavage.

Table 7.6.1. THF SEC Results for DEASti-*alt*-MAn and (DEASti-*alt*-MAn)-*b*-ACMO Copolymers Chain Extended with ACMO.

Copolymer	Time (h)	M_n (g mol^{-1})	DP[b]	PDI	Block Copolymer	Time (h)	M_n (g mol^{-1})	DP[b] (ACMO)	PDI
(DEASti-*alt*-MAn[a] (1)	3.5	12000	35	1.13	**(DEASti-*alt*-MAn)-*b*-ACMO[c] (1)**	4.0	45000	231	1.24
(2)	4.0	15000	42	1.25	**(2)**	3.0	22000	50	1.25
(3)	4.0	17000	49	1.26	**(3)**	3.5	33000	114	1.33
(4)	4.0	17000	49	1.13	**(4)**	4.0	45000	195	1.24

[a] For copolymerization of DEASti-*alt*-MAn , CDB, and AIBN were used with [CTA]:[I] of 2:1 at 60 °C in THF. [b] degree of polymerization [c] For the chain extension of DEASti-*alt*-MAn , AIBN was used with [CTA]:[I] of 2:1 at 60 °C in THF

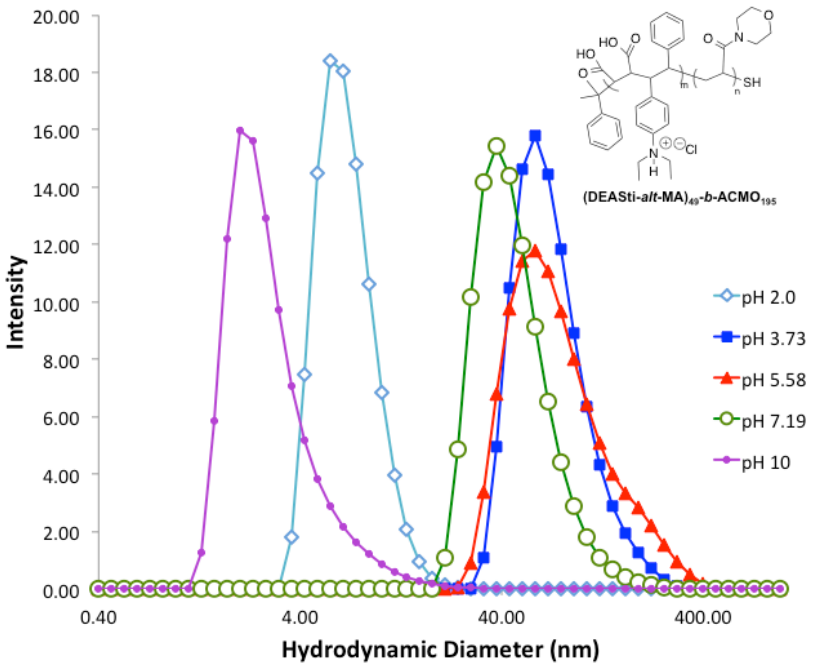

Figure 7.6.1 pH responsiveness of DHBC-(4) at 1 mg mL^{-1} by using DLS to monitor PIC hydrodynamic diameter at pH between 2–10.

DLS was used to monitor the size of DHBC-(4) (M_n = 45000 g mol^{-1} with DEASti-*alt*-MAn of 17000 g mol^{-1} M_n) in 1 mg ml^{-1} polymer solutions at different pH. PICs were assumed to contain a spherical shape. The PIC hydrodynamic diameter increased as the pH approached the IEP (4.32 pH)[8] of the DHBC (Figure 7.4.1). At intermediate pH (4.0–7.5), hydrodynamic diameter of the PIC measured between 40–60 nm. At high (11 pH) and low (2 pH), the size of PIC aggregates drastically decreased to 2–6 nm (likely mostly single chains) (Figure 7.6.1). PIC formation was found between 4.0–7.5 pH. As a control, the pH responsiveness of ACMO (M_n = 15000 g mol^{-1}, and PDI= 2.5) was measured by monitoring (volume-average diameter) hydrodynamic diameter in varying pH solutions. The size (hydrodynamic diameter) of the ACMO polymer chains did not change within the pH range of interest (4.0-7.5 pH) (Figure 7.6.2). Similar experiments were attempted

for DEASti-*alt*-MA copolymers (without the flexible block). However, the semi-rigid copolymers were insoluble at high pH conditions and at the IEP pH.

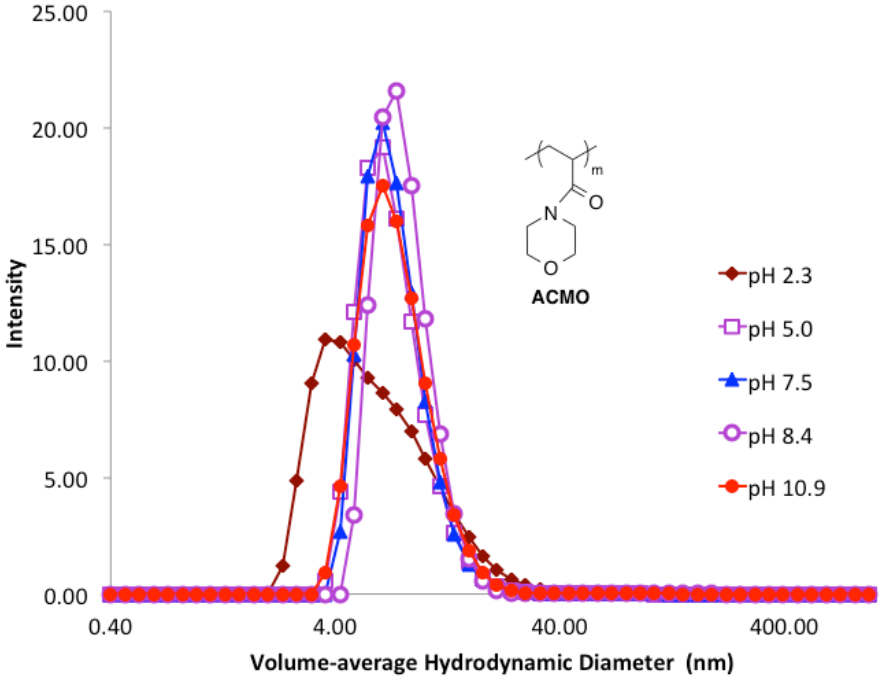

Figure 7.6.2 pH responsiveness of ACMO homopolymers at 1 mg mL^{-1} by using DLS to monitor PIC hydrodynamic diameter at pH between 2.0 and 11.

The DHBC-(4) was stable (hydrodynamic diameter <1000 nm) up to 2.0 M ionic strength (starting pH of 6.6). At higher ionic strengths (>2.5 M), two particle sizes appear (141 nm and 712 nm) but particles remain less than 1000 nm. There was a systematic increase of hydrodynamic diameter as the ionic strength of the solution was adjusted from 0.01–2.0 M (Figure 7.6.3) with no visible solution clouding. At very low ionic strengths (low [NaCl] (0.01-0.08 M)), there is a small decrease in PIC hydrodynamic diameter (Figure 7.6.4).

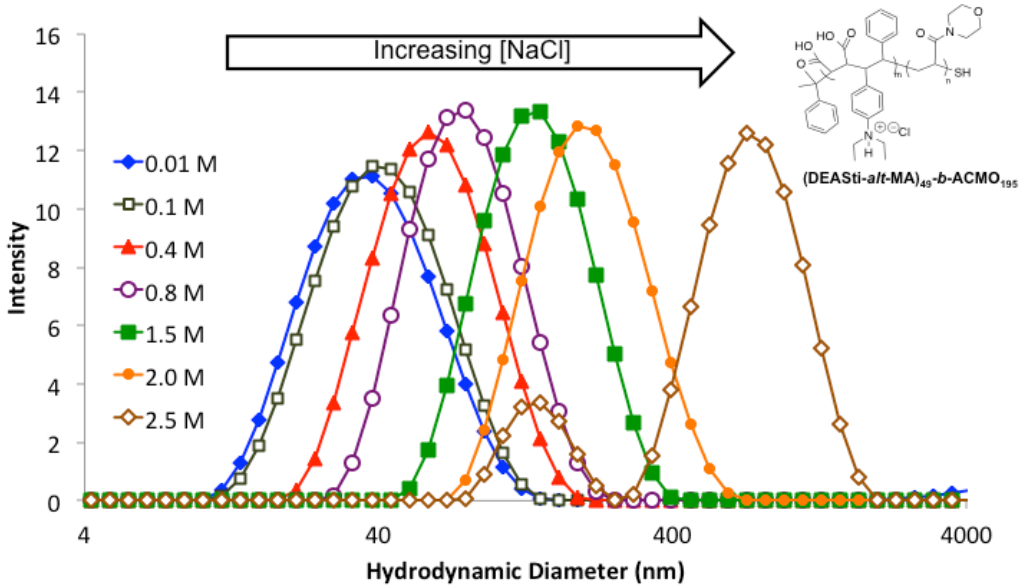

Figure 7.6.3 Salt (NaCl) responsiveness of DHBC-(4) by using DLS to monitor PIC hydrodynamic diameter with increasing ionic strength (0.01–2.5 M) (starting polymer concentration of 1 mg mL^{-1} at 6.6 pH).

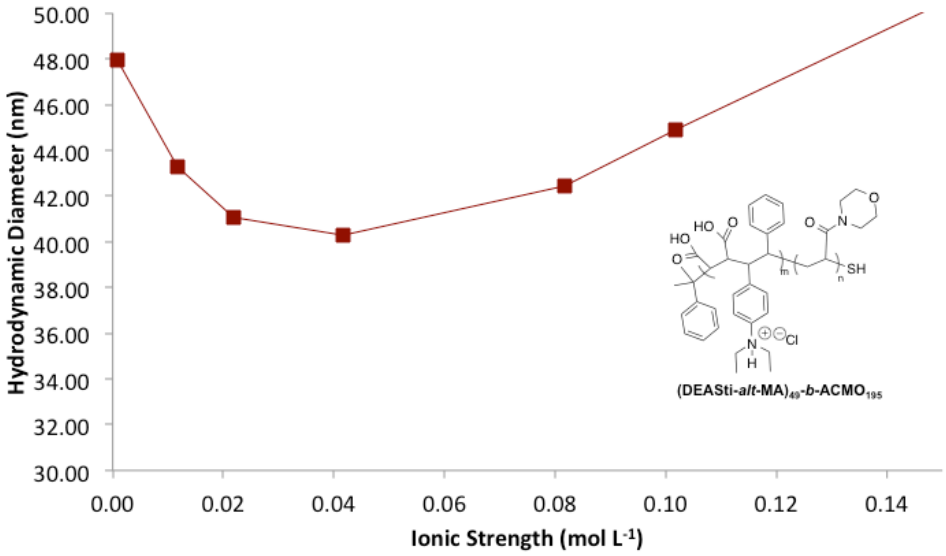

Figure 7.6.4 Salt (NaCl) responsiveness of DHBC-(4) by using DLS to monitor PIC hydrodynamic diameter with increasing ionic strength (0.0–0.1 M) (starting polymer concentration of 1 mg mL^{-1} at 6.6 pH).

The hydrodynamic diameters of all four DHBCs (1–4) were measured individually at pH 7.0 as the ionic strength was increased by the addition of 4.0 M NaCl (Figure 7.6.5). DHBC-(2) ((DEASti-*alt*-MA):ACMO DP ratio of 1:1) appeared to have the lowest solubility (hydrodynamic diameter > 1000) as the ionic strength increased and began to cloud at 0.08 M ionic strength. DHBC-(3 and 4) ((DEASti-*alt*-MA):ACMO DP ratio of 1:4 or 1:5) were both soluble at high ionic strength (hydrodynamic diameter< 750 nm) with no visible cloud point ≤ 2.0 M ionic strength.

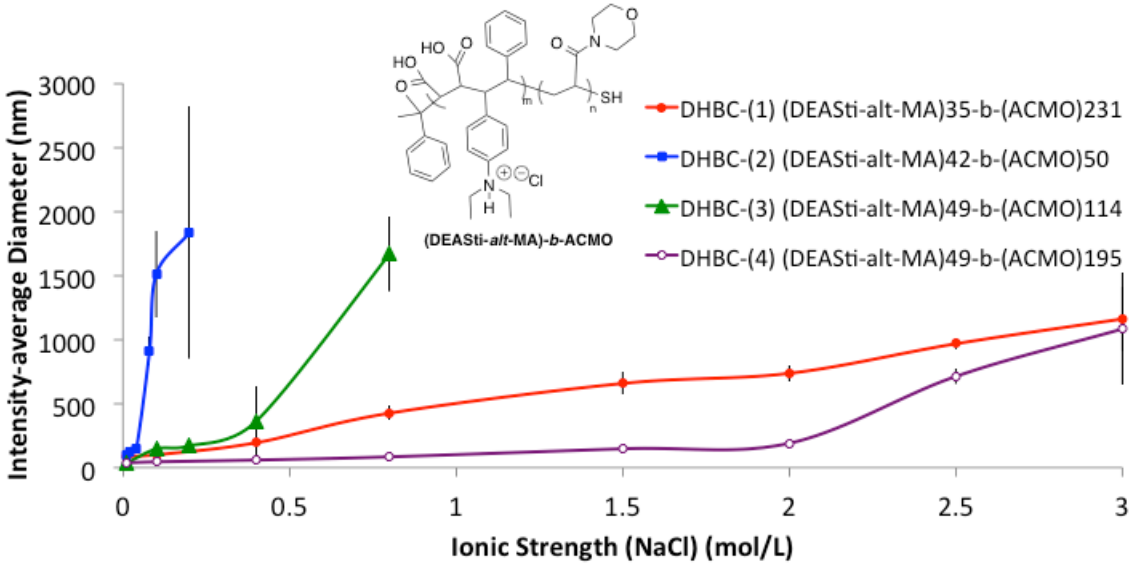

Figure 7.6.5 Salt (NaCl) responsiveness of DHBC-(1–4) by using DLS to monitor PIC hydrodynamic diameter with increasing ionic strength (0.0–3.0 M) (starting polymer concentration of 1 mg mL^{-1} at 7.0 pH).

For DHBC-(1) (M_n = 45000 g mol^{-1} with DEASti-*alt*-MAn of 12000 g mol^{-1} M_n), the salt response was monitored with NaCl, $CaCl_2$, and $NaBF_4$, individually (Figure 7.6.6), at 7.0 pH. NaCl, $CaCl_2$, and $NaBF_4$ were used to measure hydrodynamic diameter of the PIC as a function of ionic strength. Similar results appeared for the NaCl responsiveness of DHBC-(1) compared to DHBC-(4). For $CaCl_2$ and $NaBF_4$, DHBC-(1) was stable to 1.0 M and 0.02 M ionic strength, respectively, with hydrodynamic diameters < 1000 nm and PIC hydrodynamic diameter increased as ionic strength increased. However, the PICs flocculated and a cloud-point was reached at these concentrations. Figure 7.6.7 represents the same salt responsive experiments but focused on the very low ionic strengths (0.01–0.1 M). No decrease was observed in PIC hydrodynamic diameter for $NaBF_4$ or $CaCl_2$.

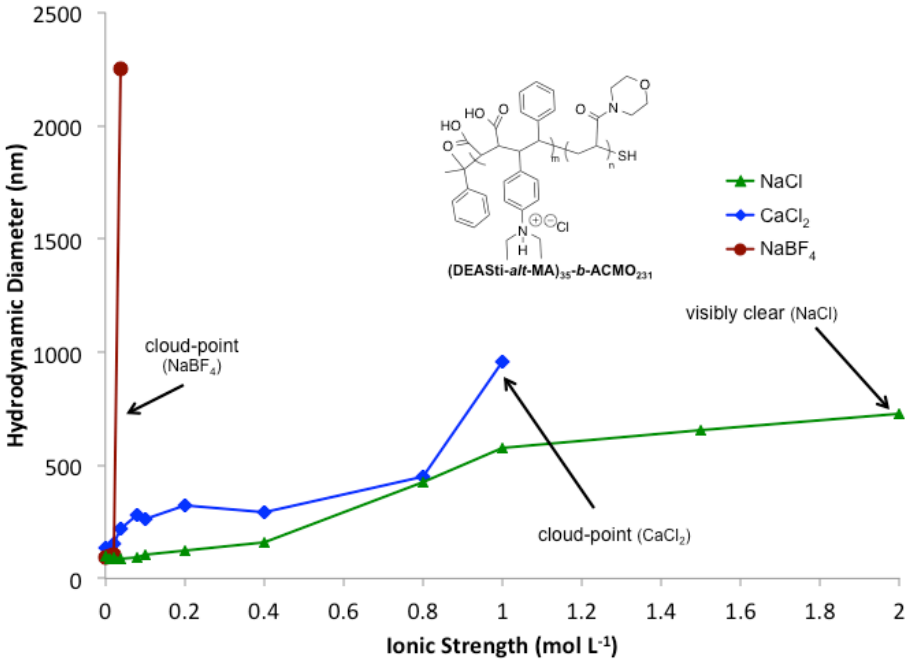

Figure 7.6.6 NaCl, $CaCl_2$, and $NaBF_4$, salt responsiveness of DHBC-(1) by using DLS to monitor PIC hydrodynamic diameter with increasing ionic strength (0.0–2.0 M) with starting polymer concentration of 1 mg mL^{-1} at 7.0 pH).

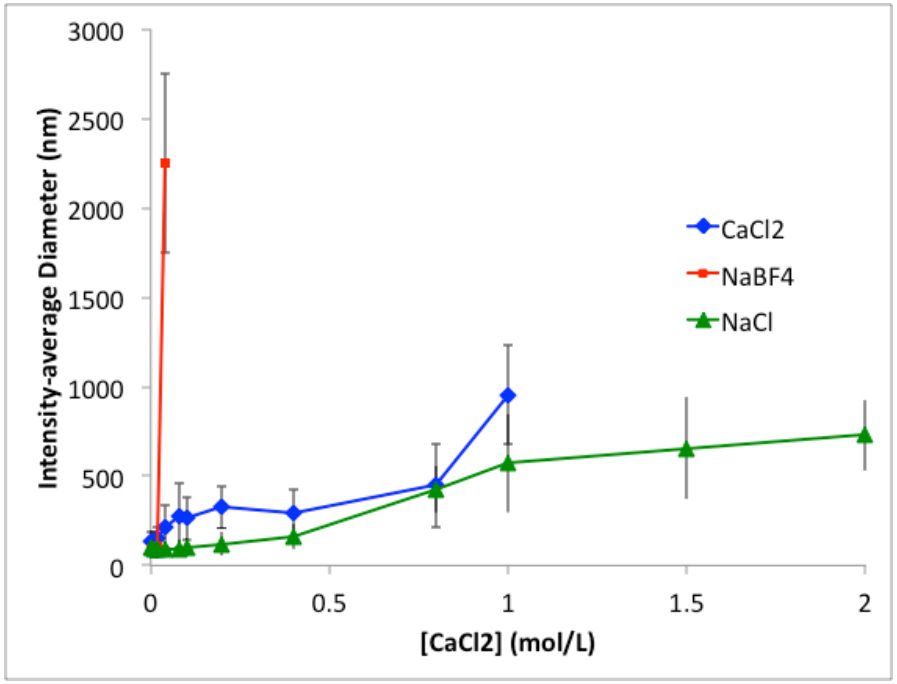

Figure 7.6.6.2 NaCl, $CaCl_2$, and $NaBF_4$, salt responsiveness of DHBC-(1) (including error bars) by using DLS to monitor PIC hydrodynamic diameter with increasing ionic strength (0.0–2.0 M) with starting polymer concentration of 1 mg mL^{-1} at 7.0 pH).

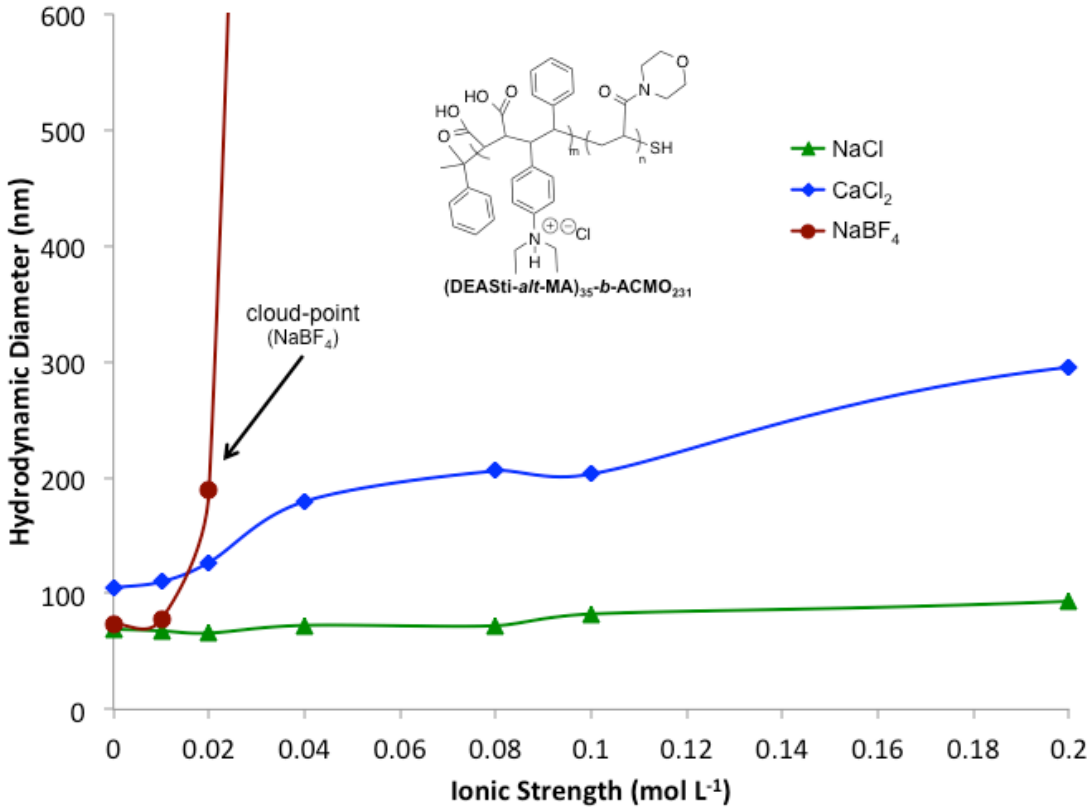

Figure 7.6.7 NaCl, $CaCl_2$, and $NaBF_4$, salt responsiveness of DHBC-(1) by using DLS to monitor PIC hydrodynamic diameter with increasing ionic strength (0.0–0.2 M) with starting polymer concentration of 1 mg mL^{-1} at 7.0 pH).

7.5 *Discussion*

7.5.1 pH Responsiveness of (DEASti-*alt*-MA)-*b*-ACMO (DHBC-(4))

At the pH extremes (11 and 2.0 pH), the smallest particle size appears possibly due to the more polyelectrolytic nature of the DHBCs (Figure 7.6.1) and are likely due to single

chains. The diethylaniline residues have a 5.5 pK_a[23] and the maleic acid residues contain two distinct pKas of 4 and 10. [11,17,18] At 2.0 pH, all residues are protonated and the DHBC contains only cationic residues. In contrast, at 11 pH, all residues have been deprotonated and the DHBC contains only anionic residues. When the DHBC contains significantly more cationic (at 2.0 pH) or anionic (at 11 pH) charges along the polymer backbone, the formation of PICs is drastically reduced and polymer or polymer aggregate size is decreased. At these pHs, electrostatic intermolecular interactions decrease due the loss of the ampholytic character (containing cationic and anionic groups) of the DHBC.

For most polyampholytes at intermediate pH, an increase of electrostatic inter– and intramolecular interactions occurs due to the more ampholytic nature of the polyampholyte at these pH and can alter the aggregate or polymer coil size. For these DHBCs, the PIC size increases as the pH approached the IEP (4.3 pH)[8] of the DHBC-(4) at which the polyampholyte is electrically neutral.[13,24] Due to the ampholytic character (containing cationic and anionic charges) of the DHBCs at intermediate pH (near the IEP), PIC complexes form with hydrodynamic diameter between 30–70 nm (Figure 7.6.1). Hydrophobic interactions[25] of the DEASti-MA repeat units could have also promoted this PIC formation, but it is likely due to electrostatic interactions of the cationic and anionic residues. This pH responsiveness closely resembles the results of work done previously reported on the OEGMA-*b*-(TEDASti-*alt*-MAn) copolymers.[9]

To confirm the pH response is due to the semi-rigid segments, the size of the ACMO homopolymer chains was monitored as a function of pH. The hydrodynamic size did not

change within the pH range of interest (4.0-7.5 pH) (Figure 7.6.2). Therefore, the pH responsiveness of these DHBCs can be assigned to the semi-rigid, polyampholyte, DEASti-*alt*-MA copolymer segments.

7.5.2 NaCl Responsiveness of (DEASti-*alt*-MA)-*b*-ACMO (DHBC-(1)).

The NaCl responsiveness of DHBC-(4) is measured by monitoring the PIC hydrodynamic diameter at varying ionic strengths (0.0–3.0 M) (Figure 7.6.3). As the ionic strength increases, the PIC size increases and appears stable (hydrodynamic diameter <1000 nm, no clouding, and unimodal) up to 2.0 M ionic strength. This salt response is known as the antipolyelectrolyte effect[26] and is possibly due to the ampholytic nature and "like-charge" attraction mechanism described above. Compared to the DHBCs reported previously,[9] DHBC-(4) is stable at ionic strengths four times higher than the (OEGMA-*b*-(TEDASti-*alt*-MAn)) DHBCs. This increased solubility could be due to either the unbalanced charge density of DHBC-(1–4) (one basic residue to two acid residues) or the solubiltiy of the ACMO, flexible homopolymer block. At 2.5 M ionic strength, the PIC complex sizes are bimodal and possible incomplete aggregation. At this concentration, the PICs are no longer considered stable due to this bimodality. However, solutions remained visibly clear. Also, at very low ionic strength (<0.01–0.10 M), there is a slight decrease in PIC size possibly due to a reduction of electrostatic intramolecular interactions or charge screening of the vicinal diacids of the maleic acid moieties. This has previously been reported for other charge imbalanced flexible polyampholytes.[27-29]

7.5.3 Salt Responsiveness of (DEASti-*alt*-MA)-*b*-ACMO (DHBC-(1–4)).

To probe this increased solubility of the ACMO segment compared to the OEGMA segment, the salt (NaCl) responsiveness of DHBCs with varying molar mass of ACMO blocks is measured. The hydrodynamic diameters of all four DHBCs (1–4) were monitored individually at pH 7.0. All four DHBCs showed an antipolyelectrolyte effect but PICs exhibited differing stabilities. DHBC-(2) and DHBC-(3) displayed the lowest solubility by reaching a cloud-point at 0.08 M and 0.8 M ionic strength, respectively. Whereas, neither DHBC-(1) or DHBC-(4) never reached a cloud-point and remained unimodal for ionic strengths < 2.0 M. When comparing block length ratios of DEASti-*alt*-MA to ACMO, DHBC-(1) contains equal block lengths with a DP ratio of 1:1; DHBC-(3) contains a block length ratio of 1:2; and DHBC-(1) and DHBC-(4) contains a block lengths ratio of 1:5 and 1:4, respectively. Therefore, the higher molar mass (DP) of the ACMO block (compared to the DEASti-*alt*-MA) appears to stabilize the DHBCs at higher ionic strengths. Since, as discussed earlier, ACMO polymers are non-repsonsive, the ACMO polymer block only serves to stabilize and solubilize the DEASti-*alt*-MA semi-rigid block.

7.5.4 $CaCl_2$ and $NaBF_4$ Responsiveness of (DEASti-*alt*-MA)-*b*-ACMO (DHBC-(1)).

By using DLS, the salt response for DHBC-(1) is measured using two more salts, $CaCl_2$, and $NaBF_4$. These salts were used to investigate the "like-charge" attraction mechanism with counterions of different size (BF_4^-) and different valency (Ca^{2+}). Again, DHBC-(1) exhibits an antipolyelectrolyte effect with an increase of ionic strength; however, DHBC-

(1) reaches a cloud-point at much lower ionic strengths (Figure 7.6.6.1) and appears to be less stable in $CaCl_2$, and $NaBF_4$ salt solutions. Possibly, the increased counterion sizes of Ca^{2+}, and BF_4^-, compared to NaCl, could have increased the hydrophobicity of the polymer chains by decreasing the ionic character of the charged residues on the polymer; thus, decreasing the solubility of DHBC-(1) and reaching a cloud-point.

7.6 *Conclusions*

In summary, four DHBCs composed of semi-rigid and flexible block segments were synthesized. These DHBCs exhibited a pH and ionic strength responsiveness. PICs hydrodynamic diameter increased as the pH approached the IEP of the DHBC. The DHBCs also exhibited an antipolyelectrolyte effect with three different salts. This behavior is consistent with the "like-charge" attraction of the semi-rigid polymer backbone of the DEASti-*alt*-MA segments, the DHBCs displayed an antipolyelectrolyte effect. Further investigation into the solution properties and stimuli responsive nature of DHBCs with both flexible block segments is underway and will be reported in the future.

7.7 *References*

(1) Cabane, E.; Zhang, X. Y.; Langowska, K.; Palivan, C. G.; Meier, W. Stimuli-responsive polymers and their applications in nanomedicine, *Biointerphases* **2012**, *7*, 1–27.

(2) Hu, J.; Zhang, G.; Ge, Z.; Liu, S. Stimuli-responsive tertiary amine methacrylate-based block copolymers: Synthesis, supramolecular self-assembly and functional applications, *Prog. Polym. Sci.* **2014**, *39*, 1096–1143.

(3) Cabane, E.; Zhang, X. Y.; Langowska, K.; Palivan, C. G.; Meier, W. Stimuli-responsive polymers and their applications in nanomedicine, *Biointerphases* **2012**, *7*.

(4) Goldblatt, M. Wastewater treatment, *Chem. Eng. Prog.* **2008**, *104*, 35–36.

(5) Colfen, H. Double-hydrophilic block copolymers: Synthesis and application as novel surfactants and crystal growth modifiers, *Macromol. Rapid Commun.* **2001**, *22*, 219–252.

(6) Colfen, H.; Antonietti, M. Crystal design of calcium carbonate microparticles using double-hydrophilic block copolymers, *Langmuir* **1998**, *14*, 582–589.

(7) Wibowo, A.; Osada, K.; Matsuda, H.; Anraku, Y.; Hirose, H.; Kishimura, A.; Kataoka, K. Morphology control in water of polyion complex nanoarchitectures of Double-hydrophilic charged block copolymers through composition tuning and thermal treatment, *Macromolecules* **2014**, *47*, 3086–3092.

(8) Savage, A. M.; Ullrich, E.; Chin, S. M.; Kiernan, Z.; Kost, C.; Turner, S. R. Synthesis and characterization of double hydrophilic block copolymers containing semi-rigid and flexible segments, *J. Polym. Sci. Pol. Chem.* **2014**.

(9) Mao, M.; Turner, S. R. Aggregation of rod-coil block copolymers containing rigid polyampholyte blocks in aqueous solution, *J. Am. Chem. Soc.* **2007**, *129*, 3832–3833.

(10) Li, Y.; Zhang, M.; Mao, M.; Turner, S. R.; Moore, R. B.; Mourey, T. H.; Slater, L. A.; Hauenstein, J. R. Chain stiffness of stilbene containing alternating copolymers by SAXS and SEC, *Macromolecules* **2012**, *45*, 1595–1601.

(11) Li, Y.; Savage, A. M.; Zhou, X.; Turner, S. R.; Davis, R. M. Solution properties of stilbene-containing sterically crowded alternating polyanions, *J. Polym. Sci. Pol. Phys.* **2013**, *51*, 1565–1570.

(12) Dobrynin, A. V.; Colby, R. H.; Rubinstein, M. Polyampholytes, *J. Polym. Sci. Pol. Phys.* **2004**, *42*, 3513–3538.

(13) Lowe, A. B.; McCormick, C. L. Synthesis and solution properties of zwitterionic polymers, *Chem. Rev.* **2002**, *102*, 4177–4189.

(14) McCormick, C. L.; Johnson, C. B. Water-soluble copolymers. 29. Ampholytic copolymers of sodium 2-acrylamido-2-methylpropanesulfonate with (2-acrylamido-2-methylpropyl)dimethylammonium chloride: solution properties, *Macromolecules* **1988**, *21*, 694–699.

(15) Manning, G. S. Limiting laws and counterion condensation in polyelectroyte solutions. I. Colligative properties, *J. Chem. Phys.* **1969**, *51*, 924–933.

(16) Ha, B. Y.; Liu, A. J. Counterion-mediated attraction between two like-charged rods, *Phys. Rev. Lett.* **1997**, *79*, 1289–1292.

(17) Sauvage, E.; Amos, D. A.; Antalek, B.; Schroeder, K. M.; Tan, J. S.; Plucktaveesak, N.; Colby, R. H. Amphiphilic maleic acid-containing alternating copolymers - 1. Dissociation behavior and compositions, *J. Polym. Sci. Pol. Phys.* **2004**, *42*, 3571–3583.

(18) Garrett, E. R.; Guile, R. L. Potentiometric titrations of a polydicarboxylic acid: maleic acid-styrene copolymer, *J. Am. Chem. Soc.* **1951**, *73*, 4533–4535.

(19) Jo, Y. S.; van der Vlies, A. J.; Gantz, J.; Antonijevic, S.; Demurtas, D.; Velluto, D.; Hubbell, J. A. RAFT homo- and copolymerization of *N*-acryloyl-morpholine,

piperidine, and azocane and their self-assembled structures, *Macromolecules* **2008**, *41*, 1140–1150.

(20) Torchilin, V. P.; Shtilman, M. I.; Trubetskoy, V. S.; Whiteman, K.; Milstein, A. M. Amphiphilic vinyl-polymers effectively prolong liposome circulation time in-vivo, *BBA - Biomembranes* **1994**, *1195*, 181–184.

(21) Li, W.; Nakayama, M.; Akimoto, J.; Okano, T. Effect of block compositions of amphiphilic block copolymers on the physicochemical properties of polymeric micelles, *Polymer* **2011**, *52*, 3783–3790.

(22) Li, Y.; Mao, M.; Matolyak, L. E.; Turner, S. R. Sterically crowded anionic polyelectrolytes with tunable charge densities based on stilbene-containing copolymers, *ACS Macro Lett.* **2012**, *1*, 257–260.

(23) Kolling, O. W.; Garber, D. A. Potentiometric study of base strengths in the binary solvent, acetic acid-p-dioxane, *Anal. Chem.* **1967**, *39*, 1562–1567.

(24) Alfrey, T.; Morawetz, H.; Fitzgerald, E. B.; Fuoss, R. M. Synthetic electrical analog of protiens *J. Am. Chem. Soc.* **1950**, *72*, 1864–1864.

(25) Garnier, G.; Duskova-Smrckova, M.; Vyhnalkova, R.; Van de Ven, T. G. M.; Revol, J.-F. Association in solution and adsorption at an air-water Interface of alternating copolymers of maleic anhydride and styrene, *Langmuir* **2000**, *16*, 3757–3763.

(26) Andrew, B. L.; Charles, L. M. Stimuli Responsive Water-Soluble and Amphiphilic (Co)polymers In *Stimuli-Responsive Water Soluble and Amphiphilic Polymers*; ACS Symposium Series, American Chemical Society: 2000; Vol. 780, p 1–13.

(27) Lee, W. F.; Chen, C. F. Poly(2-hydroxyethyl methacrylate-co-sulfobetaine)s hydrogels: 3. Synthesis and swelling behaviors of the [2-hydroxyethyl methacrylate-

co-N,N'-dimethyl (acrylamido propyl) ammonium propane sulfonate] hydrogels, *Polymer Gels and Networks* **1998**, *6*, 493–511.

(28) Mccormick, C. L.; Johnson, C. B. Water-soluble polymers .33. ampholytic terpolymers of sodium 2-acrylamido-2-methylpropanesulfonate with 2-acrylamido-2 methylpropanedimethylammonium chloride and acrylamide - synthesis and aqueous-aolution behavior, *Polymer* **1990**, *31*, 1100–1107.

(29) Mccormick, C. L.; Salazar, L. C. Water-soluble copolymers .44. Ampholytic terpolymers of acrylamide with sodium 2-acrylamido-2-methylpropanesulfonate and 2-acrylamido-2-methylpropanetrimethylammonium chloride, *Polymer* **1992**, *33*, 4384–4387.

7.8 *Supporting Information*

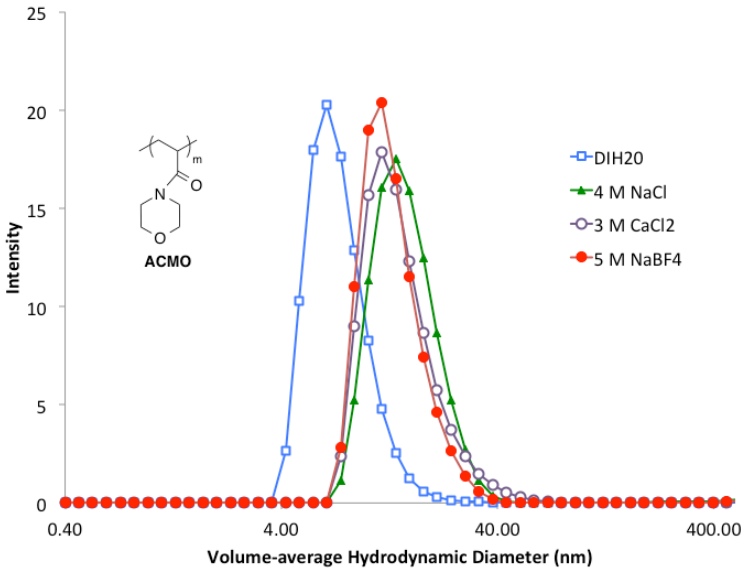

Figure 7.10.1 Salt responsiveness of ACMO homopolymer at 1 mg mL^{-1} (in DIH_2O, 4.0 M NaCl, 3.0 M $CaCl_2$, and 5.0 M $NaBF_4$) by using DLS to monitor volume-average hydrodynamic diameter at pH 7.0.

Although there is a slight increase in hydrodynamic diameter (6.5 nm–13 nm), we assume this is insignificant in the "like-charge" attraction mechanism where the PIC increase from 40 nm to >1000 nm.

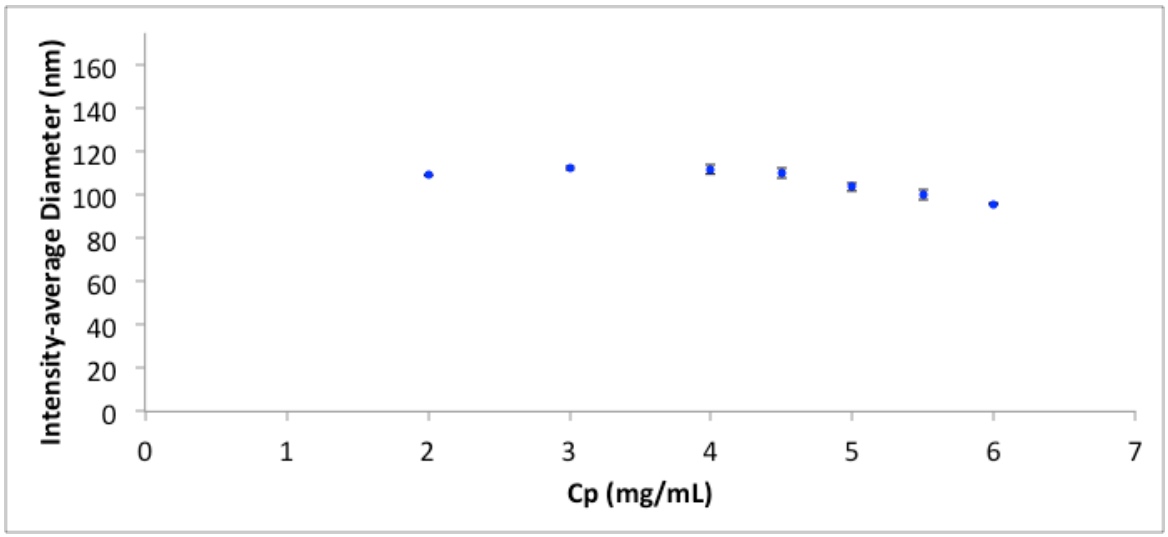

Figure 7.10.2 Effects of polymer concentration (Cp) on hydrodynamic diameter of DHBC-(4) by using DLS to monitor PIC hydrodynamic diameter with increasing Cp at 7.0 pH).

Chapter 8: **Overall Summary, Conclusions, and Future Work**

A study investigating the incorporation of substituted stilbene monomers in anionic and ampholytic copolymer systems is described. These alternating copolymers are classified as semi-rigid with sterically congested copolymer backbones. Their subsequent solution properties are evaluated.

Chapter 3

The carboxylated polyanions synthesized from *tert*-butyl ester protecting-groups as described in Chapter 3 afford copolymers with tunable amounts of carboxylate anions per repeat unit after deprotection and neutralization. In deionized water, these polyanions exhibited a polyelectrolyte affect with extended polymer chains in dilute solutions. Statistical segment length calculations revealed the polyanion chains were extended and exhibited behavior consistent with rigid-rods in salt-free solutions; possibly due to electrostatic (Coulombic) repulsive intramolecular interactions of the vicinal diacids and other anions. However, in salt solutions, salt screening occurred and the alternating polyanions collapsed to their original intrinsic, semi-rigid statistical segment lengths. Potentiometric titrations revealed multi-step dissociation behavior attributed to the vicinal diacids of the maleic acid functional groups. The close proximity along the backbone of these vicinal diacids enables the anions to share counterions, which then results in two distinct carboxyl pK_as. Overall, the statistical segment length calculations of these

uncommon semi-rigid polyanions were confirmed through the rheological experiments. The polyanions remained like rigid-rods in water and then collapsed back to the intrinsic segment length.

For future work, the same experiments and calculations outlined in this paper should be applied to the maleimide-containing copolymers. This would extend the physical characterization of the series of polyanions described in Chapter 3 and 4. With few examples of semi-rigid polymers in the literature, it would be interesting to investigate how these semi-rigid polyanions interact with other flexible, semi-rigid, or rigid polycations to form polyelectrolyte complexes. As the rigidity of polymers in these complexes can affect complex stability, size, and conformation, this new class of semi-rigid polymers offers a synthetic pathway to systematically increase the polymer rigidity (by changing the comonomer structure) and to probe how the increased rigidity affects the solution behavior of these complexes.

Chapter 4

Using the same carboxylated polyanions described in Chapter 3 and polyanions containing carboxy-*N*-phenylmaleimide comonomers, the anti-HIV activities were evaluated against four viral strains as shown in Chapter 4. Lower molar mass dicarboxystilbene-*alt*-maleic acid polyanions exhibited lower IC_{50} values (higher efficacy) against the IIIb and BaL strains. As a whole, the polyanions had excellent anti-HIV activities against all four viral strains: IIIb, BaL, JRCSF, and 92UG037, as well as exhibiting one of the lowest IC_{50} values reported. Possibly, the more extended polymer

chains resulting from the semi-rigid backbone increased the efficacy of these polyanions. With more extended polymer chains, the semi-rigid polyanions appear to more easily bridge and neutralize the gp120 (glycoprotein) complex as compared to flexible polyanions such as poly(sodium styrene sulfonate) and exhibit an almost 100 fold increase in activity. Polymer rigidity is introduced as a new drug design parameter for these nanodrugs, where the semi-rigid backbone of these polyanions increased the efficacy. To the best of our knowledge, this is the first time that polymer backbone rigidity is introduced as a contributing factor to inhibiting HIV-1 infection.

As mentioned in Chapter 4, lower molar mass samples of some of the polyanions are needed to investigate the effects of charge density and rigidity within the series of polymers. Currently and in the future, these polyanions and other polyelectrolytes synthesized in our laboratory are being assayed against other viruses, which would broaden the scope and impact of polymer rigidity on other antiviral activities.

Chapter 5

In Chapter 5, a series of sulfonated alternating polyanions and block polyanions were synthesized using controlled radical polymerization techniques. For the first time, diffusion-ordered NMR (DOSY-NMR) was used to measure the molar mass of the resulting polyanions. These characterized sulfonated polyanions were also assayed against the IIIb and BaL HIV-1 strains and exhibited excellent anti-HIV activities; albeit, less efficacy than the carboxylated analogs in Chapter 4.

Again, lower molar mass polyanions would be needed and synthesized to optimize the polyanions for potential anti-HIV microbicides. Because of the previous success with other polyanionic microbicides, the efficacy of these polyanions and carboxylated polyanions should also be assayed against other sexually transmitted viruses such as HSV, HPV, Neisseria gonorrhoeae, and Chlamydia trachomatis due to previous success with other similar polyanionic microbicides. C* (overlap concentration of polymer coils) must be measured for these DOSY experiments to insure the solutions are in the dilute regime without aggregation. To do this, the intrinsic viscosity of these polyanions in the same conditions of the DOSY-NMR experiment should be measured. Also, CSty-*alt*-CPMI copolymers of different molar mass were synthesized. The molar mass of the deprotected polyanions is estimated by using the molar mass of the organic-soluble precursors; thus, this family of polyanions can be used as a model for the DOSY-NMR experiments.

Chapters 6 and 7

The synthesis of two new stilbene monomers (3-methyl-(*E*)-stilbene, 3MSti, and 4-diethylaminostilbene, DEASti) and their controlled radical polymerizations were described in Chapter 6. The substitution of the stilbene monomer drastically affected its copolymerizability with maleic anhydride under RAFT polymerization conditions. Pseudo-first order reaction conditions were demonstrated for both 3MSti-*alt*-MAn and DEASti-*alt*-MAn copolymers. Block copolymers were then synthesized by chain extension of DEASti-*alt*-MAn with acryloylmorpholine. After acid hydrolysis, the resulting polyampholyte contained semi-rigid and flexible segments of differing molar masses. Potentiometric titrations revealed the same multi-step dissociation behavior seen

in Chapter 3 attributed to the maleic acid repeat units. In this chapter, the steric hindrance of the stilbene monomers is highlighted by the difficulties in the RAFT polymerizations with maleic anhydride and the resulting two-step dissociation behavior of the final polyampholyte.

The solution properties of these double hydrophilic block copolymers (DHBCs) were described in Chapter 7. The DHBCs formed polyion complexes (PICs) in aqueous solution that were pH-responsive and exhibited an antipolyelectrolyte effect with high salt solubility (>2.0 M NaCl). The salt responsiveness of these DHBCs, described as having a "like-charge" attraction, appeared in this polyampholyte system. The PIC size systematically increased with increasing ionic strength and seems likely due to the attraction/aggregation of the semi-rigid polyampholyte chains. The solubility of these DHBCs varied with different salts (NaCl, $NaBF_4$, or $CaCl_2$) and increased with increasing molar mass of the acryloyl morpholine flexible block segment. Although the antipolyelectrolyte is common to most polyampholytes, the semi-rigid polymer backbone tends to promote the "like-charge" attraction mentioned above, where there is a systematic increase in PIC size from 40–1000 nm.

Measured by using cryo-TEM, the identity of the self-assembled structure of the PICs is needed in the future to elucidate and/or confirm the solution behavior of the higher-ordered aggregates at low and high salt concentrations. In addition, the synthesis of fully anionic and fully cationic semi-rigid segments chain-extended with ACMO would be needed in the future to investigate how these DHBCs, which contain semi-rigid and

flexible block segments, self-assemble in solution. The ACMO homopolymer block would provide solubility in aqueous solutions at various conditions. This uncommon pairing of semi-rigid and flexible block segments could have potential as antiviral agents, water purification additives, or drug delivery vehicles.